

# Resistance to Flow in Alluvial Channels

---

GEOLOGICAL SURVEY PROFESSIONAL PAPER 422-J



# Resistance to Flow in Alluvial Channels

By D. B. SIMONS *and* E. V. RICHARDSON

PHYSIOGRAPHIC AND HYDRAULIC STUDIES OF RIVERS

---

GEOLOGICAL SURVEY PROFESSIONAL PAPER 422-J



---

UNITED STATES GOVERNMENT PRINTING OFFICE, WASHINGTON : 1966

**UNITED STATES DEPARTMENT OF THE INTERIOR**  
**STEWART L. UDALL, *Secretary***

**GEOLOGICAL SURVEY**  
**William T. Pecora, *Director***

## CONTENTS

	Page		Page
Abstract .....	J1	Variables—Continued	
Introduction .....	1	Resistance coefficient—Continued	
Experimental equipment and data collection .....	2	Size of bed material .....	19
Forms of bed roughness and flow phenomena .....	4	Fall velocity .....	19
Bed configuration without sediment movement .....	4	Apparent viscosity and density .....	22
Ripples .....	5	Gradation of bed material .....	23
Dunes .....	6	Prediction of form of bed roughness .....	24
Plane bed with sediment movement .....	7	Velocity distribution .....	26
Antidunes .....	8	Plane bed with sediment movement .....	26
Chutes and pools .....	9	Roughness coefficients .....	28
Regimes of flow in alluvial channels .....	10	Evaluation of resistance to flow .....	29
Lower flow regime .....	11	Evaluating resistance to flow by adjusting slope ..	30
Upper flow regime .....	11	Evaluating resistance to flow by adjusting depth	
Transition .....	11	of flow .....	38
Comparison of flume and field conditions .....	12	Adjusting depth to average alluvial grain	
Variables .....	12	roughness .....	41
Concentration of bed-material discharge .....	14	Alluvial sand-bed roughness .....	41
Fine-sediment concentration .....	14	Baffle and cube roughness .....	45
Dependent variable .....	15	Adjusting depth to smooth boundary rough-	
Change of variables .....	15	ness .....	46
Shape factor for the reach and cross section .....	15	Baffle and cube roughness .....	48
Seepage force .....	16	Gravel and cobble roughness .....	48
Resistance coefficient .....	16	Alluvial sand-bed roughness .....	49
Slope .....	16	Determination of average velocity .....	52
Depth .....	J18	Summary and conclusions .....	56
		Literature Cited .....	60

## ILLUSTRATIONS

		Page
FIGURE	1. Size-distribution curves for the sands used in the 8-foot-wide flume .....	J3
	2. Size-distribution curves for the sands used in the 2-foot-wide flume .....	3
	3. Idealized diagram of the forms of bed roughness in an alluvial channel .....	5
	4. Photograph showing upstream view of ripple bed .....	6
	5. Photograph showing side view of ripple bed .....	6
	6. Graph showing variation of $V$ with $V_*$ and $D$ for flow over a ripple bed .....	6
	7. Photograph showing upstream view of dune bed .....	6
	8. Photograph showing side view of the dune bed shown in figure 7 .....	7
	9. Photograph showing upstream view of plane bed .....	8
	10. Graph showing comparison of resistance to flow for flow over a plane bed with	
	and without movement of the bed material .....	8
11-15.	Photographs showing:	
	11. Downstream view of antidune flow .....	8
	12. Side view of the antidune flow shown in figure 11 .....	9
	13. Downstream view of chute-and-pool flow .....	10
	14. Downstream view of the chute and breaking antidune shown in figure 13	10
	15. Side view of the breaking antidune shown in figure 14 .....	10
	16. Graph showing relation of average velocity and stream power for runs using sand I	10
	17. Plan view of alternate bar development in the large flume at large width-depth	
	ratio .....	13
	18. Photograph showing large alternate bar in Marala Ravi Canal, Pakistan .....	14

	Page
FIGURE 19-45. Graphs showing:	
19. Change in Darcy-Weisbach $f$ with slope, depth, and fall velocity of bed material .....	J17
20. Relation of depth to discharge, Elkhorn River near Waterloo, Nebr. ....	19
21. Approximate relation of length of dunes to median fall velocity of bed material, at constant depth .....	20
22. Change in resistance to flow with temperature .....	21
23. Variation in resistance to flow with concentration of fine sediment .....	21
24. Apparent kinematic viscosity of water-bentonite dispersions .....	22
25. Variation of fall velocity with percentage of bentonite in water .....	22
26. Variation of fall velocity with temperature .....	23
27. Variation of resistance to flow with slope as a function of size distribution of bed material .....	23
28. Relation of form of bed roughness to stream power and median fall diameter of bed material .....	24
29. Relation of $\tau_0^2 V/R^{3/2}$ , $V_*$ , and regime of flow for laboratory and field conditions .....	25
30. Typical vertical-velocity-distribution curves in alluvial channel .....	26
31. Variation of slope of vertical-velocity distribution and shear velocity for plane bed with sediment movement .....	27
32. Relation between intercept of vertical-velocity distribution and shear velocity .....	28
33. Comparison of roughness height with $d_{85}$ size of bed material .....	29
34. Comparison of equation $C/\sqrt{g} = 7.4 \log (D/\xi)$ with relation between Chezy discharge coefficient and depth for a plane bed with sediment movement .....	29
35. Comparison of resistance data from the 8-foot-wide flume with Einstein and Barbarosa's (1952) bar-resistance relation for rivers and with Einstein and Kalkanis' (1959) relation for flumes .....	30
36-38. Relation between slope adjustment, shear stress, bed configuration, and depth:	
36. Sand I .....	32
37. Sand II .....	33
38. Sand III .....	34
39-41. Relation between slope adjustment, slope, bed configuration, and depth:	
39. Sand I .....	35
40. Sand II .....	36
41. Sand III .....	37
42. Relation between slope adjustment, shear stress, bed configuration, and depth for sand IV .....	38
43. Relation between $C_*$ , shear stress, and depth for sand IV .....	39
44. Relation between $C_*$ , depth, and slope for dune-bed configuration .....	39
45. Comparison of computed velocity and measured velocity .....	40
46. Diagram showing typical flow pattern over two-dimensional ripple and dune roughness elements .....	40
47. Sketch illustrating effective depth and effective velocity .....	41
48-64. Graphs showing:	
48. Effect of bed configuration on resistance to flow for sand I .....	41
49-54. Relation between depth adjustment, depth, and slope for:	
49. Ripples and dunes (sand I) .....	42
50. Ripples and dunes (sand II) .....	42
51. Ripples and dunes (sand III) .....	43
52. Dunes (sand IV) .....	43
53. Dunes (flume and field data, $d_{50} = 0.15-0.25$ mm) .....	44
54. Dunes (flume and field data, $d_{50} = 0.25-0.35$ mm) .....	45
55. Comparison of computed velocity with measured velocity .....	46
56. Relation between discharge coefficient and Reynolds number for different $\Delta D/D$ ratios .....	46
57. Relation between depth adjustment and depth with type of form roughness in a rigid-boundary flume .....	46
58. Relation between discharge coefficient, depth, and slope .....	47
59. Relation between resistance coefficient, depth, and temperature .....	47

	Page
FIGURE 48-64. Graphs showing—Continued	
60. Relation between depth adjustment and depth for baffle and cube roughness elements -----	J48
61. Resistance diagram relating $C/\sqrt{g}$ , $R_*$ , and $\Delta D/D$ for baffle roughness--	49
62. Resistance diagram relating $C/\sqrt{g}$ , $R_*$ , and $\Delta D/D$ for cube roughness--	50
63. Relation of depth adjustment to depth for rock roughness in a flume ----	50
64. Resistance diagram relating $C/\sqrt{g}$ , $R_*$ , and $\Delta D/D$ for rock roughness in a flume -----	50
65. Photograph showing typical San Luis Valley, Colo., canal with cobble roughness--	51
66-76. Graphs showing:	
66. Relation of depth adjustment to depth for San Luis Valley canals with cobble roughness -----	51
67. Resistance diagram relating $C/\sqrt{g}$ , $R_*$ , and $\Delta D/D$ for San Luis Valley canals with cobble roughness -----	51
68-71. Relation between depth adjustment, depth, and slope for:	
68. Ripples -----	51
69. Dunes -----	52
70. Plane bed (sand I) -----	52
71. Antidunes (sand II) -----	52
72. Resistance diagram relating $C/\sqrt{g}$ , $R_*$ , and $\Delta D/D$ for ripples and dunes	53
73. Relation between hydraulic-radius adjustment, hydraulic radius, and slope for Punjab canal data -----	54
74. Resistance diagram relating $C/\sqrt{g}$ , $R_*$ , and $\Delta R/R$ for Punjab canal data	54
75. Relation between hydraulic-radius adjustment, hydraulic radius, and slope for Pakistan canal data -----	55
76. Resistance diagram relating $C/\sqrt{g}$ , $R_*$ , and $\Delta R/R$ for Pakistan canal data	56

TABLES

	Page
TABLE 1. Comparison of the various characteristics of ripples and dunes with fall velocity of the bed material -----	J20
2. Data from a stable reach of the Rio Grande at similar discharges but different stream temperature -----	22
3. The slope $A_*$ and intercept $B_*$ of the velocity profiles for a plane bed with sediment movement -----	27
4. Values of $B$ when $\xi = d_{90}$ , and of $\xi$ when $B = A$ -----	28
5. Equation for $C_*$ as a function of bed form and grain size -----	31
6. Bed configurations and range in size of bed material for which figures 49-52 can be used to determine the $\Delta D$ adjustment based on an average grain roughness -----	43

GLOSSARY OF TERMS

**Alluvial channel.** A channel whose bed is composed of non-cohesive sediment that has been or can be transported by the flow.

**Antidunes.** Bed forms of curved symmetrically shaped sand waves that may move upstream, remain stationary, or move downstream. They occur in trains that are inphase with and strongly interact with gravity water-surface waves. The water-surface waves have larger amplitudes than the coupled sand waves. At large Froude number, the waves generally move upstream and grow until they become unstable and break like surf (breaking antidunes). The agitation accompanying the breaking obliterates the antidunes, and the process of antidune initiation and growth is repeated. At smaller Froude numbers

the antidunes generally remain stationary and increase and then decrease in amplitude without breaking (standing waves).

**Breaking antidune.** Curved symmetrically shaped waves on the water surface and on the channel bottom that build up with time and then break like surf.

**Bed configuration.** A complex of bed forms covering the bed of an alluvial stream.

**Bed form.** A generic term used to denote any irregularity produced on the bed of an alluvial channel by flowing water and sediment.

**Bed material.** The material of which a streambed is composed.

- Bed-material discharge.** Sediment discharge that consists of particles large enough to be found in appreciable quantities in the streambed.
- Clay.** Sediment finer than 0.004 mm (millimeters) regardless of mineralogical composition.
- Chutes and pools.** The flow phenomenon and bed configuration accompanying flows that occur at steep slopes and large bed-material discharges. The flow occurs at slopes steeper than for antidunes and consists of a series of pools in which the flow is tranquil, connected by steep chutes where the flow is rapid. A hydraulic jump forms at the downstream end of each chute where it enters the pool. The bed configuration consists of triangle-shaped elements with a steep upstream slope, a flat, almost horizontal back, and a gentle downstream slope. The chutes and pools move slowly upstream.
- Dunes.** Large bed forms having triangular profiles, a gentle upstream slope, and a steep downstream slope. They form in tranquil flow and, thus, are out of phase with any water-surface disturbance that they may produce. They travel slowly downstream as sand is moved across their comparatively gentle, upstream slopes and deposited on their steeper, downstream slopes. The downstream slopes are approximately equal to the angle of repose of the bed material. Dunes are smaller than sand bars but larger than ripples. They generally form at higher velocities and larger sediment discharges than do ripples, but at lower velocities and smaller sediment discharges than do antidunes. However, ripples form on the upstream slopes of dunes at lower velocities.
- Fall diameter or standard fall diameter.** The diameter of a sphere that has a specific gravity of 2.65 and the same terminal uniform settling velocity as the particle (any specific gravity) when each is allowed to settle alone in quiescent distilled water of infinite extent and at a temperature of 24°C.
- Fine sediment.** That part of the sediment discharge that consists of sediment so fine that it is about uniformly distributed in the vertical and is only an inappreciable fraction of the sediment in the streambed (referred to by some writers as washload). Its upper size limit at a particular time and cross section is a function of the flow as well as of the sediment particles.
- Flow regime.** A range of flows producing similar bed forms, resistance to flow, and mode of sediment transport.
- Lower flow regime.** A category for flows producing bed forms of ripples, ripples on dunes, or dunes. In this flow regime, flow is tranquil, water-surface undulations are out of phase with bed undulations, and resistance to flow is large.
- Median diameter.** The midpoint in the size distribution of sediment such that half the weight of the material is composed of particles larger than the median diameter and half is composed of particles smaller than the median diameter.
- Plane bed.** A bed form in which there are no irregularities larger in amplitude than a few grain diameters.
- Ripples.** Small triangular-shaped bed forms that are similar to dunes but have much smaller and more uniform amplitudes and lengths. Wave lengths are less than about 2 feet, and heights are less than about 0.2 foot.
- Sand.** Sediment particles that have diameters between 0.062 and 2.0 mm.
- Sand bar.** A dune-shaped bed form whose upstream surface is extremely long in relation to the geometry of the channel (length, 2-3 times the width of the channel). The bar may often protrude above the flow.
- Sand waves.** Crests and troughs (such as ripples, dunes, sand bars, antidunes, or standing waves) on the bed of an alluvial channel that are formed by the movement of the bed material.
- Sediment.** Fragmental material that originates from weathering of rock and is transported by, suspended in, or deposited by water or air.
- Sediment concentration.** The ratio of dry weight of sediment to total weight of the water-sediment mixture, expressed in parts per million.
- Sediment discharge.** The amount of sediment that is moved by water past a section in a unit of time.
- Silt.** Sediment particles whose diameters are between 0.004 and 0.062 mm.
- Standing waves.** Curved symmetrically shaped waves on the water surface and on the channel bottom that are virtually stationary. When standing waves form, the water and bed surfaces are roughly parallel and inphase.
- Suspended sediment.** Sediment moving in suspension in a fluid as a result of turbulent currents and (or) colloidal suspension.
- Transition.** A category for flows that occur between the lower and upper flow regimes and produce bed forms ranging from those typical of the lower flow regime to those typical of the upper flow regime.
- Upper flow regime.** A category for flows producing bed forms of plane bed with sediment moving, standing waves, antidunes, or chutes and pools. In the upper flow regime, water-surface undulations are inphase with bed undulations, except in breaking antidune or chute and pool flow.

SYMBOLS

	<i>Units</i>	
<i>A</i>	Slope of the $v_y/\sqrt{gDS}$ versus $\ln y/\xi$ relation. ( $A = 1/K$ ).	
$A_*$	Slope of the $v_y$ versus $\ln y$ relation .....	fps per $\ln$ unit
<i>B</i>	Intercept of the $v_y/\sqrt{gDS}$ versus $\ln y/\xi$ relation.	
$B_*$	Intercept of the $v_y$ versus $\ln y$ relation .....	fps
<i>C</i>	Wave celerity equal to $\sqrt{gL/2\pi \tanh \frac{2\pi D}{L}}$ ;	
	$C = \sqrt{gD}$ when $L$ is large relative to $D$ , and	
	$C = \sqrt{\frac{gL}{2\pi}}$ when $L$ is small relative to $D$ .....	fps
$C_*$	Correction term applied to the grain-roughness equation for a plane bed to obtain the resistance coefficient for other bed forms ( $C = \sqrt{S'/S}$ ).	
$C_T$	Concentration of bed-material discharge .....	ppm
$C_f$	Concentration of fine sediment .....	ppm
$C_s$	Suspended-sediment concentration .....	ppm
$C/\sqrt{g}$	The dimensionless Chezy discharge coefficient equivalent to	
	$\sqrt{\frac{8}{f}} = V/\sqrt{gRS}$ ,	
	where $\sqrt{gRS} = \sqrt{gDS}$ for two-dimensional flow.	
$C'/\sqrt{g}$	The dimensionless Chezy discharge coefficient for a channel having either grain roughness or hydraulically smooth boundary, or for an equivalent channel having either grain roughness or hydraulically smooth boundary.	
<i>D</i>	Average depth of flow .....	ft
$D_r$	The average depth of flow in a channel with ripple or dune roughness corrected for the separation zones .....	ft
$D'$	The average depth of flow a channel would have for the measured slope and discharge if only an average grain roughness affects the flow, $D' = \frac{VD}{V'}$ .....	ft
$D'_s$	The average depth of flow a channel would have for the measured slope and discharge if the resistance to flow was that of a hydraulically smooth boundary, $D'_s = \frac{VD}{V'}$ , where $V'$ is determined using the equation of Tracy and Lester (1961) .....	ft
$\Delta D$	Increase in average depth resulting from the form roughness and wave activity, $\Delta D = D - D'$ or $D - D'_s$ .....	ft
<i>d</i>	Fall diameter of the bed material .....	mm or ft
$d_{50}$	Median fall diameter of the bed material .....	mm or ft
<b>F</b>	Froude number of the flow; the ratio of average velocity ( $V$ ) to wave celerity ( $C$ ). $F = V/\sqrt{gD}$ when $L$ is large relative to $D$ .	
$f_s$	Seepage force caused by the water flowing through the streambed .....	lb per sq ft
<i>f</i>	Darcy-Wiesbach resistance coefficient;	
	$f = 8 (C/\sqrt{g})^2 = \frac{8gRS}{V^2}$ .	
$f'$	Resistance coefficient for a channel having grain roughness.	
$\Delta f$	Increase in resistance coefficient caused by form roughness and wave activity; $\Delta f = f - f'$ .	
<i>g</i>	Acceleration of gravity .....	ft per sec per sec
<i>h</i>	Wave height from trough to crest .....	ft
<i>L</i>	Wave length (from crest to crest or trough to trough) of either water-surface waves or sand waves .....	ft
<i>P</i>	The wetted perimeter .....	ft
<i>Q</i>	Discharge of water-sediment mixture .....	cu ft per sec
<i>R</i>	Hydraulic radius (area/wetted perimeter). For wide channels $R \approx D$ .....	ft
$R'$	Hydraulic radius a channel would have for the measured slope and discharge if the only resistance to flow was grain roughness .....	ft
$R'_s$	Hydraulic radius a channel would have for the measured slope and discharge if the resistance to flow was that of a hydraulically smooth boundary; equation of Tracy and Lester (1961) .....	ft
$\Delta R$	Increase in hydraulic radius resulting from form roughness and wave activity; $\Delta R = R - R'$ or $\Delta R = R - R'_s$ .....	ft
<b>R</b>	Reynolds number; $VD/\nu$ or $VR/\nu$ .	

	<i>Units</i>
$R_*$ Ratio of the Reynolds number to the Chezy discharge coefficient; $R/(C/\sqrt{g}) = V_*D/\nu$ or $V_*R/\nu$ .	
$S$ Slope of energy-grade line equal to water-surface slope with equilibrium flow.	
$S'$ The slope the channel would have for the measured depth and velocity if there was only grain roughness.	
$\Delta S$ Increase in slope required to compensate for the energy dissipated by form roughness and wave activity; $\Delta S = S - S'$ .	
$S_c$ Shape factor of the channel cross section.	
$S_p$ Shape factor of the sediment particle.	
$S_r$ Shape factor for the reach of the stream; sinuosity and change in area with distance.	
$T$ Temperature	°C or °F
$t$ Time	sec or min
$V$ Average velocity based on continuity principle	ft per sec
$V'$ The velocity of flow for a channel without energy dissipation caused by form roughness and antidune activity	ft per sec
$V_e$ Velocity of flow when the area of the separation zones are subtracted from the area of flow; $V_e D_e = VD$	ft per sec
$v_y$ Velocity at the point $y$ , where $y$ is the distance from the bed	ft per sec
$V_*$ The shear velocity, $V_* = \sqrt{\tau_0/\rho} = \sqrt{gDS}$ or $\sqrt{gRS}$	ft per sec
$\gamma$ Specific weight of the water-sediment mixture	lb per cu ft
$\gamma_w$ Specific weight of water	lb per cu ft
$\gamma_s$ Specific weight of the sediment particles	lb per cu ft
$\Delta\gamma$ Difference between the specific weights of sediment and water	lb per cu ft
$\kappa$ Von Karman's kappa.	
$\mu$ Apparent dynamic viscosity of the water-sediment mixture	lb-sec per sq ft
$\nu$ Apparent kinematic viscosity of the water-sediment mixture	sq ft per sec
$\xi$ Height of the roughness element	ft
$\rho$ Mass density of the water-sediment mixture	Slug per cu ft
$\rho_w$ Density of water	Slug per cu ft
$\rho_s$ Density of sediment	Slug per cu ft
$\sigma$ A measure of the gradation of the sediment distribution.	
$\tau_0$ The shear stress on the bed. $\gamma DS$ or the average shear stress $\gamma RS$	lb per sq ft
$\omega$ Fall velocity of sediment particles	ft per sec

## ENGLISH-METRIC CONVERSIONS

<i>Principal items</i>	<i>English unit</i>	<i>Factor</i>	<i>Metric unit</i>
Length	ft	0.3048	m
		30.48	cm
		304.8	mm
Area	sq ft	929.0	sq m
		.09290	sq m
Velocity	ft per sec	0.3048	m per sec
		30.48	cm per sec
Discharge	cu ft per sec (cfs)	0.02832	cu m per sec
		$2.832 \times 10^4$	cu cm per sec
Acceleration of gravity	ft per sec per sec	0.3048	m per sec per sec
		30.48	cm per sec per sec
Force per unit area	lb per sq ft	478.8	Dynes per sq cm
		.4882	gm per sq cm
		4.882	kgm per sq m
Dynamic viscosity	lb sec per sq ft	0.04788	gm per cm-sec (Poise)
		.4482	gm-sec per sq cm
Kinematic viscosity	sq ft per sec	929.0	sq cm per sec (Stokes)
Specific weight	lb per cu ft	0.01602	gm per cu cm
Mass density	slug per cu ft	0.5154	gm per cu cm

# PHYSIOGRAPHIC AND HYDRAULIC STUDIES OF RIVERS

## RESISTANCE TO FLOW IN ALLUVIAL CHANNELS

By D. B. SIMONS and E. V. RICHARDSON

### ABSTRACT

Resistance to flow in alluvial channels is intimately related to the bed configurations. Flume and field studies have proved that the bed configuration in alluvial channels will be ripples, ripples on dunes, dunes, plane bed, antidunes, chutes and pools, or some combination thereof. These bed configurations are classified into either a lower or an upper flow regime, or into an intermediate, transition zone. The lower flow regime (ripples, ripples on dunes, and dunes) is characterized by small bed-material discharge and large resistance to flow ( $7.0 \leq C/\sqrt{g} \leq 13.2$ , or  $0.04 \leq f \leq 0.16$ ). The upper flow regime (plane bed, antidunes, and chutes and pools) is characterized by large bed-material discharge and, except in chute and pool flow, low resistance to flow ( $0.02 \leq f \leq 0.07$ , or  $10.7 \leq C/\sqrt{g} \leq 20$ ). In the transition stage, the bed forms are extremely variable, ranging from dunes to antidunes. Knowledge of the relation between bed forms and associated flow conditions provides a means of relating depositional features to environmental conditions in both recent and ancient settings.

Bed forms and the resulting resistance to flow vary with the slope of the energy grade line, depth of flow, fall velocity, physical size and gradation of the bed material, seepage force, and shape and sinuosity of the channel. In the transition stage antecedent form of the bed roughness influences the bed configuration. These independent variables are interrelated in their effect on the bed form, so that isolation of the effect of any one variable on resistance to flow is very difficult. However, the flume experiments and field studies were used to qualitatively and, in some tests, quantitatively determine the effect of each variable on the mechanics of flow. These studies confirmed the essential role of depth, slope, and fall velocity of the bed material in determining resistance to flow. The studies also proved that changes in fall velocity with such changes in fluid properties as can occur in natural rivers will substantially alter resistance to flow. Thus, although depth, slope, and fall velocity are primary factors in determining resistance to flow, the effects of the other variables are not inconsequential.

Fine sediment dispersed in water has a definite effect on the viscosity and specific weight of the fluid mixture, and thus on fall velocity, bed configuration, resistance to flow, and sediment transport. Tests made with a Stormer viscosimeter in water whose temperature was 24°C showed that the apparent kinematic viscosity of an aqueous dispersion of bentonite (10 percent bentonite by weight) was 8.75 times greater than that of pure water.

Methods are presented for estimating the resistance to flow and the average velocity of the flow for both analysis and design purposes. The methods depend on knowledge of,

or methods for, estimating the bed configuration for given fluid, flow, bed material, and channel characteristics. A relation between stream power, median diameter of the bed material, and bed configuration was developed, from the field and laboratory data, for estimating the bed configuration. The methods of determining the resistance to flow are based on adjusting the measured depth or measured slope to an equivalent depth or slope in a channel having grain roughness or hydraulically smooth rigid-boundary roughness. The methods are applicable to most types of roughness (rigid or alluvial boundary) in all types of channels, flumes, canals, and rivers.

Utilizing the foregoing concepts of the mechanics of flow in alluvial channels gives valuable insight into the difficult problem of modeling the behavior of alluvial channels and the concepts assist in the development of a better understanding and control of the dominant factors affecting the geomorphology of streams and rivers. These concepts can be utilized in designing stable irrigation canals constructed in alluvium and in determining the discharge that occurred in a natural channel during a runoff event if only residual information is available.

### INTRODUCTION

Many significant aspects of resistance to flow in open channels are still only vaguely understood after nearly two centuries of study. In contrast to knowledge about resistance to flow through closed conduits, the lack of progress is a result of the problems created by the free surface and unsymmetrical cross section, the large variety of roughness elements, and the lack of any concerted sustained study since that of Darcy and Bazin in 1865. Other problems exist because many open channels have a movable or alluvial boundary rather than a fixed or rigid boundary.

An alluvial boundary is formed in cohesive or noncohesive materials that have been and can be transported by the stream. The noncohesive material generally consists of silt (0.004–0.062 mm (millimeter)), sand (0.062–2.0 mm), gravel (2.0–64 mm), or cobbles (64–256 mm), or any combination of these; silt, however, normally is not present in appreciable quantities in streams having larger bed materials.

The alluvial boundary, as shown by Gilbert (1914), can be molded into many bed configurations by the

flow, and changes in resistance to flow result. In addition, experiments of Vanoni (1946), Elata and Ippen (1961), Bagnold (1954), and Simons, Richardson, and Hauschild (1963), showed that the fluid properties and turbulent characteristics of the flow are changed by the moving sediment. The movable alluvial boundary thus adds another dimension to the resistance-to-flow problem and increase its complexity; not only the fluid, flow, and boundary characteristics but also the sediment characteristics must be included in the study of alluvial channels. At some discharges the material forming the boundary may not move, and the alluvial channel behaves as a rigid channel. Therefore, the flow conditions under which the material forming the boundary begins to move must be known.

To determine resistance to flow and bed-material discharge in alluvial channels, a systematic study was undertaken by the U.S. Geological Survey. Part of the investigation is being conducted at Colorado State University, where the study is limited to steady equilibrium flow over sand-bed material, although some qualitative preliminary studies have been made for unsteady flow (Simons and Richardson, 1962b). The median fall diameter of the bed material ranged from 0.19 mm to 0.93 mm. Each bed material was investigated from beginning of motion of the individual sand particles to antidune flow. Depths of flow ranged from 0.3 foot to 1.0 foot, velocities from less than 1 fps (foot per second) to more than 8 fps, and discharges from 3 cfs (cubic feet per second) to 22 cfs. Special studies have been made to determine the effect of changes in viscosity, either real or apparent, and the effect of the gradation of the bed material on the bed configuration, resistance to flow, and bed-material transport.

This report describes the bed configurations which form in an alluvial channel and the corresponding resistances to flow, as measured by the Darcy-Weisbach discharge coefficient or by the related Darcy-Weisbach resistance coefficient. These bed forms are classified into lower flow regime, transition, or upper flow regime. Knowledge of why the bed configurations form and the mechanics of their formation is not known. Thus, no perfect method is known for predicting the bed forms that will exist in an alluvial channel for particular flow conditions. However, a qualitative method for predicting the bed form that appears to have merit is presented. The variables that influence the form of the bed configuration and resistance to flow are quantitatively and, in some instances, qualitatively discussed. Some practical aspects of the effect of bed configuration

or change in bed configuration on flow in rivers and artificial waterways are described, and equations and methods for predicting resistance to flow and velocity of flow are developed on the basis of current fluid mechanics theory and a study of the collected data. The equations, developed from a study of the flume data, apply to flow in natural alluvial rivers and in artificial waterways. The equations can also be applied to flow in rigid-boundary open channels, as well they should be if there is any theoretical justification for them. With a method available for predicting the bed form and the resistance to flow, procedures are described for designing stable water-conveyance channels to carry a known water discharge or to determine water discharge in a channel when slope, bed-material, size, cross section, and water viscosity are known.

Only a brief description of the sands, equipment, and procedure used in the data collection is given. A more detailed description of the procedure is given together with the basic data in a companion publication by Guy, Simons, and Richardson (1965).

The authors acknowledge the advice, assistance, and encouragement given by Messrs. L. B. Leopold, P. C. Benedict, R. W. Carter, Thomas Maddock, Jr., F. C. Ames, W. L. Hauschild, D. W. Hubbell, W. W. Sayre, F. M. Chang, H. P. Guy, and C. F. Nordin, Jr., of the Geological Survey, during the study and in the preparation of this report. We also thank Messrs. M. L. Albertson and A. R. Chamberlain of Colorado State University for their assistance during the investigation.

#### EXPERIMENTAL EQUIPMENT AND DATA COLLECTION

The basic studies were conducted in a tilting recirculating flume 150 feet long, 8 feet wide, and 2 feet deep. The slope in the flume could be varied from 0 to 0.013 foot per foot, and the discharge, from 0 to 22 cfs. A smaller tilting recirculating flume 60 feet long, 2 feet wide, and 2.5 feet deep was used for special studies. Slope in the smaller flume could be varied from 0 to 0.025 foot per foot, and discharge, from 0.5 cfs to 8 cfs. The special studies in the 2-foot-wide flume were made to determine the effect of viscosity (Simons and others, 1963; Hubbell and Al-Shaikh Ali, 1961), density of the bed material (W. H. Hauschild and R. K. Fahnestock, written comm., 1962), and gradation of the bed material (Daranandana, 1962) on flow in alluvial channels.

The size distribution of bed materials used in the 8-foot-wide flume studies are given in figure 1. Those for materials used in the 2-foot-wide flume studies are given in figure 2. The size distribution is in

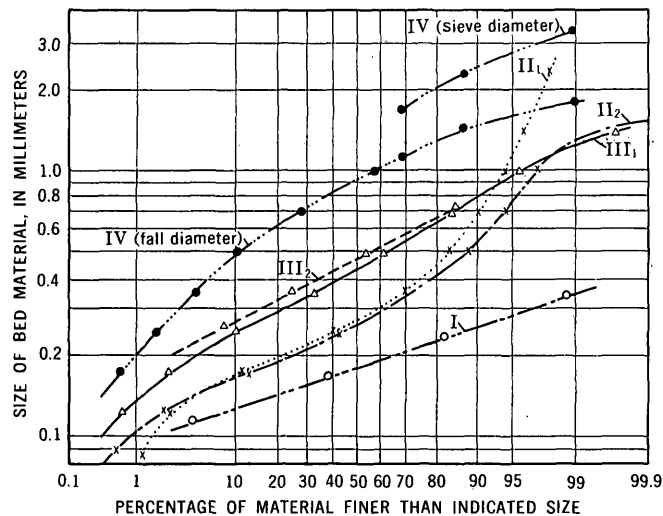


FIGURE 1.—Size-distribution curves for the sands used in the 8-foot-wide flume.

terms of the fall diameter (Colby and Christensen, 1956) unless specified otherwise. The curves shown in figures 1 and 2 are the average curves for a group of runs, determined from an averaging of the size analyses of 10 grab samples of the bed material per run.

Sand I (median diameter 0.19 mm) was pure quartz sand obtained from a decomposed sandstone deposit near Denver, Colo. Sands II (median diameter about 0.28 mm) were almost pure quartz obtained from the bed of the Elkhorn River near Waterloo, Nebr. The difference between the size distributions of sands II<sub>1</sub> (0.28 mm) and II<sub>2</sub> (0.27 mm) resulted from screening the coarse sand fraction from sand II<sub>1</sub>. The difference between sands II<sub>2</sub> and II<sub>3</sub> (0.32 mm) resulted from natural changes during the experiments. Sands III (median diameter about 0.45 mm), consisting of a mixture of feldspar and quartz with some mica, were obtained

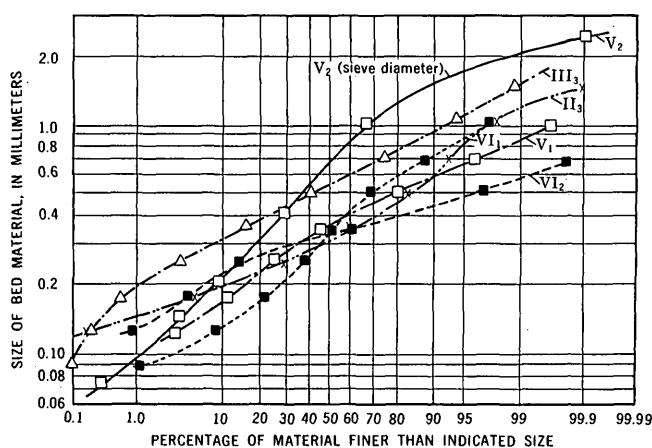


FIGURE 2.—Size-distribution curves for the sands used in the 2-foot-wide flume.

by screening the gravel from a sand deposit of the Cache la Poudre River at Fort Collins, Colo. The differences in the size distribution among sands III<sub>1</sub> (0.45 mm), III<sub>2</sub> (0.47 mm), and III<sub>3</sub> (0.54 mm) were caused by natural changes of the bed material as they were used in the experiments. Sand IV (0.93 mm) was a natural river sand, mostly quartz, obtained by screening the material coarser than 5 mm from the bed material of the North Platte River near Scottsbluff, Nebr. Bed material V, for which both the sieve size (0.68 mm) and the fall-diameter size (0.36 mm) distributions are given, was a light-weight aggregate (expanded illite) marketed by the Ideal Cement Co. under the trade name Idealite. Sands VI (0.33 mm) were almost pure silica obtained from the Black Hills Silica Corp., Hill City, S. Dak. Sand VI<sub>1</sub> passed through a U.S. standard No. 40 sieve and was retained on a No. 60 sieve, whereas sand VI<sub>2</sub> was prepared by mixing six sands in predetermined proportions to obtain a graded sand having the same median diameter as sand VI<sub>1</sub>. The sands were placed in the flumes to a depth of about 0.7 foot.

The general procedure for each run was to recirculate a given discharge of the water-sediment mixture until equilibrium flow conditions were established. Equilibrium flow is defined as flow which has established a bed configuration and slope consistent with the fluid, flow, and bed-material characteristics over the entire length of the flume, neglecting entrance- and exit-affected reaches—that is, the time-average water-surface slope of the flow is essentially constant and parallel to the time-average bed surface, and the time-average concentration of the bed-material discharge is constant. Equilibrium flow should not be confused with steady uniform flow; in equilibrium flow, velocity may vary at a point or from point to point. Steady uniform flow, as classically defined ( $\partial V/\partial t = 0$ ,  $\partial V/\partial x = 0$ ), does not occur in an alluvial channel unless the bed is plane and the flow is steady.

After equilibrium flow was established, average water-surface slope ( $S$ ), discharge of the water-sediment mixture ( $Q$ ), water temperature ( $T$ ), depth ( $D$ ), velocity distribution in the vertical ( $v_v$ ), total sediment concentration ( $C_T$ ), and the geometry of bed configuration (length,  $L$ ; height,  $h$ ), and shape) were determined.

Water-surface slope was measured with a Lory point gage and a precision level by determining water-surface elevations at definite intervals along the flume (every 5 ft in the 8-ft-wide flume; every 2 ft in the 2-ft-wide flume). Average water-surface

slope was obtained by averaging several individual slope determinations made during a run. Discharges were measured with calibrated orifice meters located in the return-flow pipes. Water temperature was measured to the nearest 0.1°C with a mercury thermometer. Depth was determined by subtracting mean bed elevation from mean water-surface elevation. Velocity distribution in a vertical was measured with a calibrated Prandtl pitot tube; however, the mean velocity of the cross section was computed from the discharge and cross-sectional-area data,  $V = Q/A$ . Total sediment concentration was measured by traversing the outflow nappe at the end of the flume with a width-depth integrating sampler. Suspended-sediment concentration was measured with a depth-integrating sampler. Bed configuration was measured with the Lory point gage and, in later runs, with a newly developed sonic depth sounder (Richardson and others, 1961). Photographs of the bed and water surfaces for all runs were taken with a still camera; normal and time-lapse sequences of the flow of water and sediment were photographed with a 16-mm movie camera.

Many of the flow phenomena observed are recorded in the Geological Survey film "Flow in Alluvial Channels." The filming was done by the Survey staff, assisted by personnel from Bandolier Films, Albuquerque, N. Mex., in the laboratory at Colorado State University and in the field near Albuquerque, on the Rio Grande.

A complete documentation and description of all basic data collected from 1956 to 1961 by the Geological survey at Colorado State University is included in a data report, Professional Paper 462-L.

#### FORMS OF BED ROUGHNESS AND FLOW PHENOMENA

The bed configurations (roughness elements) that may form in an alluvial channel are plane bed without sediment movement, ripples, ripples on dunes, dunes, plane bed with sediment movement, anti-dunes, and chutes and pools. These bed configurations are listed in their order of occurrence with increasing values of stream power ( $V\gamma DS$ ) for bed materials having  $d_{50}$  less than 0.6 mm. For bed materials coarser than 0.6 mm, dunes form instead of ripples after beginning of motion at small values of stream power. The typical form of each bed configuration is shown in figure 3.

These bed-roughness elements are not mutually exclusive occurrences in time and space in a flume or a natural river. They may form side by side in a cross section or reach of a natural stream, giving

a multiple roughness; or they may form in sequence, in time, producing variable roughness.

Multiple roughness is spatially related to variation in shear stress ( $\gamma DS$ ), stream power ( $V\gamma DS$ ), or alluvial bed material. The greater the width-depth ratio of a stream or flume, the greater is the probability of a spacial variation in shear stress, stream power, or bed material. Thus, the occurrence of multiple roughness is closely related to the width-depth ratio of the stream or flume. Multiple roughness in these experiments occurred when the width-depth ratio was greater than 20.

Variable roughness is related to changes in shear stress, stream power, or reaction of bed material to a given stream power. An example of the effect of changing shear stress or stream power is the change in bed form which occurs with changes in depth during a runoff event; this action has frequently been observed in natural rivers. An example of the effect of the bed-material-stream-power relation is the change in bed form that occurs with change in the viscosity of the fluid as the temperature or concentration of fine sediment varies. It should be noted that a transition occurs between the dune-bed and the plane bed; either bed configuration may occur for the same value of stream power.

In the following sections, bed configurations and their associated flow phenomena are described in the order of their occurrence with increasing stream power.

#### BED CONFIGURATION WITHOUT SEDIMENT MOVEMENT

If the bed material of a stream moves at one discharge but not at a smaller discharge, the bed configuration at the smaller discharge will be a remnant of the bed configuration formed when sediment was moving. The problems are in knowing when beginning of motion of the bed material occurs (Kramer, 1935; Shields, 1936; and White, 1940) and which bed form may develop. The bed configuration after the beginning of motion may be any of the preceding ones, depending on flow and bed material. Prior to the beginning of motion, the problem of resistance to flow is one of rigid-boundary hydraulics. After beginning of motion the channel is alluvial, and the problem related to defining resistance to flow under the alluvial condition is the main subject of this report.

Plane bed without movement was studied to determine the shear stress for the beginning of motion and the bed configuration that would form after beginning of motion. A plane bed for this study was

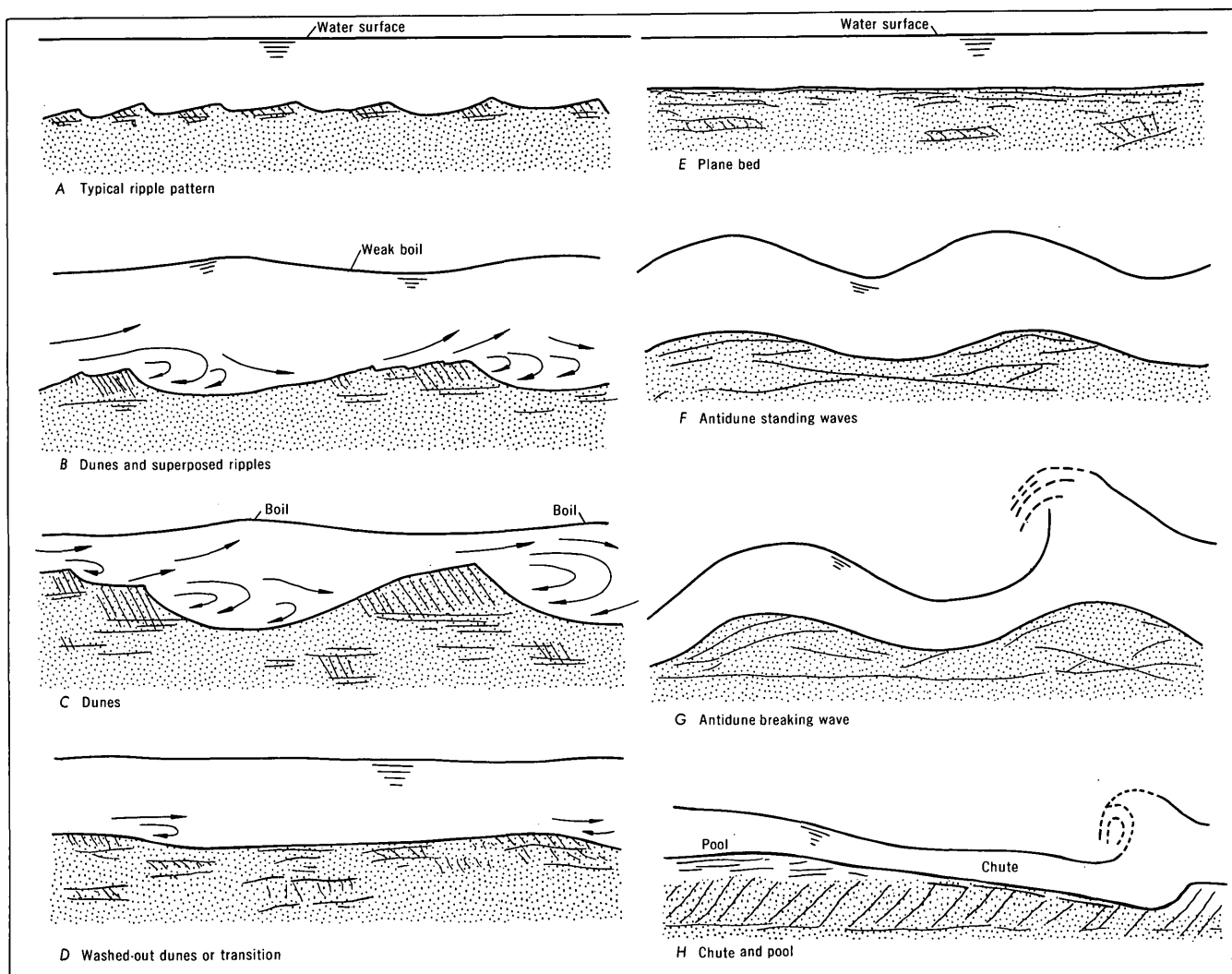


FIGURE 3.—Forms of bed roughness in an alluvial channel.

obtained artificially by screeding the bed. Within the accuracy of visual observation, Shields' relation for the beginning of motion was adequate. After beginning of motion, the plane bed changed to ripples for sand smaller than 0.5 mm, and to dunes for 0.93-mm sand. This was contrary to Liu's (1957) findings; he reported a plane bed for a range of shear stresses after beginning of motion. Knoroz (1959) reported that a plane bed did not persist after the beginning of motion and that ripples do not form for coarser sands. Resistance to flow is small for a plane bed without sediment movement. In the flume runs, values of  $C/\sqrt{g}$  ranged from 15 to 20.

#### RIPPLES

Ripples are small triangle-shaped elements having gentle upstream slopes and steep downstream slopes. In this study they ranged from 0.4 foot to 2 feet in length and from 0.02 foot to 0.2 foot in height and

were narrow normal to the direction of flow. (See figs. 4 and 5.) Resistance to flow is large, and the resulting discharge coefficient ( $C/\sqrt{g}$ ) ranged from 7 to 12. As depth increased, resistance to flow due to roughness decreased. (See fig. 6.) Thus, there is a relative roughness effect produced by the ripple bed. Figure 6 shows that resistance to flow is independent of sand size when the bed configuration is one of ripples. This is because the ripple shape is independent of sand size and the effect of grain roughness is small relative to the form roughness. Knoroz observed that the length of the separation zone when the bed form was either ripples or dunes was about 10 times the height of the ripple or the dune. The separation zone downstream from a ripple causes very little, if any, disturbance on the water surface, and the flow contains little suspended bed material. The water is clear enough that the bed configuration can be photographed through the run-





FIGURE 8.—Side view of the dune bed shown in figure 7. Note the bottom-set, foreset, and top-set layering of the sand.

Field observations by the authors indicated that dunes form in any channel, irrespective of the size of bed material, if the stream power is sufficiently large to cause general transport of the bed material without exceeding a Froude number of unity. Also, the length and shape of the dunes are functions of the fall velocity of the bed material; dune height did not appear to be a function of fall velocity of the bed material. The length of the dunes increased and the angle of the upstream and downstream faces decreased as fall velocity decreased. Dunes formed of fine sand ( $d_{50} < 0.4$  mm) were longer and less angular than those formed of coarser sand.

Resistance to flow caused by dunes is large, but not as large as that caused by ripples formed of finer sand and at shallow depth. For dunes, the discharge coefficient  $C/\sqrt{g}$  varied from 8 to 12. Resistance to flow increased with an increase in depth for coarser sands ( $d_{50} > 0.3$  mm) and decreased with an increase in depth for finer sands ( $d_{50} < 0.3$  mm). Also, when dunes were more than 10 times longer than they were high, the grain roughness on the back of the dunes influenced resistance to flow. Knoroz (1959) observed that resistance to flow for dunes depended on the grain roughness, in addition to the form roughness, whereas, that for ripples did not depend on grain roughness.

Dunes cause large separation zones in the flow. These zones, in turn, cause large boils to form on the surface of the stream. Measurements of flow velocities within the zone of separation showed that velocities in the upstream direction existed that were  $\frac{1}{2}$ – $\frac{1}{3}$  the average stream velocity. Boundary shear stress was sometimes sufficient to cause formation of ripples oriented in a direction opposite to that of the

primary flow in the channel. With dunes, as with any tranquil flow over an obstruction, the water surface is always out of phase with the bed surface. The flow accelerates over the crest of dunes and decelerates over the trough, thereby contracting the flow over the crest and expanding it over the trough.

Some investigators do not agree that there is a difference between ripple- and dune-bed configurations. Vanoni, Brooks, and Kennedy (1961), for example, saw little reason for distinguishing between ripples and dunes because the mechanisms by which they are formed and by which they move are similar. The following factors, however, indicate that there are major differences, in addition to the difference in size, between the two bed configurations:

1. The effects of a change in depth on resistance to flow are opposite: an increase in depth causes a decrease in the resistance to flow for flow over a ripple bed, but an increase in depth causes an increase in the resistance to flow for flow over a dune bed when the bed material is coarser than 0.3 mm, and a decrease in the resistance to flow when the bed material is finer than 0.3 mm.
2. Ripples do not form if the median diameter of the bed material is larger than 0.6 mm.
3. Resistance to flow caused by ripples is independent of the grain size of the bed material, whereas that caused by dunes is dependent on the grain size.

This question might seem academic if it were not for the fact that ripple beds are dominant in flume investigations and dune beds are dominant in the field. Taylor and Brooks (1962) pointed out that if there is a fundamental difference between ripples and dunes, the problems of roughness analysis and of modeling alluvial channels cannot be resolved by small-scale laboratory studies.

#### PLANE BED WITH SEDIMENT MOVEMENT

A plane bed is a bed without elevations or depressions larger than the largest grains of the bed material (fig. 9). The resistance to flow for flow over a plane bed results largely from grain roughness and  $C/\sqrt{g}$  is large, ranging from 14 to 23. Grain roughness is not of the usual type, however, because grains roll, hop, and slide along the bed. For flow over a plane bed with sediment movement, the resistance to flow is slightly less than that for flow over a static plane bed, which is essentially an artificial rigid-boundary condition that exists after screeding when stream power is insufficient to cause significant

transport of the bed material. The difference in resistance to flow between that on a plane bed with sediment moving and that on a static plane is shown in figure 10. This lower resistance to flow for flow over a plane bed with motion has been observed by many experimentors and was attributed by Vanoni and Nonicos (1960) to dampening of the turbulence by the suspended sediment. Elata and Ippen (1961) indicated that the structure of the turbulence was not damped by the suspended bed material but that the structure was changed by the movement of the sediment at the boundary.

The magnitude of the stream power ( $\tau_0 V$ ) at which the dunes or transition roughness changes to the plane bed depends mainly on the fall velocity of



FIGURE 9.—Upstream view of plane bed. Bed material is sand II; slope = 0.00153, depth = 0.60 foot, discharge 14.9 cfs,  $C/\sqrt{g} = 18.1$ .

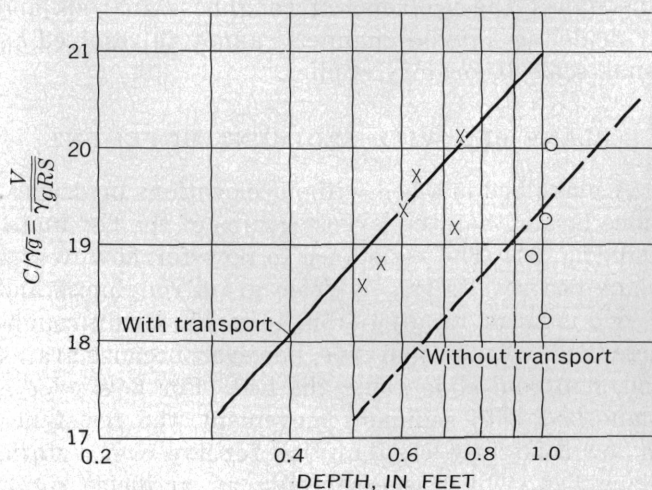


FIGURE 10.—Comparison of resistance to flow for flow over a plane bed with and without movement of the bed material. (Sand II.)

the bed material. Dunes of fine sand (low fall velocity) are washed out at lower values of stream power than are dunes of coarser sand. Consequently, in the flume experiments, where the depths were shallow (0.5–1.0 ft), the plane bed formed with finer sands at smaller slopes than it did with coarser sands; the result was smaller velocities and smaller Froude numbers ( $F$ ). The plane bed with the fine sand occurred at slopes such that the Froude number, based on average depth and average velocity, was as small as 0.3, and it existed until the Froude number increased to about 0.8. If coarse sands are involved, larger slopes are required to effect the change from transition to the plane bed; the result is larger velocities and larger Froude numbers. Hence, in a flume containing fine sand, the plane-bed condition commonly exists after the transition and persists over a wide range of Froude numbers ( $0.3 \leq F \leq 0.8$ ). If the sand is coarse and the depth is shallow, however, transition may not terminate until the Froude number is so large that the subsequent bed form may be antidunes rather than plane bed. In natural streams, because of their greater depths, the change from transition to plane bed may occur at a much lower Froude number than in the flumes.

ANTIDUNES

Antidunes form as a series or train of inphase (coupled) symmetrical sand and water waves. (See figs. 11 and 12.) The height and length of these waves depend on the scale of the flow system and the characteristics of the fluid and the bed material. In

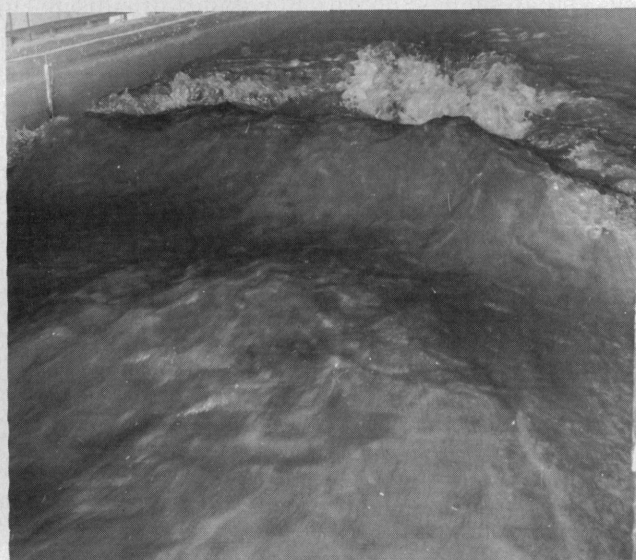


FIGURE 11.—Downstream view of antidune flow. Bed material is sand II; slope = 0.0059, depth = 0.56 foot, discharge = 21.2 cfs,  $C/\sqrt{g} = 14.6$ .

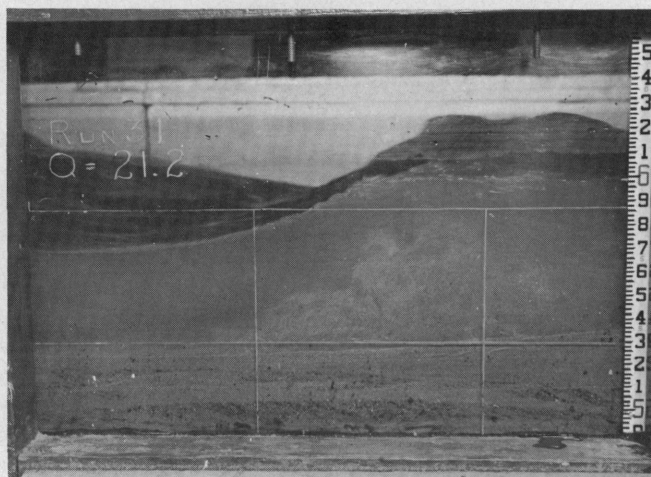


FIGURE 12.—Side view of the antidune flow shown in figure 11.

the 8-foot-wide flume, the height of the sand waves (from the bottom of the trough to the top of the crest) ranged from 0.03 foot to 0.5 foot, and the height of the water waves was 1.5–2 times the height of the sand waves. The length of the waves, from crest to crest or trough to trough, ranged from 5 to 10 feet. In natural streams, such as the Rio Grande or the Colorado River, much larger antidunes form. In these streams surface waves 2–3 feet high and 10–20 feet long have been observed.

Antidunes do not exist as a continuous train of waves that never change shape; rather, they form as trains of waves that gradually build up from a plane bed and a plane water surface. The waves may grow in height until they become unstable and break like the sea surf, or they may gradually subside. The former have been called breaking antidunes, or antidunes; and the latter, standing waves. As the antidunes form and increase in height, they may move upstream, downstream, or remain stationary. Their upstream movement led Gilbert (1914) to name them antidunes.

Resistance to flow due to antidunes depends on how often the antidunes form, the area of the reach that they occupy, and the violence and frequency of their breaking. If the antidunes do not break, resistance to flow is about the same as for a plane bed, and  $C/\sqrt{g}$  ranges from 14 to 23. The acceleration and deceleration of the flow through the nonbreaking antidunes (frequently called standing waves) causes resistance to flow to be slightly more than that for flow over a plane bed. If many antidunes break, resistance to flow can be very large because the breaking waves dissipate a considerable amount of energy. With breaking waves,  $C/\sqrt{g}$  may range from 10 to 20.

With antidune flow, the fact that the water and bed surfaces are in phase is a positive indication that the flow is rapid ( $F > 1$ ). With dunes, the fact that the water surface is out of phase with the bed surface is a positive indication that the flow is tranquil ( $F < 1$ ). In both instances the Froude number, which is based on the ratio of the mean velocity of the flow to the velocity of a gravity wave ( $C$ ), must take into account the wave length ( $L$ ). That is,  $C^2 = \frac{gL}{2\pi} \tanh \frac{2\pi D}{L}$  and cannot be approximated by  $C^2 = \sqrt{gD}$ , as is often done in open-channel flow, unless  $L/D \geq 10$ . Also, the mean velocity must be for the flow in the section of the stream where the antidunes are forming and not for the entire cross section of the stream.

Kennedy (1961) made a detailed study of antidune flow. His conclusions were:

1. The wave length of antidunes is given by  $L = 2\pi V^2/g$ .
2. Where a limited range of depth and velocity exists, antidunes will form only if an initial surface wave is introduced.
3. The Froude number ( $V/C$ ) for the occurrence of antidunes decreases as the depth of flow increases or as the size of the sand grains decreases.
4. Two-dimensional waves (those that occupy the full width of the flume) break when the ratio of wave height to wave length reaches a value of approximately 0.14. This value of 0.14 agrees with the theoretical value for deep-water waves.

From Kennedy's first conclusion it is obvious that the wave length is independent of depth of flow and, hence, the Froude number. However, Kennedy (1963) revised his first conclusion and stated instead that only the minimum length is given by  $2\pi V^2/g$  and that, for each bed material, there is a characteristic wave length dependent on velocity and depth.

#### CHUTES AND POOLS

At very steep slopes, alluvial-channel flow changes to what has been called chutes and pools. In the large, 8-foot-wide flume, this type of flow and bed configuration occurred only in runs using sands I and II. Chute-and-pool flow could not be attained when coarser sands were used because the steeper slope required could not be set up in the flume. This type of flow consisted of a long chute (10–30 ft) in which the flow accelerated rapidly, a hydraulic jump at the end of the chute, and then a long pool (10–30

ft) in which the flow was tranquil but was accelerating. (See figs. 13, 14, and 15.) The chutes and pools moved upstream at velocities of about 1–2 fpm (feet per minute). The elevation of the sand bed varied within wide limits, although at no time was the flume floor exposed. Resistance to flow was large, and  $C/\sqrt{g}$  ranged from 9 to 16. This type of flow was frequently accompanied by a decrease in the mean velocity of the flow in the flume even though there was an increase in stream power (fig. 16).

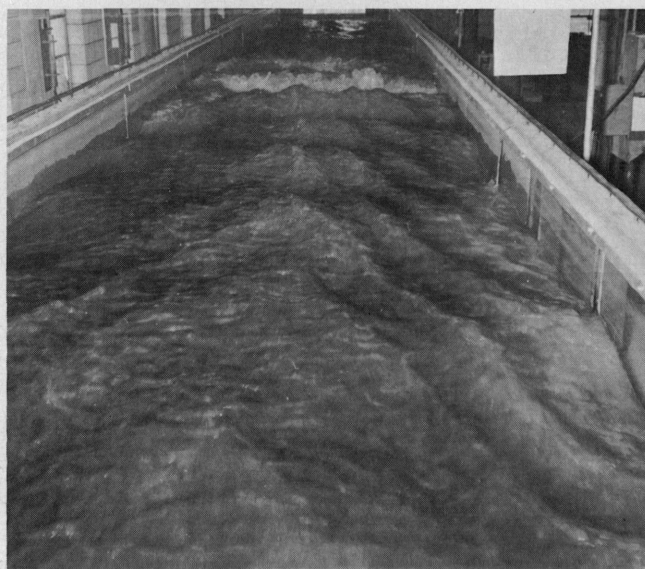


FIGURE 13.—Downstream view of chute-and-pool flow. Note the pool in the foreground and the breaking wave in the background, at the downstream end of the chute. Bed material is sand II; slope = 0.0095, depth = 0.45 foot, discharge = 15.4 cfs,  $C/\sqrt{g} = 11.5$ .



FIGURE 14.—Downstream view of chute (foreground) and breaking antidune shown in figure 13. Standing waves are terminating in the breaking antidune.

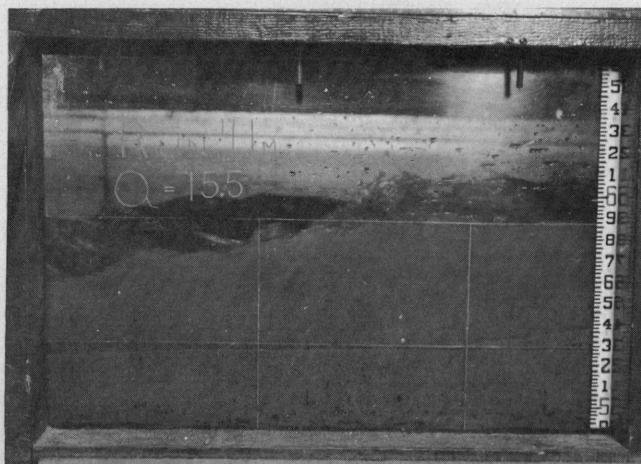


FIGURE 15.—Side view of the breaking antidune illustrated in figure 14. Note the large quantity of bed material in suspension.

REGIMES OF FLOW IN ALLUVIAL CHANNELS

The flow in alluvial channels is divided into two flow regimes with a transition zone between (Simons and Richardson, 1963). These two flow regimes are

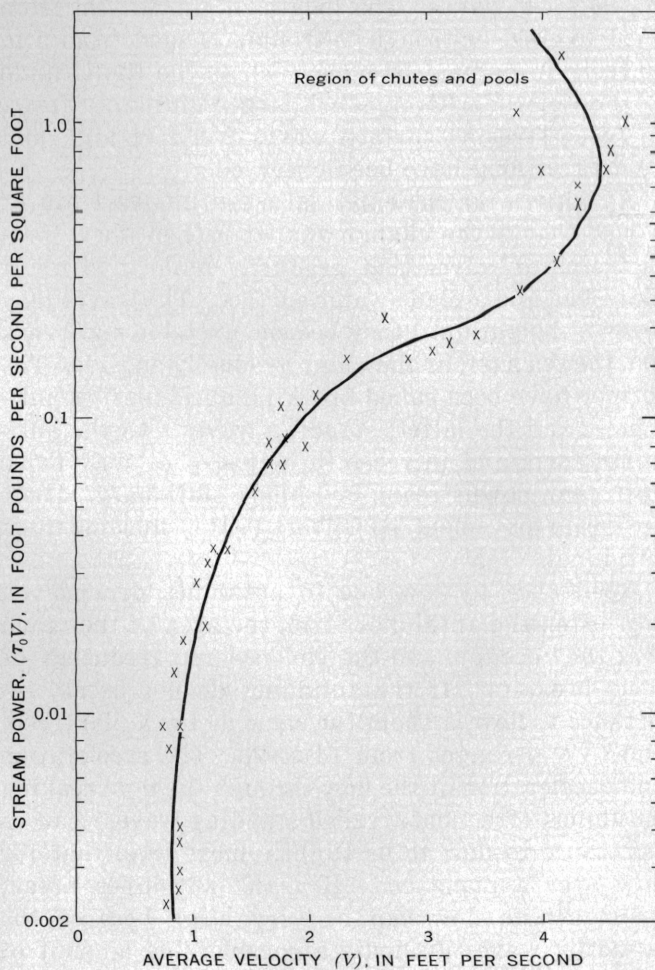


FIGURE 16.—Relation of average velocity to stream power for runs with sand I as the bed material.

characterized by similarities in the shape of the bed configuration, mode of sediment transport, process of energy dissipation, and phase relation between the bed and water surfaces. The two regimes and their associated bed configurations, discussed in the following sections, are listed as follows:

*Classification of bed forms into flow regimes*

Lower flow regime (smallest values of shear,  $\gamma DS$ , or stream power,  $V\gamma DS$ ):

1. Ripples
2. Dunes with ripples superposed
3. Dunes

Transition zone (bed roughness ranges from dunes to plane bed or antidunes).

Upper flow regime (largest values of shear,  $\gamma DS$ , or stream power,  $V\gamma DS$ ):

1. Plane bed
2. Antidunes
  - a. Standing waves
  - b. Breaking antidunes
3. Chutes and pools

#### LOWER FLOW REGIME

In the lower flow regime, resistance to flow is large and sediment transport is small. The bed form is either ripples or dunes or some combination of the two. The water-surface undulations are out of phase with the bed surface, and there is a relatively large separation zone downstream from the crest of each ripple or dune. Total resistance to flow is the result partly of grain roughness and dominantly roughness of form. The most common mode of bed-material transport is for the individual grains to move up the back of the ripple or dune and avalanche down its face. After coming to rest on the downstream face of the ripple or dune, the particles remain there until exposed by the downstream movement of the dunes; then the cycle of moving up the back of the dune, avalanching, and storage is repeated. Thus, most movement of the bed-material particles is in steps, of the order of magnitude of a ripple or dune length, separated by rest periods dependent on ripple or dune height and velocity. The velocity of the downstream movement of the ripples or dunes depends on their height and the velocity of the grains moving up their backs. In flume studies, the ripple bed is the configuration usually formed in the lower flow regime; in natural streams and rivers, dunes or dunes with ripples superposed are the dominant bed forms in the lower flow regime.

#### UPPER FLOW REGIME

In the upper flow regime, resistance to flow is small and sediment transport is large. The usual

bed forms are plane bed or antidunes. The water surface is in phase with the bed surface except when an antidune breaks, and normally the fluid does not separate from the boundary. A small separation zone may exist downstream from the crest of an antidune prior to breaking. Resistance to flow is the result of grain roughness with the grains moving, of wave formation and subsidence, and of energy dissipation when the antidunes break. The mode of sediment transport is for the individual grains to roll almost continuously downstream in sheets one or two grain diameters thick; when antidunes break, however, much bed material is briefly suspended, then movement stops temporarily and there is some storage of the particles in the bed.

#### TRANSITION

The bed configuration in the transition zone is erratic. It may range from that typical of the lower flow regime to that typical of the upper flow regime, depending mainly on antecedent conditions. If the bed configuration is dunes, the depth or slope can be increased to values more consistent with those of the upper flow regime without changing the bed form; or, conversely, if the bed is plane, depth and slope can be decreased to values more consistent with those of the lower flow regime without changing the bed form. Often in the transition from the lower to the upper flow regime, the dunes will decrease in amplitude and increase in length before the bed becomes plane (washed-out dunes). Resistance to flow and sediment transport also have the same variability as the bed configuration in the transition. It was the transition zone, which unfortunately covers a wide range of shear values, that Brooks (1958) was investigating when he concluded that a single-valued function does not exist between velocity or sediment transport and the shear stress on the bed.

In many instances when the flow conditions are such that the bed form is in the transition zone, the bed configuration will oscillate between dunes and plane bed. This phenomenon can be explained by the changes in resistance to flow and, consequently, the changes in depth and slope as the bed form changes. Resistance to flow is small for flow over a plane bed; so the shear stress on the bed decreases to a value that is incompatible with the shear stress for a plane bed but compatible with the shear stress for a dune bed, and the bed form changes to dunes. The increase in resistance to flow causes an increase in the shear stress on the bed so that the dunes wash out and the bed becomes plane, and the cycle continues.

## COMPARISON OF FLUME AND FIELD CONDITIONS

The preceding comments were based on observations of bed configurations and flow phenomena that occurred in the flume experiments and in natural rivers (field conditions) and are equally true for both situations. However, there are major differences between flume and field conditions. In the usual flumes only a limited range of depth and discharge can be investigated, but slope and velocity can be varied within a wide range. In the field, a larger range of depth and discharge is common, but slope of a particular channel reach is virtually constant. Consequently, the variation in shear stress ( $\gamma DS$ ) and stream power ( $V\gamma DS$ ) is principally the result of slope variation in flume studies and of depth variation in a particular natural stream. The walls of a flume are nonerodible, and, hence, the width is constant; but in most alluvial channels the width depends on flow and bank conditions. Larger Froude numbers ( $V/\sqrt{gD}$ ) can be achieved in flume studies than will occur in most natural alluvial channels because natural banks cannot withstand prolonged high-velocity flow without eroding. This erosion increases the cross-sectional area and this causes a reduction in the average velocity and the Froude number. Rarely does a Froude number, based on average velocity and depth, exceed unity for any extended time period in a natural stream with erodible banks. In the field, where the slope of the energy grade line is constant, the Froude number is also constant unless there is a change in the resistance to flow ( $F = \frac{C}{\sqrt{g}} \sqrt{S}$ ).

Flow is more nearly two dimensional in flumes than in natural streams. However, the main current meanders from side to side in a large flume, as it does in the field, and bars of small amplitude but large area develop in an alternating pattern adjacent to the walls of the flume. (It is on these bars that the bed forms shown in fig. 3 superpose themselves.) If very large width-depth ratios are maintained in the flume by keeping depth of flow shallow, these bars may grow to the water surface. Figure 17 shows the bars that formed in the 8-foot-wide flume when the width-depth ratio was about 22, the slope was 0.0020, the total discharge was 4.0 cfs, and the bed material had a median fall diameter of 0.19 mm.

In the field it is even more obvious that the flow meanders between the parallel banks of a straight channel, and the alternate bars which form opposite the apex of the meanders are easier to distinguish. As in a flume, if the depth is decreased the alternate

bars increase in amplitude until they are close to the water surface, or even exposed. (See fig. 18.) In fact, scour in the main current adjacent to a large bar may cause the water surface there to drop slightly so that the top of the bar is exposed. This has been observed in the Rio Grande (R. K. Fahnestock, oral commun., 1962) and in other natural channels. If the banks are not stable, erosion occurs where the high-velocity water impinges, and deposition occurs on the opposite bank. The ultimate development is a meandering stream if other factors such as slope, discharge, and size of bed material are compatible (Leopold and Maddock, 1953).

## VARIABLES

Resistance to flow in alluvial channels is complicated by the large number of variables. It is further complicated by the interdependency, either real or apparent, of the variables. In fact, some variables may be altered or even determined by the flow, and changes in flow conditions may change the role of a dependent variable into that of an independent one. It is difficult, especially in field studies, to differentiate between the independent and dependent variables.

The slope of the energy grade line of an alluvial stream illustrates the changing role of a variable and the difficulty of selecting the dependent variable. If a stream is in equilibrium with its environment, slope is an independent variable. In such a stream the average slope over a period of years has adjusted so that the flow is capable of transporting only the amount of sediment supplied at the upper end of the stream and by the tributaries. If for some reason a tributary or upstream reach supplied a larger or smaller quantity of sediment than the stream was capable of transporting, the slope would change and would be dependent on the amount of sediment supplied. Clearly, it is difficult to determine if a stream is in equilibrium. Lane (1955) and Leopold and Langbein (1962) pointed out that a stream reacts quickly to any change and that the slope of the stream, although it may never reach true equilibrium (geologically, it never does), will approach its final equilibrium value in a short time. If during a runoff event in a natural stream the water and sediment discharges do not change rapidly, the slope of the water surface and the energy gradient for a reach of the stream also will not change significantly. If the discharge does change rapidly (surge), so that there is an appreciable difference in discharge between the ends of a relatively short reach, the slope

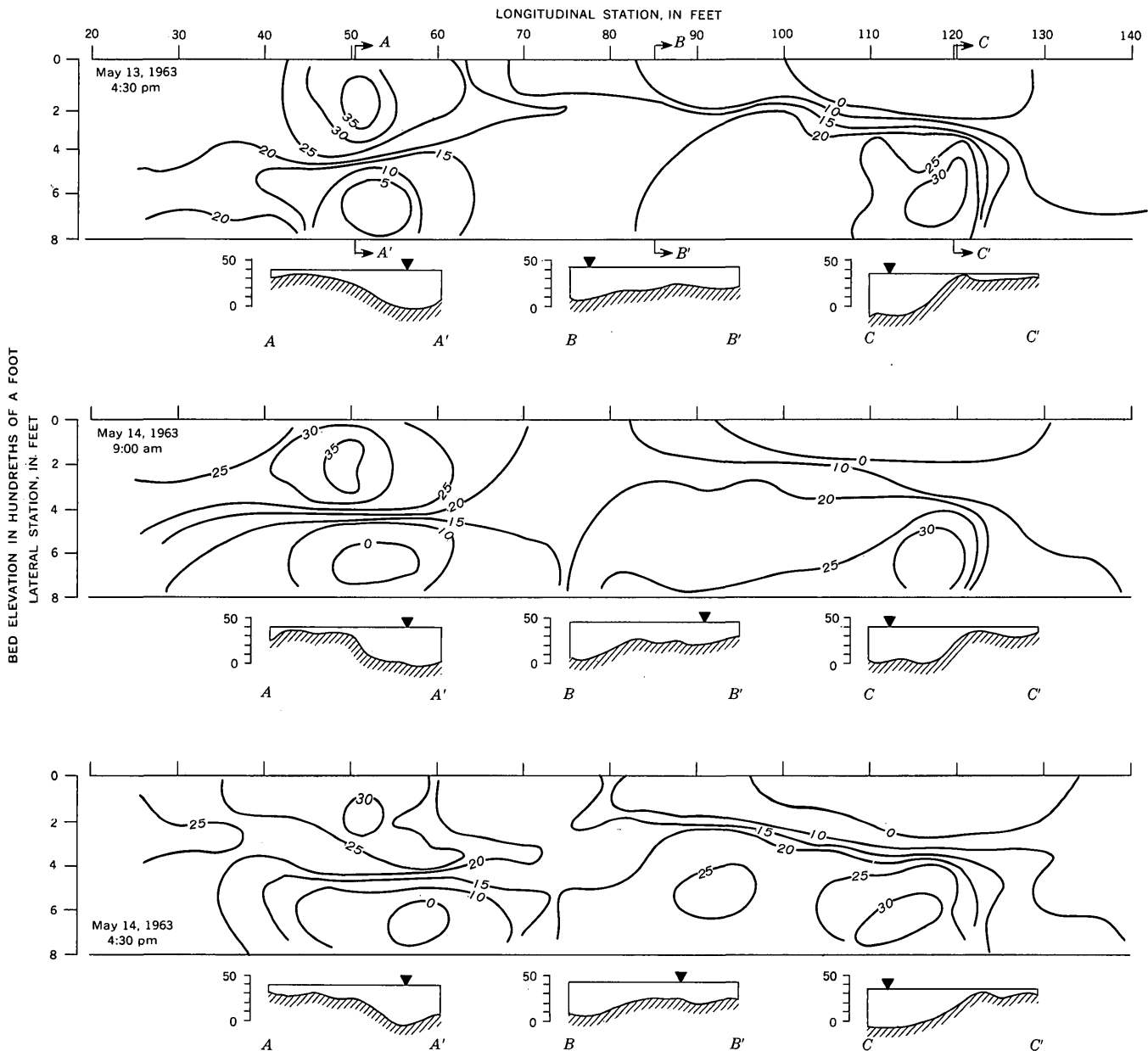


FIGURE 17.—Plan view of alternate bar development in the 8-foot-wide flume at a large width-depth ratio. Contour intervals 0.05 and 0.10 foot.

of the water surface and the energy gradient will vary.

We have given much thought to the significant variables in an alluvial channel, as have others (Rouse, 1959; Vanoni, 1946; Brooks, 1958; Einstein, 1950; and Bagnold, 1956, to mention a few), and have presented our ideas in several publications (Simons and others, 1961; Simons and Richardson, 1962a; and Richardson and others, 1962)—publications which have provoked stimulating discussions. In the following sections the variables affecting resistance to flow are listed and their dependency or independency is discussed. Also discussed are some conditions whereby a dependent variable may

become an independent one; which variables may be eliminated as a first approximation to simplify the problem; and, in general terms, the effect or importance of a variable on resistance to flow. The measure of resistance to flow used in these discussions (and in this report) will be either the Chezy discharge coefficient ( $C/\sqrt{g}$ ) or the Darcy-Weisbach resistance coefficient ( $f = 8/(C/\sqrt{g})^2$ ).

Under the restraint of equilibrium flow,

$$\frac{\partial C_T}{\partial t} = \frac{\partial C_T}{\partial x} = \frac{\partial V}{\partial t} = \frac{\partial V}{\partial x} = 0,$$

the variables that determine resistance to flow are:

$$\phi [V, D, S, \rho, \mu, g, d, \sigma, \rho_s, S_p, S_R, S_c, f_s] = 0, \quad (1)$$

where

- $C_T$  = concentration of bed-material discharge,  
 $V$  = velocity,  
 $D$  = depth,  
 $S$  = slope of the energy grade line,  
 $\rho$  = density of water-sediment mixture,  
 $\mu$  = apparent dynamic viscosity of the water-sediment mixture,  
 $g$  = gravitational constant,  
 $d$  = representative fall diameter of the bed material,  
 $\sigma$  = measure of the size distribution of the bed material,  
 $\rho_s$  = density of sediment,  
 $S_p$  = shape factor of the particles,  
 $S_R$  = shape factor of the reach of the stream,  
 $S_c$  = shape factor of the cross section of the stream, and  
 $f_s$  = seepage force in the bed of the stream.



FIGURE 18.—Large alternate bar in Marala Ravi Canal, Pakistan.

#### CONCENTRATION OF BED-MATERIAL DISCHARGE

The concentration of bed-material discharge ( $C_T$ ), which some investigators have suggested is a variable, has been left out of equation 1. Admittedly, the concentration of bed material affects the fluid properties by increasing the apparent viscosity and the density of the water-sediment mixture (Einstein, 1906; Bingham, 1922; Bagnold, 1956; and Elata and Ippen, 1961). The effect of the sediment on viscosity ( $\mu$ ) and density ( $\rho$ ) in any resistance to flow relation is accounted for by using their values for the water-sediment mixture instead of their values for pure water (Elata and Ippen, 1961; Simons, and others, 1963). Also, as Vanoni and Nomicos (1960), Vanoni and Brooks (1957), and Elata and Ippen (1961) demonstrated, the presence of sediment in the flow causes a change in the turbulence charac-

teristics and in the velocity distribution. However, Elata and Ippen found that the effects of the particles on the resistance to flow, by the change in turbulence and velocity distribution, can be accounted for by using the apparent viscosity of the mixture to evaluate  $R$  in the  $C/\sqrt{g}$  versus  $R$  diagram. Furthermore, both Vanoni and Brooks (1957) and Elata and Ippen (1961) found that the effect of the sediment concentration on resistance to flow was small. Elata and Ippen found about a 5-percent difference in  $C/\sqrt{g}$  between clear-water runs and runs in which as much as 27 percent by volume of the water-sediment mixture was neutrally buoyant granular material in suspension.

A more fundamental reason for not including the concentration of bed-material discharge in equation 1 is that, for equilibrium flow, it is a dependent variable. If, however, the flow is not in equilibrium—that is, the concentration of bed material entering the flume or reach of a stream is larger or smaller than the concentration leaving—the concentration is an independent variable and should be included as a variable. Needless to say, for nonequilibrium flow the concentration of bed-material discharge would have to be known, but determining the concentration is almost an impossibility.

#### FINE-SEDIMENT CONCENTRATION

Fine sediment is that part of the total sediment discharge that is not found in appreciable quantities in the bed material. If much fine sediment is in suspension, its effect on the viscosity of the water-sediment mixture should be taken into account (Simons and others, 1963). The effect of fine sediment on resistance to flow is a result of its effect on the apparent viscosity and the density of the water-sediment mixture; so the fine-sediment factor is not included in the list of variables, but it is included in the viscosity and density terms and is discussed in a later section.

The fundamental differences between fine sediment and bed material are in the availability of the sediment, the source of the sediment, and the capacity of the flow to carry the sediment. Fine sediment is not available in appreciable quantities from the bed, and it generally is not transported in concentrations that approach the fine-sediment transport capacity of the stream; bed material, however, is always available and is transported at the capacity of the stream. That is, fine-sediment concentration is dependent upon the availability of the sediment to the stream; and bed-material concentration is dependent upon the ability of the stream to transport a particular

size in a conglomeration of sizes and, hence, upon the variables of equation 1. Fine sediment that is in suspension at one discharge or in one stream may be bed material at another discharge or in another stream. Generally the fine sediment is uniformly distributed in the stream cross section.

#### DEPENDENT VARIABLE

The velocity ( $V$ ) was selected as the dependent variable in the present study, and the other variables were assumed to be independent. If the study had had other objectives, any one of the other variables could have been selected as the dependent variable, if the conditions of the experiment and the research objectives were properly treated. For example, the size distribution of the bed material could have been the dependent variable; then, the experiment would have been designed to determine the change in size distribution of the bed material with changes in  $V$ ,  $D$ ,  $S$ , and the other variables.

To study resistance to flow in an alluvial channel, either  $V$ ,  $D$ , or  $S$  may be selected as the dependent variable. In the present study velocity was selected because in a natural stream it is generally the unknown quantity and the other variables are measured quantities. In our experiments with given bed materials, the slope was varied and the resultant depth measured for different values of discharge. The velocity was then computed from the discharge and depth. Bed-material discharge and bed configuration were also measured, and either could be substituted in equation 1 for one of the other variables. Whether they should be included depends on the objectives of the study and the availability of data both in the laboratory and in the field. If the objective of the investigation is sediment transport or bed configuration under equilibrium conditions, then obviously the concentration or the bed configuration should replace one of the other variables. Including either one or both as independent variables in a resistance to flow study, however, might make the analysis more difficult by obscuring an essential relationship. Another reason for not including them is that they are often unknown quantities in natural streams, although by visual observation of the water surface or of the bed configuration and stratifications in the bed material after a runoff event, the bed configuration can usually be estimated. Later in this report, bed configuration is used as an independent variable in determining resistance to flow.

#### CHANGE OF VARIABLES

In equation 1, fluid viscosity, particle shape, and density can be eliminated if the fall velocity of the

bed material is included in the list of variables, giving equation 2:

$$V = \phi [D, S, \rho, g, d, \omega, S_R, S_c, f_s, \sigma]; \quad (2)$$

where fall velocity,  $\omega$ , depends on several variables,

$$\omega = \phi [d, \rho_s, \rho, g, S_p, \mu, \sigma]. \quad (3)$$

Viscosity can be eliminated because flow over an alluvial bed after the beginning of motion is fully developed, rough, turbulent flow. The laminar sub-layer, since it is very much smaller than the grain diameters, should not exist. Resistance to flow for this type of flow is independent of the flow Reynolds number ( $R$ ) and the viscosity. The changes in resistance to flow over sand beds which have been observed with changes in viscosity (Straub, 1954; Hubbell, 1956; Hubbell and Al-Shaikh Ali, 1961; Vanoni and Brooks, 1957) are the result of changes in the fall velocity of the bed material, which cause a corresponding change in the bed configuration (Hubbell and Ali, 1961; Simons and others, 1963; and Simons and Richardson, 1963).

The density and shape factors of the particles were included in equation 1 with the size of the bed material and the viscosity to account for the interaction of the fluid and the bed material. To have kept them in equation 2 with fall velocity would have resulted in a redundancy. Furthermore, it has frequently been demonstrated that fall velocity is more representative of the interaction of the fluid and the bed material than any other single variable.

The size and gradation of the bed material cannot be replaced by the fall velocity because, in addition to determining the fall velocity, they determine the grain roughness of the bed. Gradation parameters based on the physical sizes of the bed material and on fall velocities may be necessary. This is true because of the nonlinearity of the relation between the coefficient of particle drag versus  $\frac{\omega d \rho}{\mu}$ .

#### SHAPE FACTOR FOR THE REACH AND CROSS SECTION

The shape factor for the reach ( $S_R$ ) was included in equations 1 and 2 to focus attention on the energy losses resulting from the nonuniformity of the flow in a natural stream caused by the bends and the nonuniformity of the banks. Study of these losses in natural channels has long been neglected, although, as Ippen and Drinker (1962) stated, there is no net excess energy loss in bends with straight approach and exit reaches of sufficient length. In straight flumes with parallel walls, the shape factor of the reach is a constant and can be disregarded.

The shape factor for the cross section ( $S_c$ ) is a constant for the flume and can be disregarded. However, as is explained in the following paragraph, a shape factor for the cross section is needed when data from flumes of different widths are compared. Under these conditions, flow phenomena, bed configuration, and resistance to flow vary with the width of the flume.

Simons, Richardson, and Haushild (1963) noted that:

1. Ripples observed in the 8-foot-wide flume with sand III did not occur with the same sand in the 2-foot-wide flume.
2. Dune fronts in the 8-foot-wide flume seldom were continuous from one wall to the other, whereas those in the 2-foot-wide flume were continuous.
3. Antidunes in the 8-foot-wide flume could be three-dimensional and could occur in more than one row, whereas those in the 2-foot-wide flume were always two-dimensional and extended from wall to wall.

Hence, the resistance to flow was different in the two flumes for the same conditions (depth, slope, fall velocity, and so on). Vanoni and Brooks (1957) found a difference in results for their 10.5-inch-wide and 33.3-inch-wide flumes which could not be accounted for by a sidewall correction.

#### SEEPAGE FORCE

The seepage force ( $F_s$ ), which occurs whenever there is inflow or outflow through the bed material and banks of a channel in permeable alluvium, may have a significant affect on bed configuration and resistance to flow (Simons and Richardson, 1962b). The inflow or outflow through the interface between water and the bed and the bank depends on the difference in pressure across the interface and the permeability of the bed material. For flow in a flume with a rigid bed and walls, the pressure difference and the permeability of the bed material depend only on the variables in equation 1; thus, the seepage force is a dependent variable and can be eliminated from equation 2. For flow in a natural channel, however, the pressure difference will depend on the location of the water table in the alluvium and also on the variables in equation 1; now, seepage force is an independent variable insofar as resistance to flow is concerned.

If there is inflow, the seepage force acts to reduce the effective weight of the sand and, consequently, the stability of the bed material. If there is outflow, the seepage force acts in the direction of gravity and increases the effective weight of the sand and the

stability of the bed material. As a direct result of changing the effective weight, the seepage forces can influence the form of bed roughness and the resistance to flow for a given channel slope, channel shape, bed material, and discharge. For example, under shallow flow a bed material with median diameter of 0.5 mm will be molded into the following forms as shear stress is increased: Ripples, dunes, transition, standing sand and water waves, and antidunes. If this same material was subjected to a seepage force that reduced its effective weight to a value consistent with that of medium sand (median diameter,  $d = 0.3$  mm), the forms of bed roughness would be ripples, dunes, transition, plane bed, and antidunes for the same range of flow conditions. The reason for this difference in the forms of bed roughness is the reduction in effective weight and increased mobility of the bed material.

A rather common field condition is outflow from the channel during the rising stage; this process builds up bank storage and increases the stability of the bed and bank material. In the falling stage, the situation is reversed; inflow to the channel reduces the effective weight and stability of the bed and bank material and influences the form of bed roughness and the resistance to flow.

#### RESISTANCE COEFFICIENT

With the proposed simplifications and by grouping  $V$ ,  $D$ ,  $S$ ,  $\rho$ , and  $g$  into the Darcy-Weisbach resistance coefficient or into the Chezy discharge coefficient, equation 2 becomes:

$$\frac{8gRS}{V^2} = f = 8 \left( \frac{C}{g} \right)^2 = \phi [S, D, d, \omega, \sigma, g, \rho]; \quad (4)$$

or the bed configuration can be substituted for the dimensionless resistance coefficient to give:

$$\text{bed configuration} = \phi [S, D, d, \omega, \sigma, g, \rho]. \quad (4a)$$

The variables were not grouped into dimensionless parameters to present more clearly the essential role of each. Because of the interdependency of slope, depth, bed-material characteristics, bed configuration, and resistance to flow, it is difficult to isolate the effect of any one variable. For example, an increase in fall velocity may increase resistance to flow at one slope and decrease it at another slope. The relation of the variables in equations 4 and 4a to the bed configuration and resistance to flow are discussed in the following sections.

#### SLOPE

The effect of slope on bed configuration and resistance to flow for two depths and four bed materials is shown in figure 19. With constant depth and in-

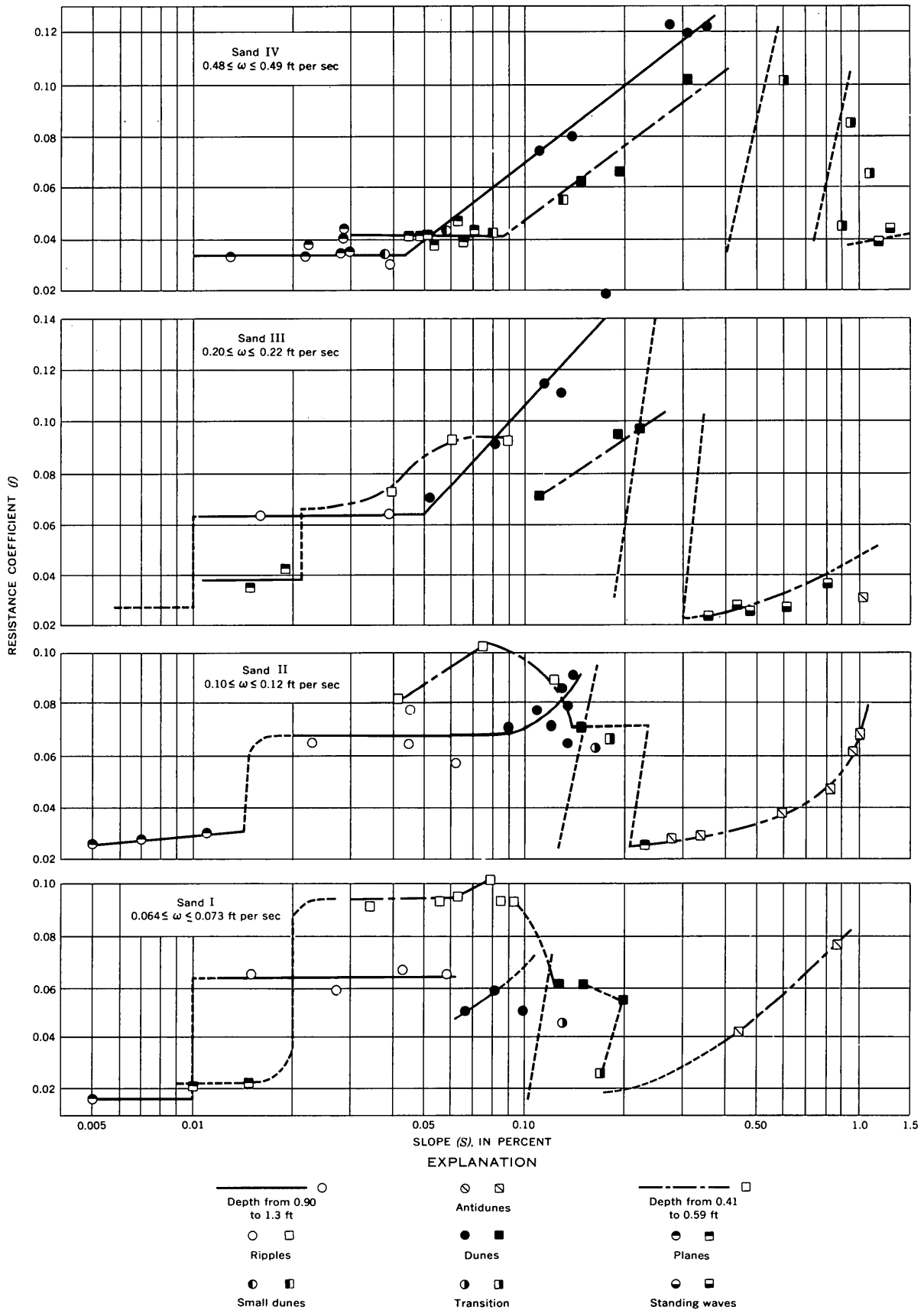


FIGURE 19.—Change in Darcy-Weisbach resistance coefficient ( $f$ ) with slope, depth, and fall velocity of the bed material in the 8-foot-wide flume.

creasing slope, the bed configurations for the bed material having a median fall velocity equal to or less than 0.22 fps (sand III) were (1) an artificial plane bed without sediment movement, (2) ripples, (3) ripples on dunes, (4) dunes, (5) transition (where the bed configuration was either dunes, plane bed, or a combination of them), (6) plane bed with sediment movement, and (7) antidunes. For the bed material having a median fall velocity of 0.48 fps (sand IV), the bed forms were the same but ripples did not form.

Resistance to flow is a function of slope even when the class of bed configurations given on page J4 does not change. For example:

1. With shallow depths and the ripple-bed configuration, resistance to flow increased with an increase in slope; at greater depths, resistance to flow did not change. At greater depths, ripples gave way to dunes; but with an increase in slope at the shallow depths, dunes did not form. The shallow depth appeared to inhibit the formation of dunes.
2. With the dune-bed configuration, an increase in slope increased resistance to flow for bed material having fall velocities greater than 0.20 fps. For those bed materials having fall velocities less than 0.20 fps, an increase in slope decreased resistance to flow at shallow depths and slightly increased resistance to flow at greater depths.
3. The slope (where the transition from flow in the lower flow regime to the upper flow regime occurred) depended on the fall velocity of the bed material and the depth of flow. Constant depth required an increase in slope with an increase in fall velocity for the occurrence of the transition. With fall velocity constant, an increase in slope and a decrease in depth were necessary for the occurrence of the transition.
4. With antidunes, resistances to flow increased with increasing slope; the magnitude of the increase of resistance to flow with an increase in slope depended on the fall velocity of the bed material. The smaller the fall velocity, the larger the increase in resistance to flow with an increase in slope.

#### DEPTH

The effect of depth on bed form and resistance to flow is not well defined because only a limited range in depths have been studied. However, just as changes in slope can change the bed configuration when depth and size of bed material are constant,

so will changes in depth change the bed configuration when slope and bed material are constant. With a constant slope and bed material, an increase in depth can change a plane bed without movement to ripples, and a ripple-bed configuration to dunes, as is illustrated in figure 19. Although not clearly shown in figure 19, flume studies (Simons and Richardson, 1962b) and field studies (Colby, 1960; Dawdy, 1961; and Culbertson and Dawdy, 1964) have demonstrated that an increase in depth, without varying slope and bed material, may cause a dune bed to change to a plane bed or antidunes, and that a decrease in depth may cause a plane bed or antidunes to change to a dune-bed configuration. Figure 20 shows a typical break in a depth-discharge relation caused by a change in bed form from dunes to plane bed or from plane bed to dunes (Beckman and Furness, 1962).

Limiting the variables to discharge and depth, resistance to flow will also vary with depth even when the bed configurations given on page J4 do not change. When the bed configuration is plane bed, either with or without sediment movement, there is a decrease in resistance to flow with an increase in depth—that is, a relative roughness effect. When the bed configuration is ripples, because their form is independent of depth, there is also a relative roughness effect—resistance to flow decreases with an increase in depth, as shown in figures 6 and 19. When the bed configuration is dune bed, although dunes increase in size when depth is increased, resistance to flow increases with an increase in depth only for sands coarser than 0.3 mm; for sands finer than 0.3 mm, resistance to flow decreases with an increase in depth. This effect is the result of a decrease in angularity of the dunes as they increase in size. Field studies indicate that at large depths, resistance to flow may decrease with an increase in depth even when the bed material is composed of sands coarser than 0.3 mm. This is true even though the size of the dunes continues to increase with an increase in depth. The anomalism may be explained by the facts that (1) the long dunes with mobile grain roughness on their backs compensate for the form effects of the separation zones downstream from the crests, and (2) at large depths the dunes, although large, may not cause appreciable nonuniformity of the flow. In the flume studies, dunes of the coarser sands created much acceleration and deceleration of the flow. Studies are needed to determine the conditions where resistance to flow for flow over a dune bed ceases to increase with an increase in depth.

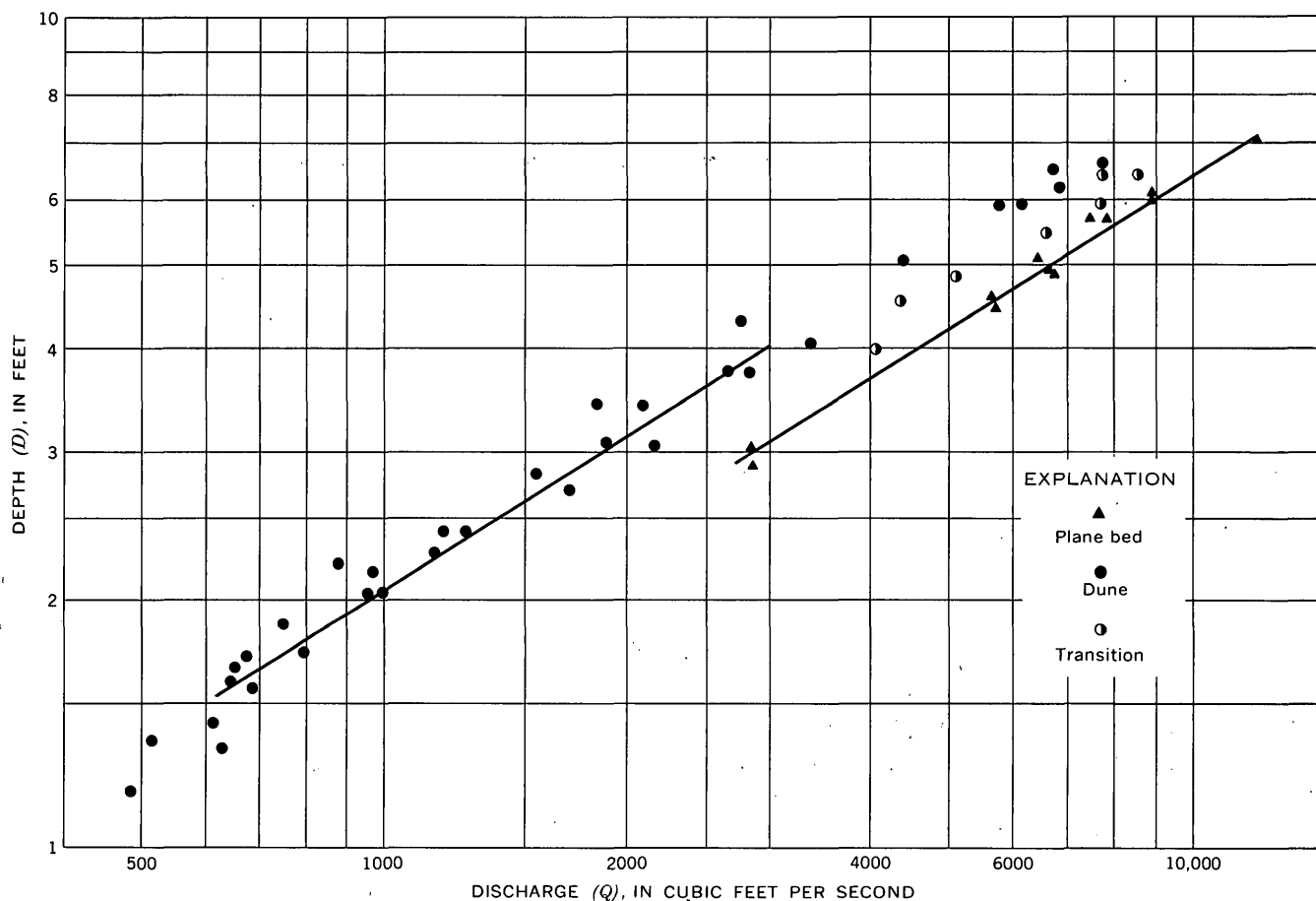


FIGURE 20.—Relation of depth to discharge for Elkhorn River near Waterloo, Nebr.

When the bed configuration is antidunes, resistance to flow increases with an increase in depth to some maximum value, then decreases as depth is increased further. This increase or decrease in flow resistance is directly related to changes in length, amplitude, and activity of the antidunes as depth is increased.

#### SIZE OF BED MATERIAL

The effects of the physical size of the bed material on resistance to flow are (1) its influence on the fall velocity, which is a measure of the interaction of the fluid and the particle in the formation of the bed configurations, (2) its effect as grain roughness, and (3) its effect on the turbulent structure and the velocity field of the flow.

The physical size of the bed material, as measured by the fall diameter (Colby and Christensen, 1956) or by sieve diameter, is a primary factor in determining fall velocity, although only in relation to the other variables in equation 3. Use of the fall diameter instead of the sieve diameter is advantageous because the shape factor and density of the particle can be eliminated as variables. That is, if only the fall diameter is known, the fall velocity of the par-

ticle in any fluid at any temperature can be computed; whereas, to make the same computation when the sieve diameter is known, knowledge of the shape factor and density of the particle are also required.

The physical size of the bed material is the chief factor in determining the friction factor for the plane-bed condition and for antidunes when they are not actively breaking. The additional dissipation of energy when antidunes are present is caused by the formation and breaking of the waves, which increases with an increase in energy input or a decrease in the fall velocity of the bed material.

The physical size of the bed material for a dune-bed configuration also has an effect on resistance to flow. The flow of fluid over the back of dunes is affected by grain roughness, although the dissipation of energy by the form roughness is the major factor. The form of the dunes is related to the fall velocity of the bed material.

#### FALL VELOCITY

Fall velocity is the primary variable that determines the interaction between the bed material and the fluid. For a given depth and slope, it determines the bed form that will occur, the actual dimensions

TABLE 1.—Comparison of the various characteristics of ripples and dunes with fall velocity of the bed material

No.	Sand		Ripples				Dunes			
	$d_{50}$ (mm)	Fall Velocity (fps)	Depth (ft)	$C/\sqrt{g}$	$L$ (ft)	$h$ (ft)	Depth (ft)	$C/\sqrt{g}$	$L$ (ft)	$h$ (ft)
I.....	0.19	0.064-.073	1.01	13.1	0.63	0.04	0.91	12.0	8.4	0.30
II.....	0.27, 0.28	.10 -.12	.96	11.1	.95	.04	.93	10.6	7.6	.30
III.....	0.45, 0.47	.20 -.22	.81	11.2	1.13	.10	.81	9.6	5.9	.30
IV.....	0.93	.48 -.49	---	---	---	---	1.02	10.8	4.7	.21

of the bed form (table 1), and, except for the contribution of the grain roughness, the resistance to flow.

The significance of fall velocity of the bed material on the spacing or length of dunes for various sizes of bed material at virtually constant depth is shown in figure 21. The dunes are not only shorter in length but are also much more angular when the fall velocity of the bed material is relatively large. For example, with sand IV (fall velocity  $\approx$  0.48 fps) the average length of dunes was 6.5 feet as compared to 11.6 feet for sand I (fall velocity  $\approx$  0.068 fps).

The differences in resistance to flow for the four sands in figure 19 are primarily the result of differences in fall velocity. The differences in resistance to flow when the bed form is plane bed, however, are caused by the differences in grain roughness for the different diameters of bed material. Nevertheless, the magnitude of depth and slope at the beginning of motion (when a plane bed without motion changes to ripples or dunes) and that when a dune bed changes to a plane bed with motion or antidunes depends primarily on the fall velocity. An increase in fall velocity requires an increase in the product of depth times slope (that is, shear stress) for the change from static plane bed to ripples or dunes, or the change from dunes to plane bed and antidunes.

Fall velocity is the critical factor in determining (1) whether ripples or dunes will form after the beginning of motion, (2) the shear stress at the beginning of motion when ripples or dunes begin to form from a plane bed, and (3) the shear stress at which ripples change to dunes. Ripples will not form in material having a fall diameter larger than 0.6 mm or a fall velocity higher than about 0.22 fps; there is some evidence, however, that the size of the bed material is a factor in determining whether ripples form. The magnitude of the shear stress required for the formation of ripples increases with an increase in fall velocity.

When the bed form is dunes, the slower the median fall velocity of the bed material is, the longer and less angular the dunes will be and, also, the smaller

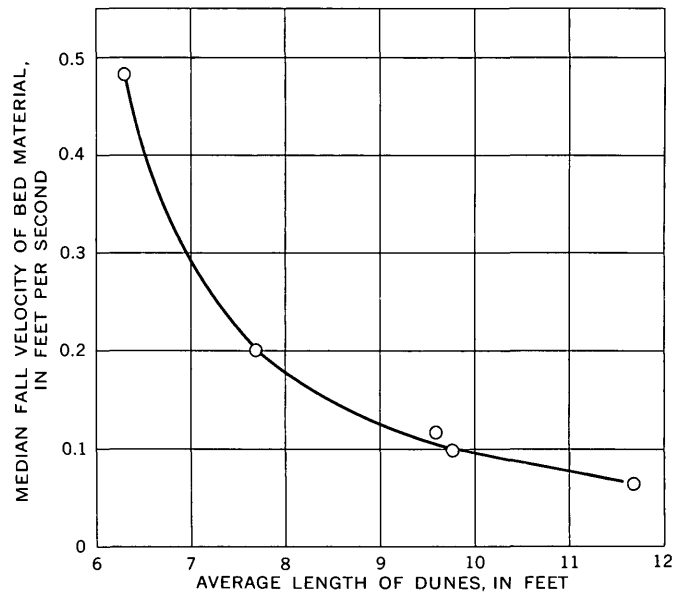


FIGURE 21.—Approximate relation of length of dunes to a median fall velocity of the bed material, at constant depth.

the range in shear stress or stream power will be within which a dune bed occurs.

For bed material having a median fall velocity equal to or greater than 0.2 fps, the range of stream power within which dunes occur is large and that within which a plane bed occurs is small. In fact, whether or not a plane bed does occur between dunes and standing waves is intimately related to fall velocity and depth. If the depth is shallow and the fall velocity of the bed material is fairly high, the bed configuration may change from transition to standing waves without the development of a plane bed.

The magnitude of the shear required for the formation of antidunes and the amount of antidune activity (formation and breaking of the antidunes) that will result from a given shear depends on the fall velocity. With a decrease in fall velocity there is a corresponding decrease in the magnitude of the shear required for the formation of the antidunes and for an increase in antidune activity. The in-

crease in antidune activity with a decrease in fall velocity causes an increase in resistance to flow.

Special flume studies verified that the changes in bed form and resistance to flow are primarily the result of changes in the fall velocity. These special studies were:

1. The fall velocity of a given bed material was varied by changing the viscosity of the water-sediment mixture. Viscosity was varied by changing either the water temperature or the concentration of fine sediment in the water-sediment mixture. A change in fall velocity caused the bed configuration and resistance to flow to change (Hubbell and Al-Shaikh Ali, 1961; Simons and others, 1963). A decrease in fall velocity resulting from an increase in fluid viscosity caused resistance to flow to decrease for a dune bed and to increase for the antidune bed. (See figs. 22 and 23.) Thus, by

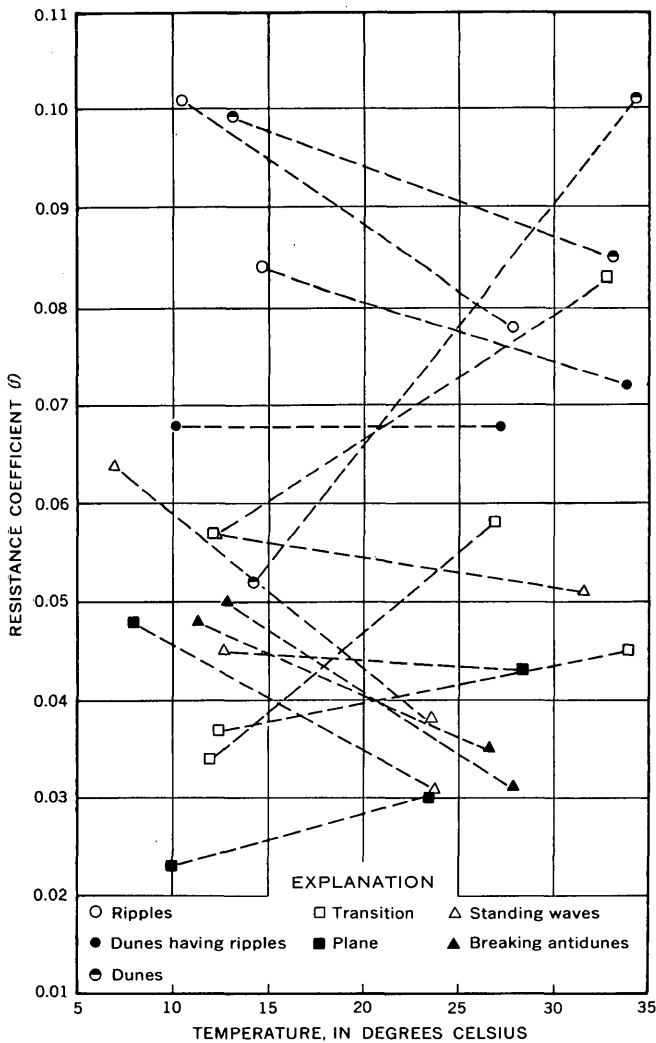


FIGURE 22.—Change in resistance to flow with temperature. Connected points represent paired runs during which temperature was the only independent variable (Hubbell and Al-Shaikh Ali, 1961).

decreasing fall velocity, a dune bed could be changed to a plane bed or a plane bed could be changed to antidunes.

2. The density of sand  $V$  was 1.87, the median fall diameter was 0.36 mm, and the median sieve diameter was 0.68 mm. (See fig. 2.) The bed configurations and the magnitude of the shear stress for the various bed configurations and for a change in bed configurations corresponded to those for a bed material with the same fall velocity but not for material with the same sieve diameter. In fact, ripples formed with this bed material, which is expected for a 0.36-mm sand but not for a 0.68-mm sand.

In addition to the flume experiments, observations of natural streams have shown that the bed con-

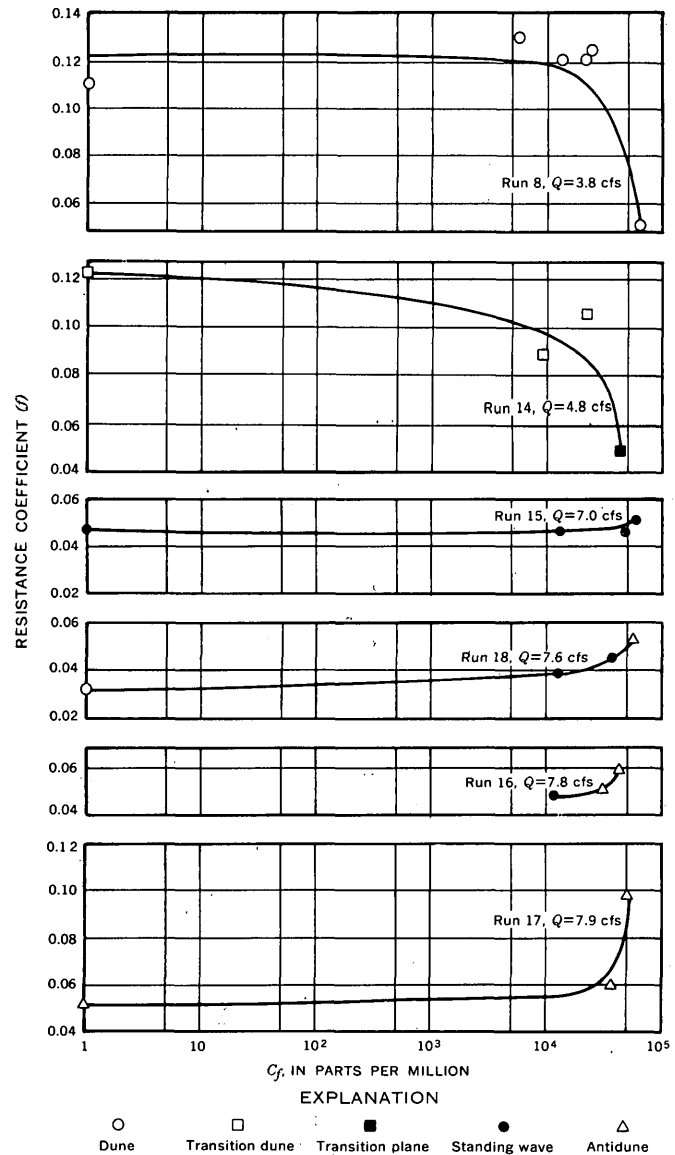


FIGURE 23.—Variation in resistance to flow ( $f$ ) with concentration of fine sediment ( $C_f$ ). Each run number represents a sequence in which concentration of fine sediment was the only independent variable.

figuration and resistance to flow will change with changes in fall velocity when the discharge and bed material are constant (Hubbell and others, 1956). For example, the Loup River near Dunning, Nebr., has bed roughness in the form of dunes in the summer when the stream fluid is warm and less viscous but has a nearly plane bed during the cold winter months. Similarly, two sets of data collected by R. K. Fahnestock (written commun., 1962) on a stable reach of the Rio Grande at similar discharges show that when the water was cold, the bed of the stream was plane, the resistance to flow was small, the depth was relatively shallow, and the velocity was large; but when the water was warm, the bed roughness was dunes, the resistance to flow was large, the depth was deeper, and the velocity was smaller. (See table 2.)

TABLE 2.—Data from a stable reach of the Rio Grande at similar discharges but different temperatures

Temperature (°F)	Velocity (fps)	Depth (ft)	Slope	Bed material (d <sub>50</sub> )	Bed roughness	C/√g
50°	4.25	2.45	0.00049	0.24	Plane	21.7
80°	2.53	3.66	.00053	.24	Dunes	10.2

APPARENT VISCOSITY AND DENSITY

The effect of the various factors given in equation 3 on fall velocity are well known. However, the effects of fine sediment in suspension on fluid viscosity and fall velocity are less well known (Simons and others, 1963). Figure 24 shows the effect of fine

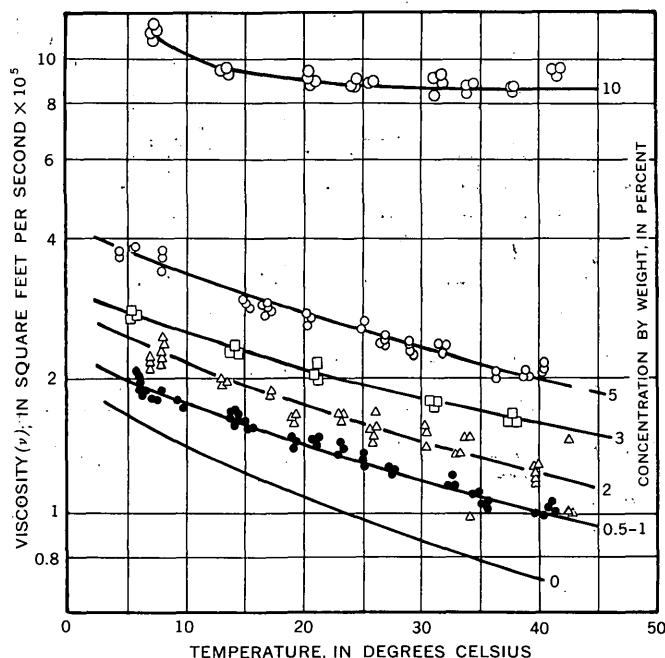


FIGURE 24.—Apparent kinematic viscosity of water-bentonite dispersions.

sediment (bentonite) on the apparent kinematic viscosity of the mixture. The magnitude of the effect of fine sediment on viscosity is large and depends on the chemical makeup of the fine sediment.

In addition to changing the viscosity, fine sediment suspended in water increases the mass density (ρ) and, consequently, the specific weight (γ) of the mixture. The specific weight (γ) of a sediment-water mixture can be computed from the relation, (Simons and others, 1963)

$$\gamma = \frac{\gamma_w \gamma_s}{\gamma_s - C_s(\gamma_s - \gamma_w)}, \tag{5}$$

where

- γ<sub>w</sub> = specific weight of the water, about 62.4 lb per cu ft (pounds per cubic foot);
- γ<sub>s</sub> = specific weight of the sediment, about 164.5 lb per cu ft; and
- C<sub>s</sub> = concentration (in percent by weight) of the suspended sediment.

A sediment-water mixture, where C<sub>s</sub> = 10 percent, has a specific weight (γ) of about 66.6 lb per cu ft, and any change in γ affects the boundary shear stress and the stream power.

Changes in the fall velocity of a particle caused by changes in the viscosity and the fluid density are evident in figure 25. For comparative purposes, the

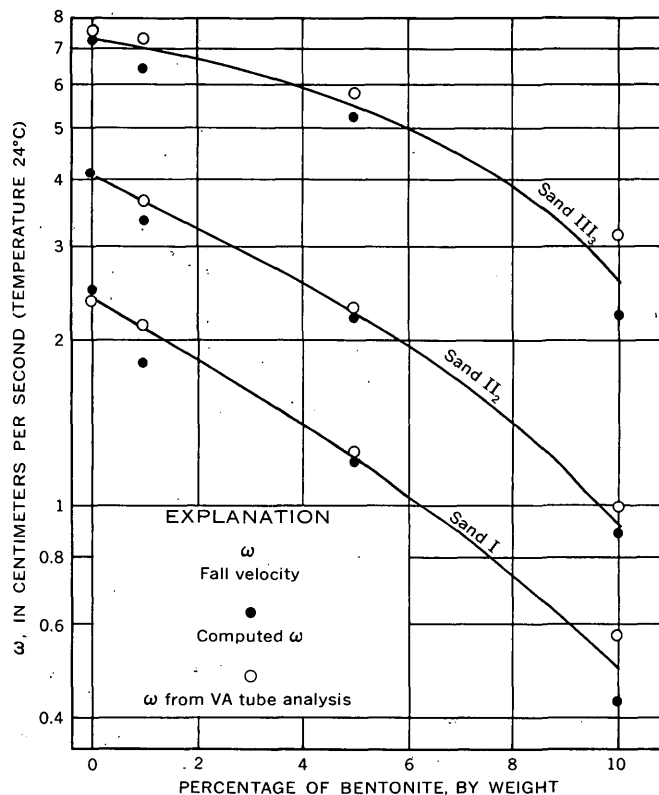


FIGURE 25.—Variation of fall velocity with percent bentonite in water.

effect of temperature on fall velocity is given in figure 26. The details of the determination of fall velocity by computation and by visual accumulation (VA) tube analysis are given in the report of Simons and others (1963).

GRADATION OF BED MATERIAL

The effect of gradation of the bed material on flow in alluvial channels was investigated by Daranandana (1962) under the supervision of the authors and the sponsorship of the U.S. Geological Survey. His study was conducted in the 2-foot by 60-foot flume using two quartz sands with the same  $d_{50}$

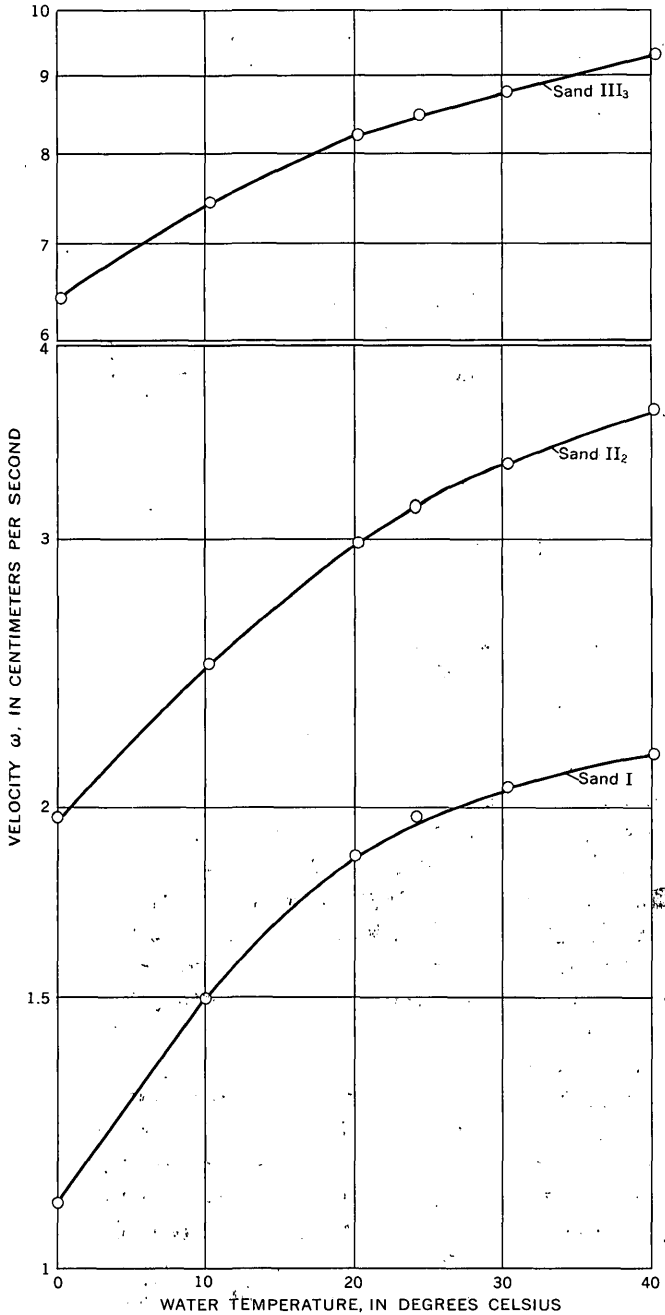


FIGURE 26.—Variation of fall velocity with temperature.

(sands VI in fig. 2;  $d_{50} = 0.33$  mm). Sand VI<sub>1</sub> had a uniform gradation coefficient ( $\sigma$ ) of 1.27, and sand VI<sub>2</sub> was graded with  $\sigma = 2.07$ , where

$$\sigma = \frac{1}{2} \left[ \frac{d_{50}}{d_{16}} + \frac{d_{84}}{d_{50}} \right] \quad (6)$$

In this study, depth and water temperature were kept constant, and the change in bed configuration, resistance to flow, and sediment transport were observed and measured for various slopes and discharges of the water-sediment mixture.

The effect of the gradation of the bed material on bed form and resistance to flow is shown in figure 27. The resistance to flow for flow over a plane bed with-

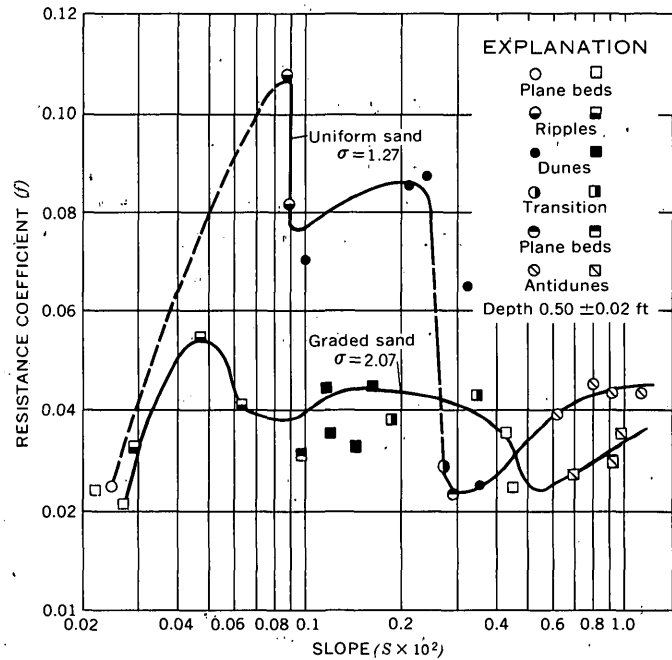


FIGURE 27.—Variation of resistance to flow with slope as a function of the size distribution of the bed material.

out motion was slightly larger for the uniform sand, whereas that on a plane bed with motion was nearly the same for the two sands. Resistance to flow was much larger for the uniform sand on beds having ripples, dunes, or antidunes. The transition from a dune bed to plane bed occurred over a narrower range of shear values for the uniform sand than for the graded sand.

Visual observation of the bed configuration provided the reason why resistance to flow was different for the two sands, but it did not show why the bed configurations were different. In the studies using the graded bed material, however, the continual sorting and remixing which took place suggested that the representative fall velocity and gradation also varied. In essence, then, the characteristics of the bed material were continually changing.

For flow over a plane bed without movement, the finer particles in the graded sand filled the voids, so that the boundary was smoother than the plane bed formed in graded sand. On the plane bed with movement, however, the effect of sediment on the turbulent structure of the flow probably had a counter-influence on resistance to flow that compensated for any filling of the large voids by fine sand, and resistance to flow was similar for the two sands.

The average height and length of ripples in runs using uniform sand were larger than those in runs using graded sand, which increased resistance to flow. Ripples formed of uniform sand averaged 0.032 foot in height and 0.86 foot in length; those formed of graded sand averaged 0.025 foot in height and 0.46 foot in length.

Dunes of the uniform sands had ripples superposed on them, whereas those of the graded sand did not. Although the dunes of the uniform sand were smaller, the effect of the ripples on their back increased resistance to flow. Dune length and height were 3.33 feet and 0.095 foot, respectively, in the uniform sand and 4.00 feet and 0.14 foot in the graded sand. Also, the longer dunes, crest to crest, decreased resistance to flow for the graded sand.

The greater resistance to flow in runs using the uniform sands cannot be explained by the differences in antidune length and amplitude. The average antidune lengths and heights were greater for the uniform sands (5.05 ft and 0.15 ft, respectively) than for the graded sand (4.3 ft and 0.085 ft, respectively). These changes do not adequately explain the large differences in resistance to flow.

Daranandana's investigation proved that there is a gradation effect on resistance to flow and emphasized that natural river sands should be used in flume experiments if the results are to be extrapolated to the field. The importance of using natural river sands in flume experiments is further emphasized by Blench's (1952) conclusion that alluvial bed material is always adjusted by the flow so that its distribution conforms to a fairly definite normal distribution law.

#### PREDICTION OF FORM OF BED ROUGHNESS

A completely satisfactory method for predicting form of bed roughness has not been developed. Various methods of predicting form roughness (Albertson and others, 1958; Simons and Richardson, 1963; and Garde, 1959) have been proposed, but none have been suitable for both laboratory and field conditions. A simple relation (fig. 28) was developed by Simons and Richardson (1964) to relate stream power,

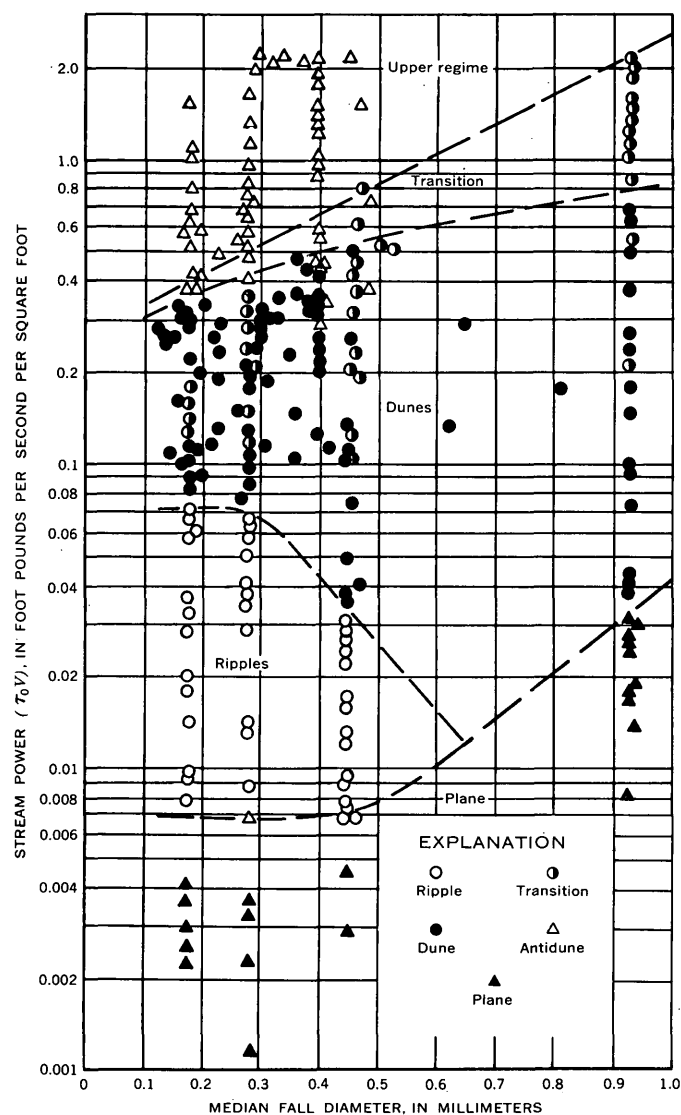


FIGURE 28.—Relation of form of bed roughness to stream power and median fall diameter of the bed material.

median fall velocity of bed material, and form roughness. This relation gives an indication of the form of bed roughness one can anticipate if the depth, slope, velocity, and fall diameter of bed material are known. Flume data were utilized to establish the boundaries separating plane bed and ripples, ripples and dunes for all sizes of bed material, and dunes and transition for the 0.93-mm bed material. The lines dividing dunes and transition and dividing transition and upper regime are based on the following field data: (1) Elkhorn River, near Waterloo, Nebr. (Beckman and Furness, 1962), (2) Rio Grande 20 miles above El Paso, Tex. (see table 2), (3) Middle Loup River at Dunning, Nebr. (Hubbell and Matejka, 1959), (4) Rio Grande at Cochiti, near Bernalillo, and at Angostura heading, N. Mex. (Culbertson and Dawdy, 1964), (5) Punjab canal data

(Simons, 1957), and (6) Harza Engineering Co., International (1963) canal data. If just the flume data were used, the dividing line between dunes and transition would occur at about 10 percent less stream power than the field data indicates. Figure 28 shows that the range of stream power in which dunes occur becomes smaller with decreasing fall diameter of bed material. Thus, a small change in

stream power can change the bed form and resistance to flow when the median fall diameter of the bed material is small.

Using additional alluvial canal and river data, Tipton and Kalmbach, Inc. (written commun., 1963) further validated the stream-power relation for predicting form of bed roughness. They also suggested using figure 29 to illustrate the large number of

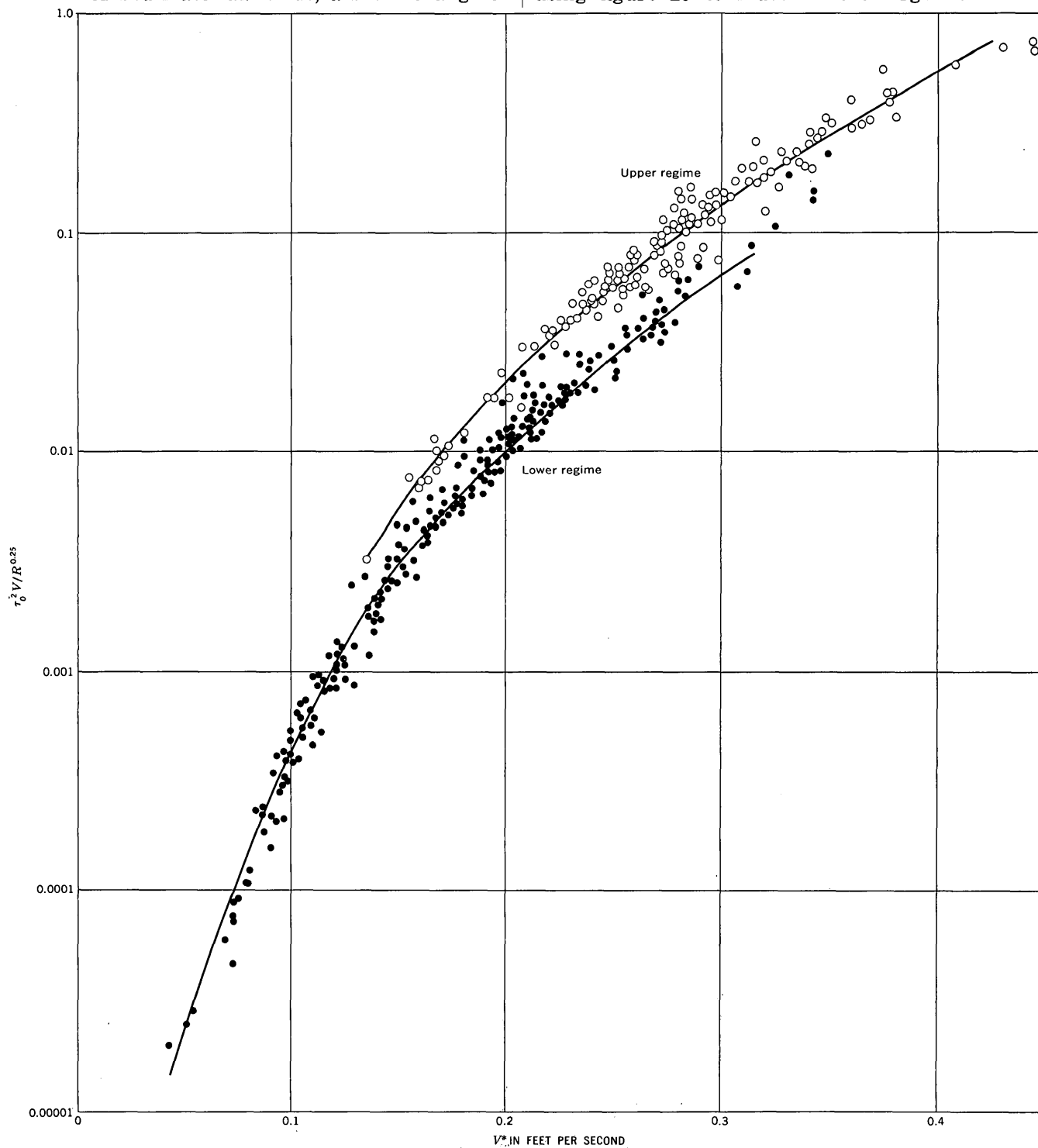


FIGURE 29.—Relation of  $\tau_0^2 V / R^{0.25}$ ,  $V^*$ , and regime of flow for laboratory and field conditions. The data are from the Rio Grande (Culbertson and Dawdy, 1964), Elkhorn River (Beckman and Furness, 1962), Pakistan canals (Harza Engineering Co., Internat., 1963), and the 8-foot-wide flume.

upper regime flows that have been observed in large irrigation canals that have fine-sand beds.

Knowledge of what the bed form is or may be under given fluid, flow, and sediment conditions is important in designing channels that will neither erode nor fill up with sediment (stable channel), determining the stage-discharge relation for natural channels, and estimating the water and sediment discharge of a stream. For example, in stable-channel, design, if dunes with a large resistance to flow are anticipated, then a small average velocity, fairly large depth, and steep slope must exist for a given discharge. With fine bed material, a small change in stream power can change the bed form, and the channel may not function as designed. The bed form may not be dunes as anticipated but may be transitional or plane and result in small resistance to flow, high average velocity, relatively shallow depth, and an unstable channel having high transport capacity.

The Marala-Ravi Canal in Pakistan is an example. This canal has bed material with a median diameter of approximately 0.16 mm and was designed to carry 21,000 cfs. When the canal was put in operation, the slope steepened from 1:10,000 to 1:8,000 because of excess sediment from the river. This resulted in a combination of slope, depth, and velocity which gave a stream power of 0.71. A stream power of this magnitude was sufficient to cause development of a plane bed and cause channel instability, large changes in channel geometry, and a bed-material discharge of 132 tons per day per foot of width.

VELOCITY DISTRIBUTION

The velocity distribution in a wide alluvial channel is as complex as the bed forms that occur. With dunes and antidunes, the velocity distribution is constantly changing with time and space. The variation of the velocity distribution in the vertical with these bed forms is so great that a detailed statistical study would be required to describe them. This would require many more profiles, covering a longer period of time over a larger area of the flume, than are available. Typical velocity profiles for ripples, dunes, and plane-bed configurations are given in figure 30.

With both plane bed and ripples, the velocity profiles are constant with time and space outside a zone near the boundary roughness. (See fig. 30.) In the following section the velocity distribution for the plane bed with sediment moving is analyzed. From this analysis an equation for the mean velocity and the roughness coefficient for the plane bed with sediment movement is evolved.

PLANE BED WITH SEDIMENT MOVEMENT

The velocity distribution in the vertical for two-dimensional flow over a plane bed with sediment movement can be described by

$$v_y = A_* \ln y + B_*, \tag{7}$$

where  $A_*$  and  $B_*$  are the slope and the intercept of the  $v_y$  versus  $\ln y$  plot. The values of  $A_*$  and  $B_*$  for the various runs are given in table 3 along with other pertinent information for the run.

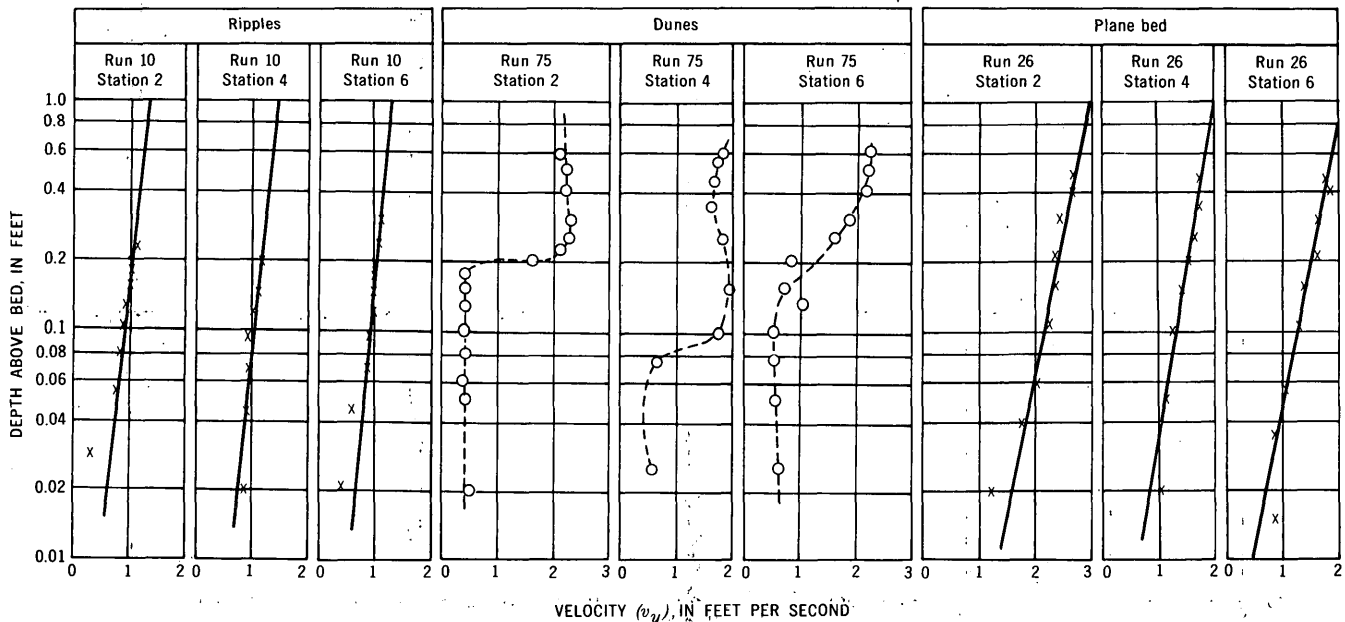


FIGURE 30.—Typical vertical-velocity-distribution curves for an alluvial channel. Data are from the runs in the 8-foot-wide flume with sand III as the bed material. Station refers to the normal distance from the flume wall.

TABLE 3.—Slope ( $A_*$ ) and intercept ( $B_*$ ) of the velocity profiles for a plane bed with sediment movement

Sand	$d_{60}$	Run	$V_*$	$A_*$	$B_*$	$\kappa$	$C_T$
I.....	0.19	10	0.167	0.561	4.22	0.30	2480
		15	.169	.595	4.50	.....	2000
		16	.190	.610	4.92	.....	2750
II.....	.27 .28	46	.199	.608	4.74	.30	1670
		22	.172	.548	3.91	.29	1540
		25	.215	.589	4.89	.34	2710
		28	.201	.545	4.69	.34	2760
III.....	45 47	26	.200	.700	5.03	.27	4580
		60	.261	1.005	6.05	.22	3290
		61	.264	.782	5.90	.31	3390
		71	.234	.826	5.43	.27	3250
		72	.238	.813	5.20	.28	5680
		70	.249	.590	5.21	.41	6310
		100	.360	1.170	7.94	.29	3440
IV.....	.93	27	.095	.261	2.02	.34	3
		32	.103	.244	2.30	.40	26
		24	.104	.261	2.30	.38	1

Velocity varies with  $\ln y$ , so it is natural to assume that the velocity distribution will have a form similar to that of the Von Karman-Prandtl velocity-distribution equation for flow near hydraulically rough boundaries:

$$v_y/V_* = A \ln (y/\xi) + B. \quad (8)$$

With flow over a rigid boundary,  $A$  ( $A = 1/k$ , where  $k$  is Von Karman's kappa) has the constant value 2.5,  $B$  varies with the roughness and form of the cross section,  $\xi$  is some roughness height, and  $V_*$  is the shear velocity ( $\sqrt{gDS}$ ). Experiments with flow over an alluvial bed have revealed that  $A$  is a variable and can exceed 2.5 (Vanoni, 1946; Ismail, 1952; Vanoni and Brooks, 1957). The difference in  $A$ , comparing flow between movable alluvial boundaries and rigid boundaries, was attributed by these investigators to a damping effect on the turbulence by the suspended sediment. Laursen and Lin (1952), in a discussion of Ismail's paper, disputed this view and held that the change in  $A$  resulted from the change in bed roughness. Vanoni and Brooks (1957) showed a good correlation between the change in  $A$  and the ratio of the power to suspend the sediment in a thin layer near the bed ( $\Delta\gamma C_s \omega \Delta y$ ) and stream power to overcome friction ( $\tau_0 V$ ). Elata and Ippen (1961) used neutrally buoyant particles to show that suspended sediment causes an increase in  $A$ . Also, by measuring turbulence they found that the change in  $A$  was not the result of damping the turbulence but of a change in its structure. Elata and Ippen's investigation indicated that the size and density of the bed material, in addition to its concentration near the boundary, affected  $A$ . Thus, the size and concentration of the bed material moving in suspension and in contact with an alluvial bed fairly conclusively affect  $A$ , but so also might changes in bed form. Also, the relative importance of the three factors (suspended sediment, contact load, or bed form)

affecting  $A$  is not known.

To determine  $A$  and  $B$ , equation 7 is equated to equation 8, from which

$$A = \frac{A_*}{V_*} \quad (9)$$

and

$$B = \frac{B_*}{V_*} + A \ln \xi. \quad (10)$$

Plotting  $A_*$  versus  $V_*$  (fig. 31),  $A$ , which is the

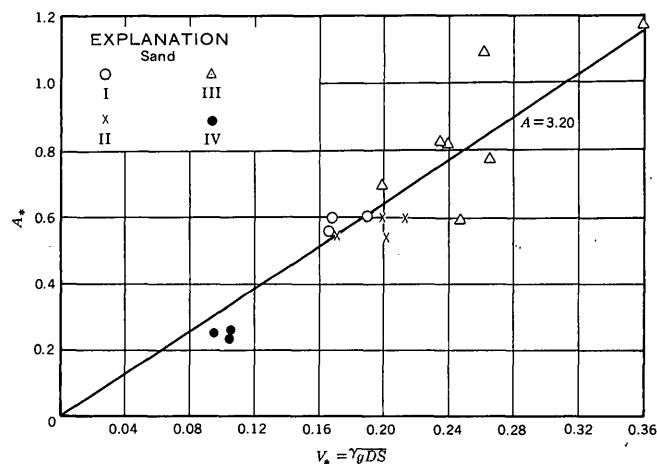


FIGURE 31.—Variation of the slope of the vertical-velocity distribution ( $A_*$ ) with shear velocity ( $V_*$ ) for a plane bed with sediment movement.

slope of the line, does not vary systematically with concentration, size of bed material, or any other variable. Thus, it appears that the slope of an average line through the plotted data represents  $A$  for the plane-bed data for sands I, II, and III. The three points representing sand IV are for plane-bed runs in which shear values were slightly larger than were required for beginning of motion, and  $A$  for this sand should be about the same as that in runs in rigid-boundary channels. The capabilities of the flume system were inadequate to obtain a plane bed with high rates of sediment movement (after the dune-bed configuration) with sand IV. The average value of  $A$  for sands I, II, and III in a channel with a moving boundary was 3.20, and that for sand IV was 2.64; these values are equivalent to kappa values of 0.31 and 0.38, respectively.

The absence of a systematic variation of  $A$  with sand size for flow over a plane bed having a moving boundary can be explained by the nature of the experiments. In experiments conducted under equilibrium plane-bed conditions, the concentration of suspended sediment and the movement of the contact bed-material discharge depend on the magnitude of the shear velocity and the size of the bed material.

Similarly,  $A_*$ , the slope of the  $v_y$  versus  $\ln y$  plot, depends on the existence of the plane bed, the concentration of the suspended sediment, the magnitude of the contact bed-material discharge, and thus on the shear velocity and the size of the bed material. If a 1:1 correspondence exists between the shear velocity for the plane bed and the effect of the shear velocity on the slope of the velocity profile irrespective of the size of the bed material, then  $A = \frac{A_*}{V_*}$  should be a constant. That is, the increase in shear velocity required by larger size bed material for the formation of a plane bed resulted in a compensating increase in the slope of the  $v_y$  versus  $\ln y$  relation so that  $A$  remained constant.

To determine  $B$  and  $\xi$  in equation 10,  $B_*$  (the intercept of the plot of  $v_y$  versus  $\ln y$ ) is plotted versus  $V_*$  in figure 32. Either  $B$  or  $\xi$  can be selected and the other solved with the aid of figure 32. Except

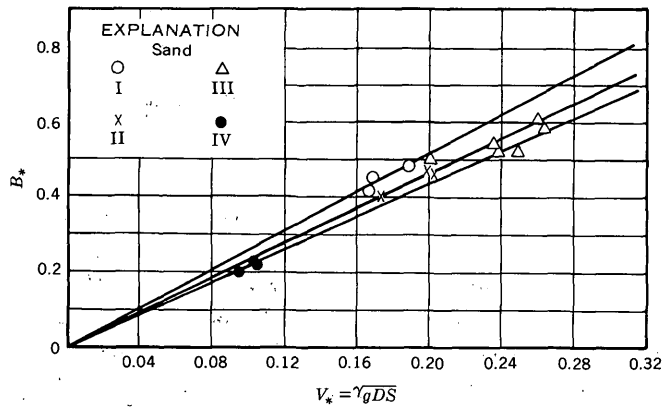


FIGURE 32.—Relation between the intercept of the vertical-velocity distribution ( $B_*$ ) and shear velocity ( $V_*$ ).

for sand IV, the slope  $M$  of the  $B_*$  versus  $V_*$  relation depends on the size of the bed material. The relation between  $B_*$  and  $V_*$  for sand IV at low rates of sediment movement is not the same as for high rates. Consequently, the slope of the  $B_*$  versus  $V_*$  relation is considered to be a function of the size of the bed material for all sand sizes.

For each bed material having a large range in sand sizes, there are many possible values of the roughness size ( $\xi$ ) and, thus, many combinations of  $B$  and  $\xi$ . From the original concept of equation 8,  $B$  should be a constant for a given roughness and channel shape. Also,  $B$  should have such a value that  $\xi$  should be a size which always occurs with the same frequency in the bed material. That is,  $\xi$  should equal the  $d_{50}$ ,  $d_{65}$ ,  $d_{90}$ , or some other size in the bed material.

TABLE 4.—Values of  $B$  when  $\xi = d_{50}$  and of  $\xi$  when  $B = A$ . [Calculated values of  $B$  assume  $\epsilon = d_{50}$ , and those of  $\xi$  assume  $B = A$ .]

Sand	$d_{50}$		$d_{85}$ (ft)	$B_*/V_*$	$B$ (fps)	$\xi$	
	mm	ft				ft	mm
I...	0.19	0.000613	0.00078	25.9	2.3	0.00083	0.25
II...	0.27, 0.28	.00090	.0015	23.3	.9	.0018	.55
III...	0.45, 0.47	.00151	.003	21.9	1.1	.0029	.88

When the  $d_{50}$  size of the bed material was substituted for  $\xi$  in equation 10,  $B$  was not a constant; but when the value of  $B$  in equation 8 was assumed to be equal to  $A$ , then  $\xi$  was approximately equal to the  $d_{85}$  size (table 4). Using  $B$  equal to  $A$  and integrating equation 8 gives a simple mean-velocity relation

$$V = V_* [A \ln(D/\xi) + (B - A)]. \quad (11)$$

However, because  $B$  varies with the shape of the cross section as well as with the grain roughness, other values of  $B$  or of  $\xi$  may have to be selected for other cross sections. With  $B = A$ , equation 8 becomes

$$v_y/V_* = 3.2 [\ln(y/\xi) + 1] \quad (12)$$

and

$$\frac{V}{V_*} = 3.2 \ln(D/\xi) = 7.4 \log D/\xi; \quad (13)$$

where

$V_* = \sqrt{gDS}$  (in eq 12) = shear velocity for the position where the velocity distribution in the vertical was measured,

$V_* = \sqrt{gRS}$  (in eq 11 and 13) = mean shear velocity for the flume, and

$\xi = d_{85}$ .

The different methods of calculating  $V_*$  are necessary because in the velocity-distribution equations (eq 7, 8, and 12) the flow is two-dimensional and the distribution is governed by the local shear ( $\gamma DS$ ). In the mean-velocity equations (eq 11 and 13) the flow is three-dimensional and the mean velocity is governed by the mean shear ( $\gamma RS$ ).

ROUGHNESS COEFFICIENTS

The measure of the roughness coefficient,  $\frac{V}{V_*} = \frac{C'}{\sqrt{g}}$ ,

given by equation 13 was evolved from a study of the velocity distribution normal to the bed under the following assumptions:

1. The velocity profiles would conform to the Von Karman-Prandtl equation (eq 8).

2. The coefficients  $A$  and  $B$  in this equation are equal.
3. The shear stress for the velocity-distribution equation is equal to  $\gamma DS$ ; thus,  $V_* = \sqrt{gDS}$  in equations 8 and 12.
4. The shear stress for the integrated equation is equal to  $\gamma RS$ ; thus,  $V_* = \sqrt{gRS}$  in equations 11 and 13.

For equation 13 to be valid, the values of  $\xi$  (calculated using  $V$  and  $\sqrt{gRS}$ ) should be approximately equal to the values of  $\xi$  calculated from the velocity-distribution equation (eq 12) using  $v_y$  and  $\sqrt{gDS}$ . As shown in figure 33, the values of  $\xi$  from equations 12 and 13 compare very well, and their height is approximately equal to that of the  $D_{85}$  size of the bed material. To further check equation 13, it was plotted on the relation between  $C'/\sqrt{g}$  and  $D$  for the plane-bed runs (fig. 34). Equation 13 fits the experimental points well and may be used as the basic velocity equation for the plane-bed runs with sediment movement. However, even though equation 13 is valid in form, it may not be the correct equation for other conditions because it was developed for an idealized situation and neglects many factors such as the shape factor for the reach and the cross section.

EVALUATION OF RESISTANCE TO FLOW

Various methods have been suggested for determining average velocity and resistance factors for

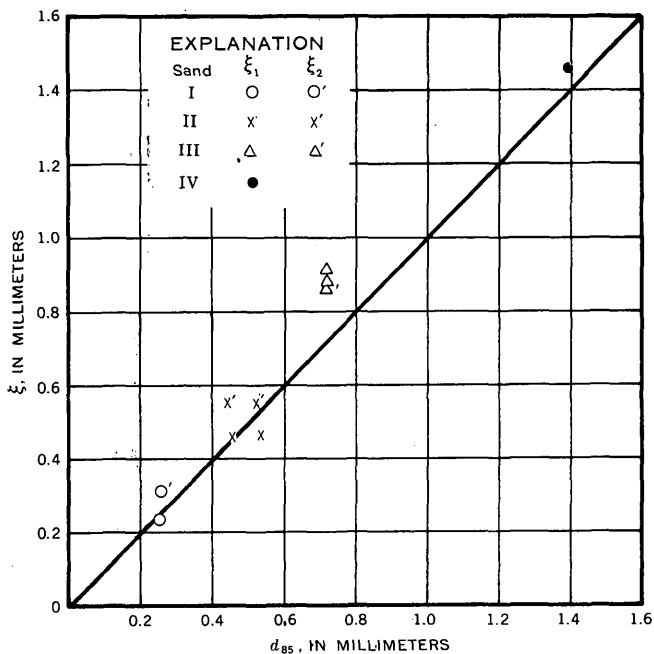


FIGURE 33.—Comparison of the roughness height ( $\xi$ ) with the  $d_{85}$  size of the bed material.  $\xi_1$  was calculated from  $C'/\sqrt{g} = 7.4 \log (D/\xi)$ ; and  $\xi_2$ , from  $v_y/V_* = 3.2 [\ln (v/\xi) + 1]$ .

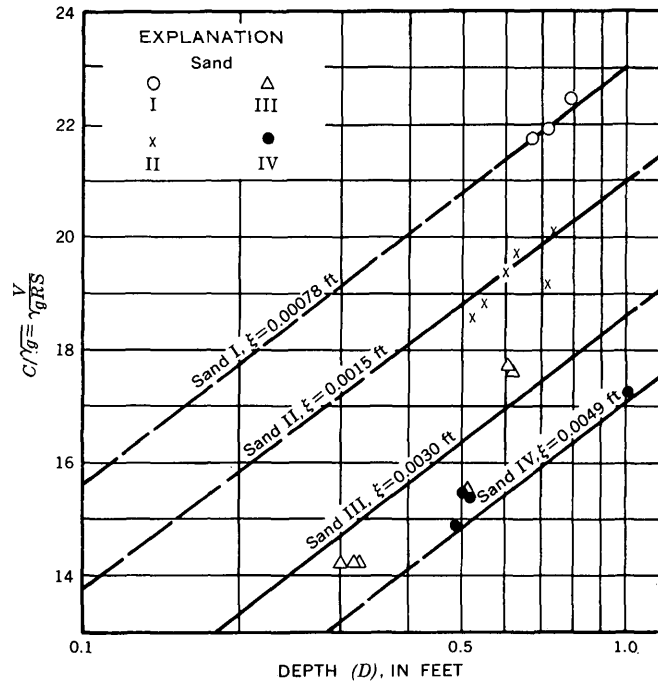


FIGURE 34.—Comparison of the equation  $C'/\sqrt{g} = 7.4 \log (D/\xi)$  with the relation between the Chezy discharge coefficient and depth for plane bed with sediment movement.

flow in alluvial channels. The Manning and Chezy equations developed for channels having rigid boundaries, the various regime equations (Inglis, 1948), and Einstein and Barbarosa's (1952) treatment of alluvial river-channel roughness have all been used to estimate channel resistance and average velocity.

The data for the 8-foot-wide flume follow those plotted in Einstein and Barbarosa's (1952) river curve, which relates  $V/\sqrt{g\Delta RS}$  to  $\Delta\gamma d/\gamma R'S$ , reasonably well within the range of  $\Delta\gamma d/\gamma R'S$  values for which ripples and dunes occur. However, for both large and small values of  $\Delta\gamma d/\gamma R'S$ , the data departs systematically and radically from the proposed curve. Therefore, some modification is required when Einstein and Barbarosa's relation is applied in the upper flow regime. (See fig. 35.)

Resistance to flow in alluvial channels is the result of one of the following processes or a combination of them:

1. Surface resistance (grain roughness). Where surface resistance occurs, the flow does not separate from the macroboundary but does separate from the grains, or microroughness. This type of resistance occurs on a plane bed, on the back of dunes, and in antidune flow.
2. Form resistance. Where form resistance occurs, the flow separates from the macroboundary. The result is a pressure reduction in the separation zone (form drag) and the generation of large-scale eddies; both processes dissipate

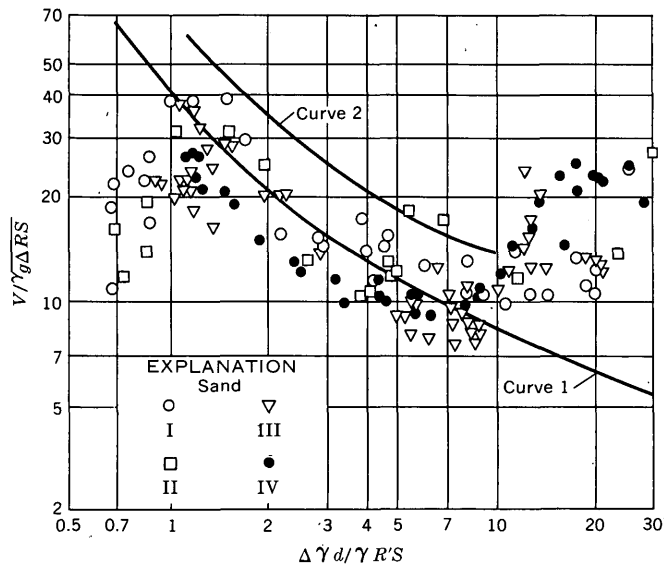


FIGURE 35.—Comparison of resistance data from the 8-foot-wide flume to Einstein and Barbarosa's (1952) bar-resistance relation for rivers (curve 1) and with Einstein and Kalkanis' (1959) relation for flumes (curve 2).

energy. This type of resistance occurs with ripples, with dunes, and, to a limited extent, with antidunes.

3. Acceleration and deceleration of the flow (non-uniform flow). With the growth and subsidence of the inphase water- and bed-surface waves, acceleration and deceleration of flow occurs. This is a source of energy dissipation in addition to that caused by the grain roughness. This type of energy dissipation occurs with antidune flow, although with dunes there is also some acceleration and deceleration of the out-of-phase flow over the roughness elements.
4. Breaking waves. The inphase water- and bed-surface waves reach an instability point and break. The eddies and turbulence generated by the breaking waves dissipate energy of the same order of magnitude as does a hydraulic jump with a Froude number slightly larger than unity. Fortunately, a breaking wave, except in chute-and-pool flow, occupies a limited amount of time and space and causes a rather small increase in resistance to flow. This type of energy dissipation occurs with antidunes and with chutes and pools.

It is very difficult to separate the processes or to mathematically describe the forms of bed roughness which occur on the bed of a sand channel. The spacing, amplitude, and shape of these roughness elements are affected by many interrelated variables. Because of this, it is very difficult to write a generalized function to determine resistance to flow. A generalized function may not exist, because (1)

more than one resistance to flow may occur for a given slope, depth, and bed material; (2) hysteresis exists in the change in bed configuration so that the bed configuration and resistance to flow depend on preceding flow conditions; and (3) the bed configuration will oscillate between a dune bed and a plane bed for a given bed material at certain slopes and discharges. The problem is further complicated by three-dimensional flow, varying depth, varying bank roughness, and nonuniformity of flow in alluvial channels. The net result is varying bed configuration from point to point on the stream bed, both longitudinally and laterally, and, consequently, varying resistance to flow. Hence, average resistance to flow is the result of the combined effects of many different roughness elements and the turbulence they create. In a straight sand channel it is not uncommon to find a plane bed under the main current of the stream, transition roughness adjacent to the bed plane, and dunes near the banks. Meanders and bars also complicate the problem; meanders are present to some extent even in straight reaches of sand-bed streams.

Various methods of treating resistance to flow and of determining the average velocity of flow are presented in the following sections. The methods are based either on adjusting the measured slope to compensate for the increase in energy loss caused by the different bed configurations, or by adjusting depth or hydraulic radius to compensate for the energy loss and the increase in flow cross section caused by the form roughness. The latter method results from the fact that there is no flow through part of the measured depth. Two methods of depth adjustment are discussed: (1) by adjusting the depth to the equivalent depth for a plane bed with grain roughness and, (2) by adjusting the depth to an equivalent depth for a smooth boundary as defined by the equation of Tracy and Lester (1961). These methods depend on knowledge of the bed configuration. If the bed configuration is not known, an estimation is made of what it was or may be, and the velocity is computed using one of the foregoing methods. With the computed velocity, shear stress, and bed-material size, figure 28 is used to determine if the selected bed configuration would occur. If the selected bed configuration would not occur, another trial is made and the velocity is recomputed.

#### EVALUATING RESISTANCE TO FLOW BY ADJUSTING SLOPE

Equation 13 can be used to calculate resistance to flow and average velocity for flow over a plane bed upon which there is sediment movement. Therefore,

it is proposed that an adjustment term be applied to the plane-bed equation to obtain the resistance to flow for the ripple, dune, antidune, or chute and pool bed configurations. This adjustment term would take into account the increase in resistance to flow caused by the form roughness, wave acceleration and deceleration, and wave breaking (all these effects will be referred to hereafter as form roughness effects). The resistance to flow is in terms of  $f'$  and  $\Delta f$ , where  $f'$  is the resistance to flow due to grain roughness and  $\Delta f$  is the increase in resistance to flow caused by various form roughness effects. This implies that

$$f = f' + \Delta f. \quad (14)$$

From equation 14, the total-resistance factor is

$$f = 8(gR/V^2)(S' + \Delta S) \quad (15)$$

or

$$f = 8(gRS'/V^2)(1 + \Delta S') = 8(gRS'/V^2)(S/S'),$$

where  $S'$  is the slope the channel would have for the same depth and velocity if the resistance to flow was only grain roughness, and  $\Delta S$  is the increase in slope required to compensate for all other types of energy dissipation. From equation 14,

$$S = S' + \Delta S. \quad (16)$$

In terms of the Chezy discharge coefficient,  $C/\sqrt{g} = V/\sqrt{gRS}$ ,

$$f = 8/(C/\sqrt{g})^2 = 8/C'^2 (S/S'), \quad (17)$$

where

$$C'/\sqrt{g} = 7.4 \log D/\xi \quad (18)$$

or

$$C/\sqrt{g} = C'/\sqrt{g} \sqrt{S'/S} = (7.4 \log D/\xi)C_*, \quad (19)$$

and  $C_*$  is the correction factor applied to equation 18 to obtain the discharge coefficient for bed forms other than a plane bed.  $V_*$  is based on the hydraulic radius  $R$  and not the depth  $D$ .

To determine  $C_*$  it is first necessary to determine  $\Delta S$ , the increase in slope of the energy grade line which results from the form roughness. The increment of slope ( $\Delta S$ ) should be a function of the bed form, shear stress on the bed, and size of bed material. Therefore,  $\Delta S = S - S'$  was calculated for all the data and was plotted versus the shear stress for each sand with bed form and depth as additional variables. For sands finer than sand IV, a linear relation existed between the logarithms of  $\Delta S$  and the shear stress (depth and bed form as additional variables). (See figs. 36-38.) Thus,

$$\Delta S = KD^M \tau_0^N, \quad (20)$$

where  $K$ ,  $M$ , and  $N$  are constants that are functions of the bed form and sand size.  $N$  is the slope of the  $\Delta S$  versus  $\tau_0$  line for the different bed forms, and  $K$  and  $M$  are determined from

$$I = KD^M = \frac{\Delta S}{\tau_0^N} \quad (21)$$

by plotting  $I$  as determined from  $\frac{\Delta S}{\tau_0^N}$  for each depth versus that depth on log paper and determining the slope  $M$  of the line and the intercept  $K$ .

The equations expressing  $\Delta S$  as a function of depth and shear are given in the preceding three figures. These figures indicate that, given bed roughness of ripples and dunes,  $\Delta S$  is independent of depth of flow for sands I and II and that it has a minor effect for sand III if the hydraulic radius is approximately equal to the depth—that is, when  $\tau_0 = \gamma RS \approx \gamma DS$ . Therefore,  $\Delta S$  was plotted against the slope. (See figs. 39, 40, and 41.) The correction factor  $C_*$  for each sand for the plane-bed equation was determined from these figures and is given in table 5.

The flume data indicate that  $\Delta S$  and  $C_*$  are independent of depth for the ripple- and dune-bed configurations in the finer sands. This requires further verification because of the small range in depth investigated. To determine if  $\Delta S$  was still independent of depth for the dune-bed configuration at large depths, field data from the Elkhorn River (Beckman and Furness, 1962), which was the source for sand II, were studied. Runs having fully developed dunes (indicated by the depth-discharge relation in fig. 20) were plotted in figure 40. As indicated in figure 40,  $\Delta S$  was also independent of depth for the Elkhorn River, where the depth ranged from 1.4 feet to 5 feet. This tends to confirm that  $\Delta S$  is independent of depth for dunes. However, additional field and laboratory studies are needed to conclusively determine whether or not  $C_*$  is independent of depth for ripples and dunes in fine sands.

TABLE 5.—Equation for  $C_*$  as a function of bed form and grain size

Bed form	Grain size		
	I (0.19 mm)	II (0.27 mm)	III (0.45 mm)
Ripples.....	$\sqrt{1 - 1.5S^{-0.09}}$	$\sqrt{1 - .62}$	$\sqrt{1 - 2.7S^{-2}}$
Dunes.....	$\sqrt{1 - 1.2S^{-0.09}}$	$\sqrt{1 - .26/S^{-1.4}}$	$\sqrt{1 - 2.6D^{-3}S^{-2}}$
Plane bed.....	1	1	1
Antidunes.....	$\sqrt{1 - \frac{34S^{-0.9}}{D^{-7}}}$	$\sqrt{1 - 700S^{-1.3}}$	$\sqrt{1 - \frac{2.9 \times 10^4 S^{-3}}{D^{2.5}}}$

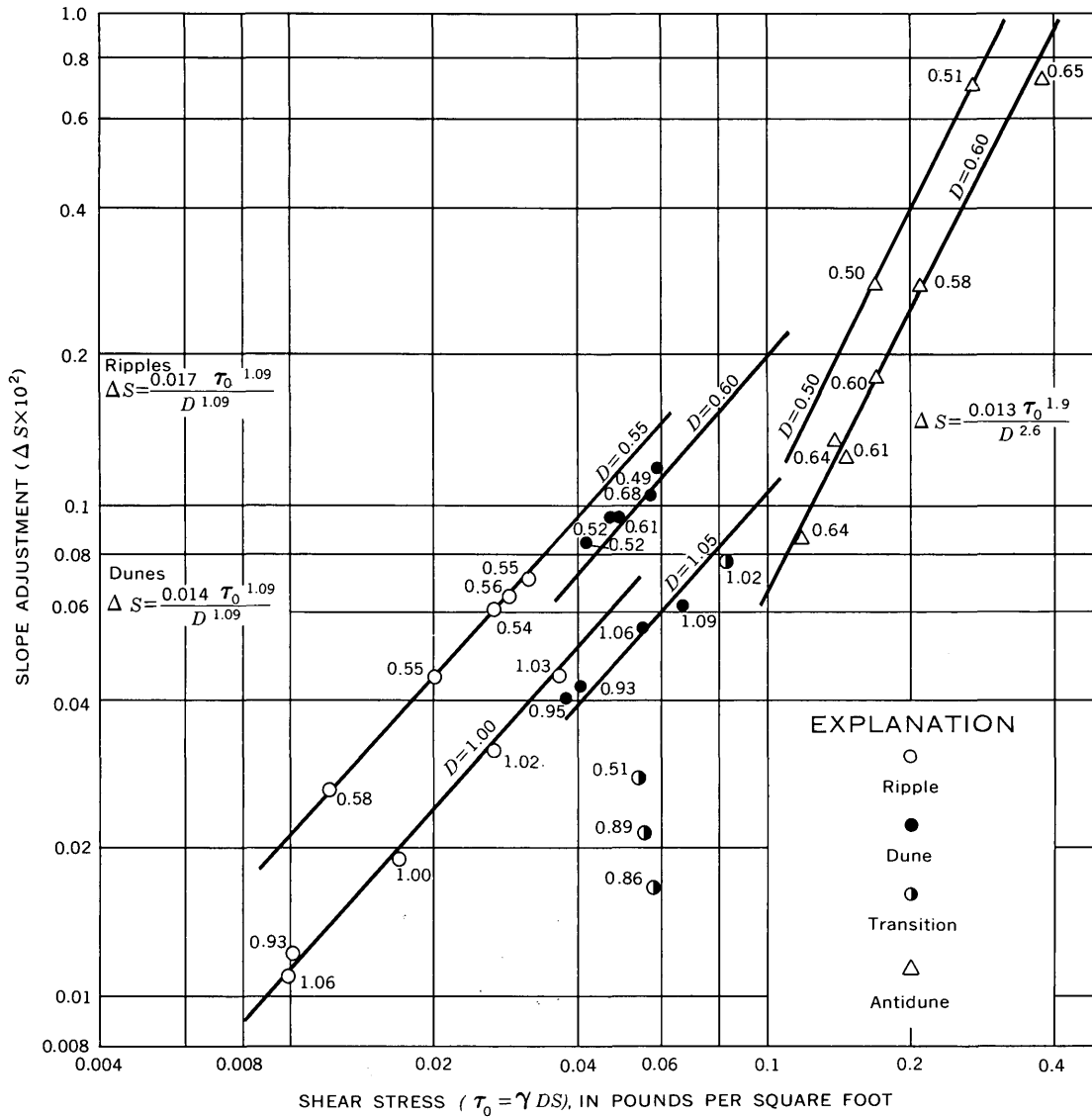


FIGURE 36.—Relation between slope adjustment ( $\Delta S$ ), shear stress ( $\tau_0$ ), bed configuration, and depth ( $D$ ) for sand I. Numeral by the point is the depth.

The lack of variation of  $\Delta S$  with depth is in conflict with prior statements concerning the effect of depth of flow on resistance to flow and with the changes in resistance to flow shown in figures 5 and 19. The only explanation is that the effect of depth is taken care of by the  $D/\xi$  term in equation 18 from which  $S'$  is determined.

With sand IV,  $\Delta S$  was not linearly related to the shear stress. (See fig. 42.) Therefore,  $C_*$  was computed for each run and plotted against the shear stress as shown in figure 43. With the dune-bed configuration,  $C_*$  was inversely related to the shear stress. An increase in shear stress, either by an increase in slope or an increase in depth, caused a decrease in  $C_*$  (that is, an increase in roughness). The variation of  $C_*$  with depth and slope in the lower flow regime is given in figure 44. When the

bed form was in transition from the lower to upper flow regimes,  $C_*$  was affected by depth and the shear stress. Also, there was a systematic change in  $C_*$  with depth and shear stress in the transition which was contrary to the results of runs using finer sands.

$C_*$  was inversely related to slope and directly related to slope and directly related to depth when flow was in the upper regime. An increase in slope resulted in a decrease in  $C_*$  (an increase in resistance to flow), and an increase in depth resulted in an increase in  $C_*$  (a decrease in resistance to flow). The effect of depth and slope on  $C_*$  has been qualitatively verified by field observations. Antidune activity and resistance to flow in natural alluvial channels will decrease with an increase in depth when slope is constant, and they will increase with an increase in slope when depth is constant. Studies

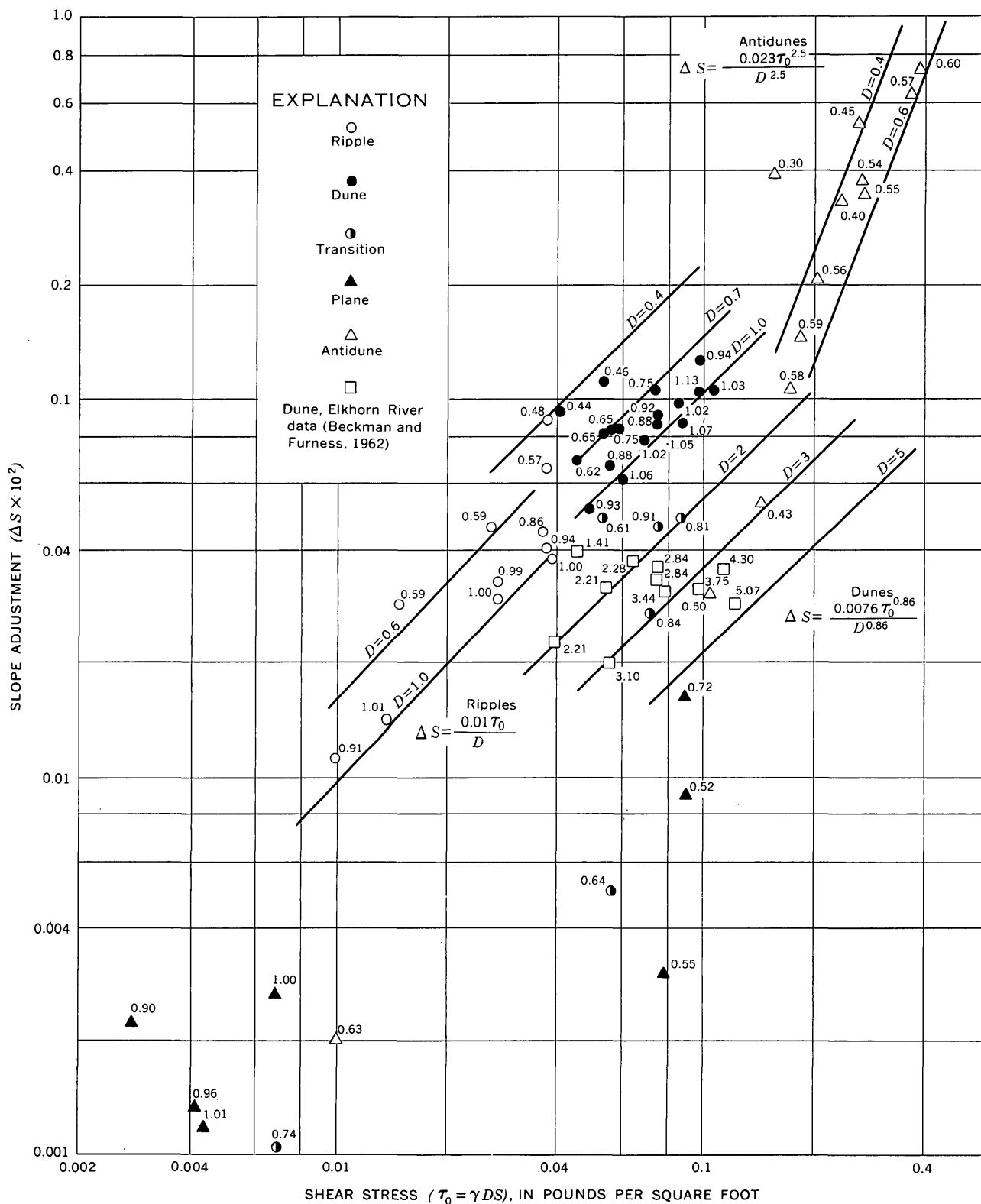


FIGURE 37.—Relation between slope adjustment ( $\Delta S$ ), shear stress ( $\tau_0$ ), bed configuration, and depth ( $D$ ) for sand II. Numeral by the point is the depth.

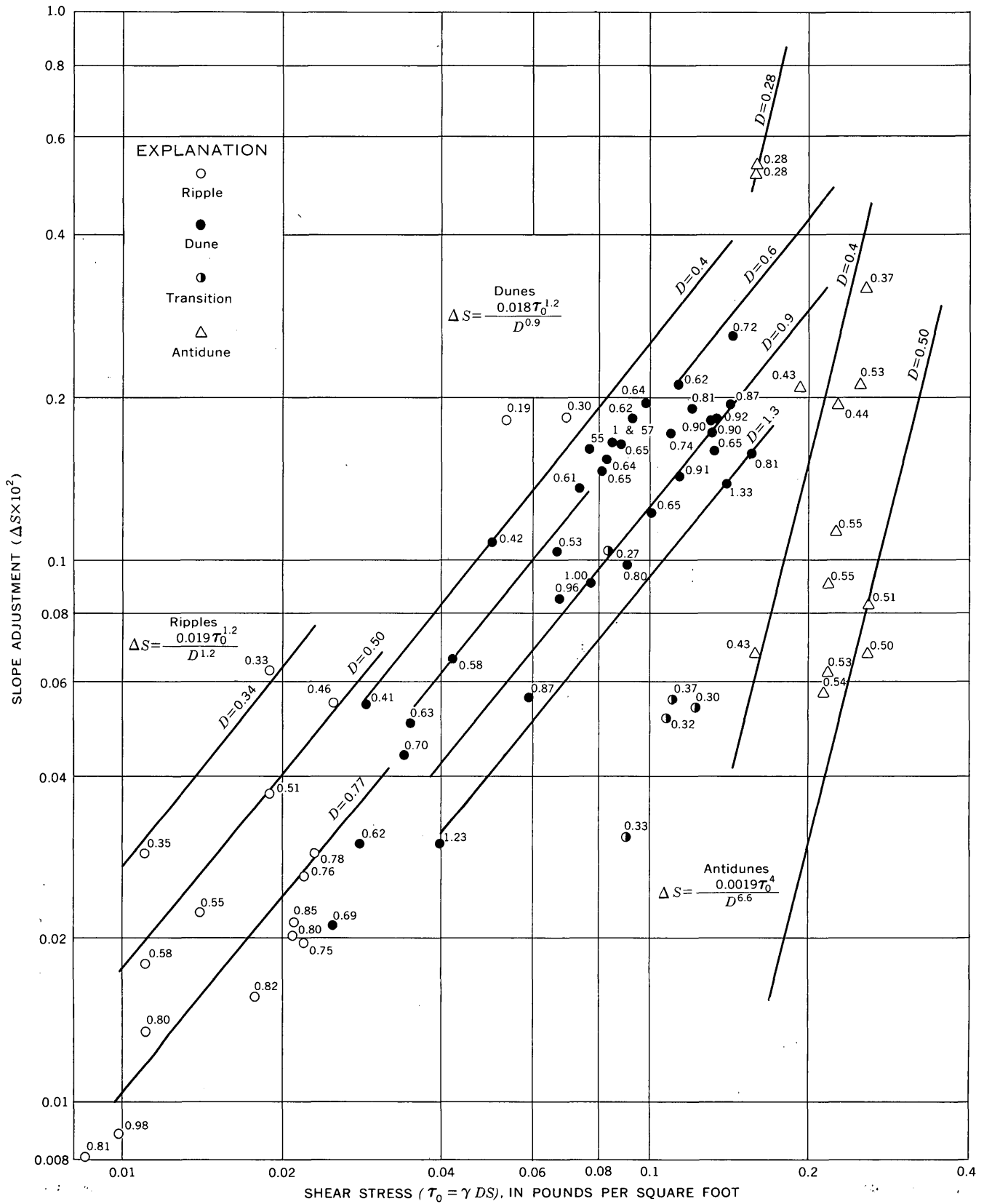


FIGURE 38.—Relation between slope adjustment ( $\Delta S$ ), shear stress ( $\tau_0$ ), bed configuration, and depth ( $D$ ) for sand III. Numeral by the point is the depth.

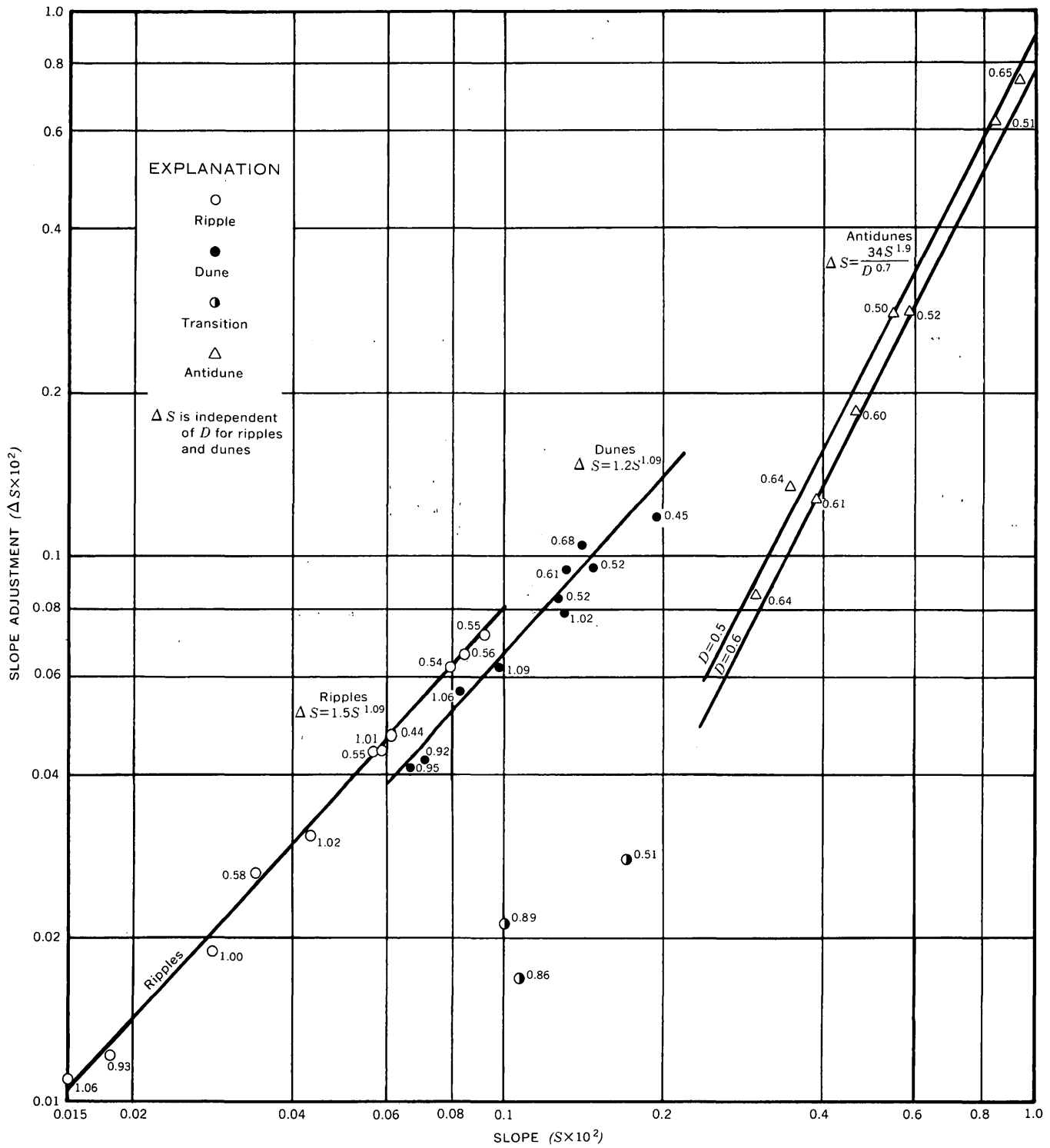


FIGURE 39.—Relation between slope adjustment ( $\Delta S$ ), slope ( $S$ ), bed configuration, and depth ( $D$ ) for sand I. Numeral by the point is the depth.

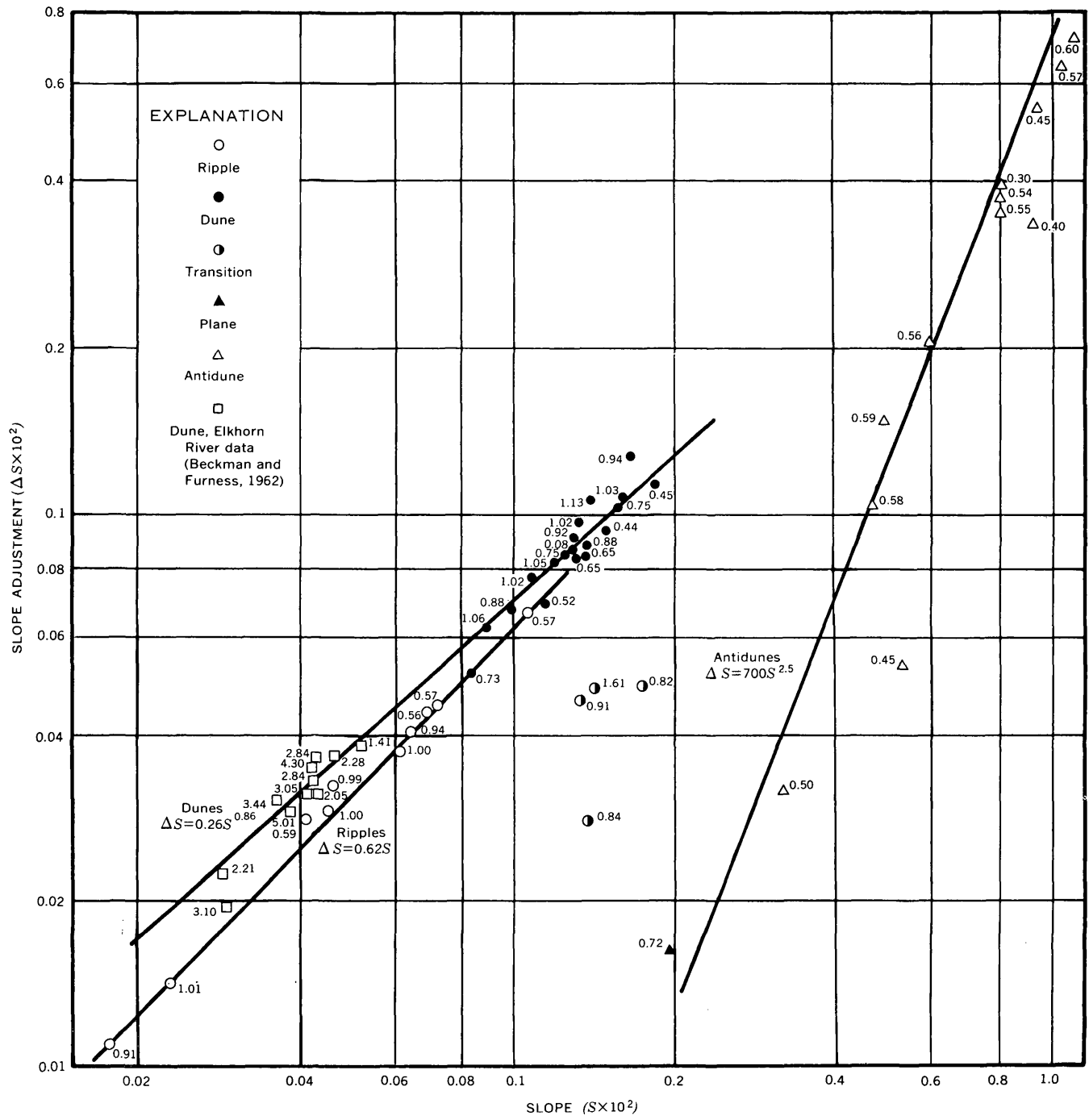


FIGURE 40.—Relation between slope adjustment ( $\Delta S$ ), slope ( $S$ ), bed configuration, and depth ( $D$ ) for sand II. Numeral by the point is the depth.

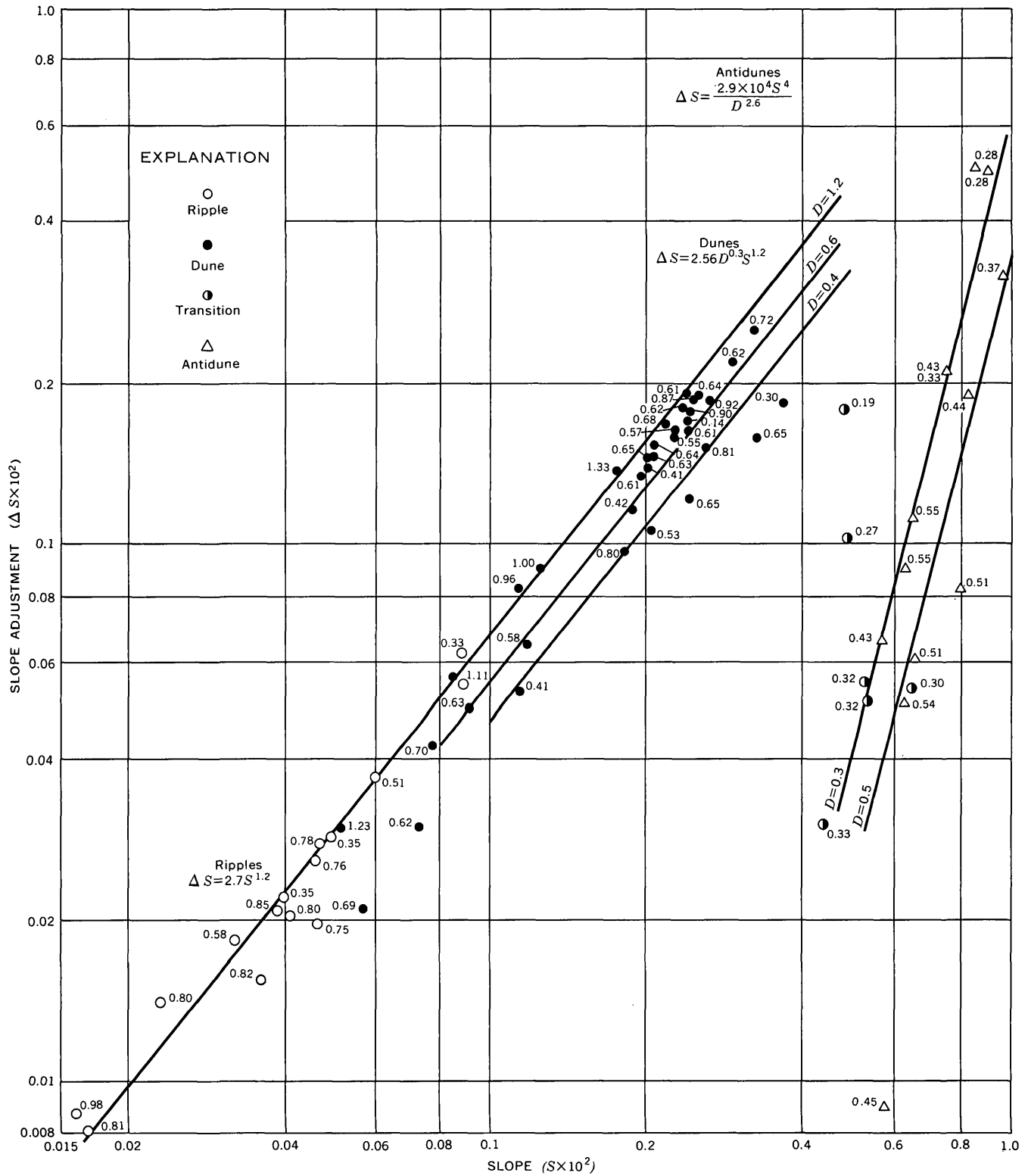


FIGURE 41.—Relation between slope adjustment ( $\Delta S$ ), slope ( $S$ ), bed configuration, and depth ( $D$ ) for sand III. Numeral by the point is the depth.

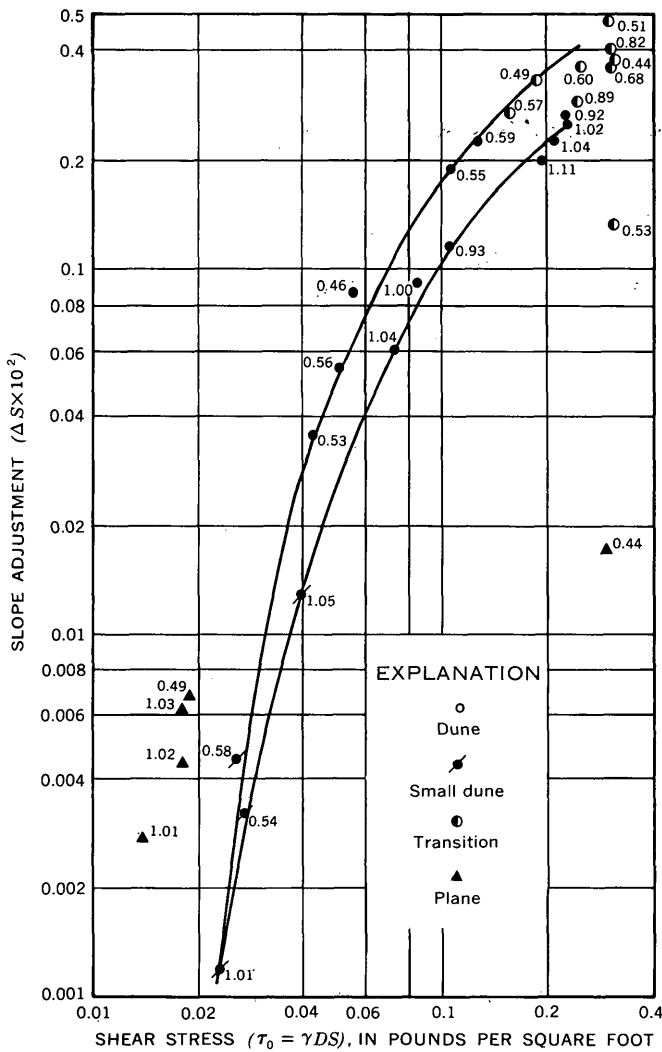


FIGURE 42.—Relation between slope adjustment ( $\Delta S$ ), shear stress ( $\tau_0$ ), bed configuration, and depth ( $D$ ) for sand IV. Numeral by the point is the depth.

in the field and laboratory are needed to quantitatively determine the relation between  $C_*$ , slope, and depth for different sand sizes.

Using equation 19 and the values of  $C_*$  from either table 5 or figure 43, the velocity was computed for all the flume runs. The computed velocity and the measured velocity are compared in figure 45.

In summary:

1. The discharge coefficient  $C'/\sqrt{g}$  for a plane bed can be determined for the flume runs by

$$C'/\sqrt{g} = 7.4 \log(D/\xi), \quad (13)$$

in which  $\xi$  is the  $d_{85}$  size of the sand in the flume (may vary for other streams), because  $\xi$  will be a function of the form of the cross section.

2. The plane-bed equation can be multiplied by a parameter  $C_*$  to obtain the discharge coefficient for the other bed configurations.

3. The parameter  $C_*$  depends on the bed form, sand size, slope, and depth.

A. In the lower flow regime:

- a. The coefficient  $C_*$  for the finer sands ( $d_{50} \leq 0.4$  mm) was independent of depth and decreased (an increase in resistance to flow) with an increase in slope. The magnitude of the decrease in  $C_*$  with an increase in slope depended on the sand size and whether the bed configuration was ripples or dunes.

- b. For the coarser sands ( $d > 0.4$  mm),  $C_*$  was dependent on the depth and the slope and decreased with an increase in depth and (or) an increase in slope. The coarser the sand, the greater was the effect of depth on the value of  $C_*$ .

B. In the upper flow regime:

- a. The value of  $C_*$  for sands finer than 0.93 mm decreased with an increase in slope and increased with an increase in depth. The magnitude of the change depended on the sand size.

C. In the transition zone:

- a. The value of  $C_*$  was undetermined for all but the coarser sands. With the 0.93-mm sand,  $C_*$  increased with an increase in slope or a decrease in depth.

4. The value of  $C_*$  can be determined from equations for sands I, II, and III (table 5), and from figure 43 for sand IV.

#### EVALUATING RESISTANCE TO FLOW BY ADJUSTING DEPTH OF FLOW

Resistance to flow or mean velocity can be determined by adjusting either slope or depth of flow. The depth adjustment takes into account the increase in energy dissipation resulting from the form roughness and the possible error in depth measurement resulting from inclusion of the separation zones downstream from ripples and dunes in the total area of flow.

The measured depth of flow includes part of the separation zones downstream from ripples and dunes. This part does not actually convey the fluid downstream. The roughness elements and their associated separation zones were observed, measured, and photographed. Together with these measurements, much attention was given to the flow pattern

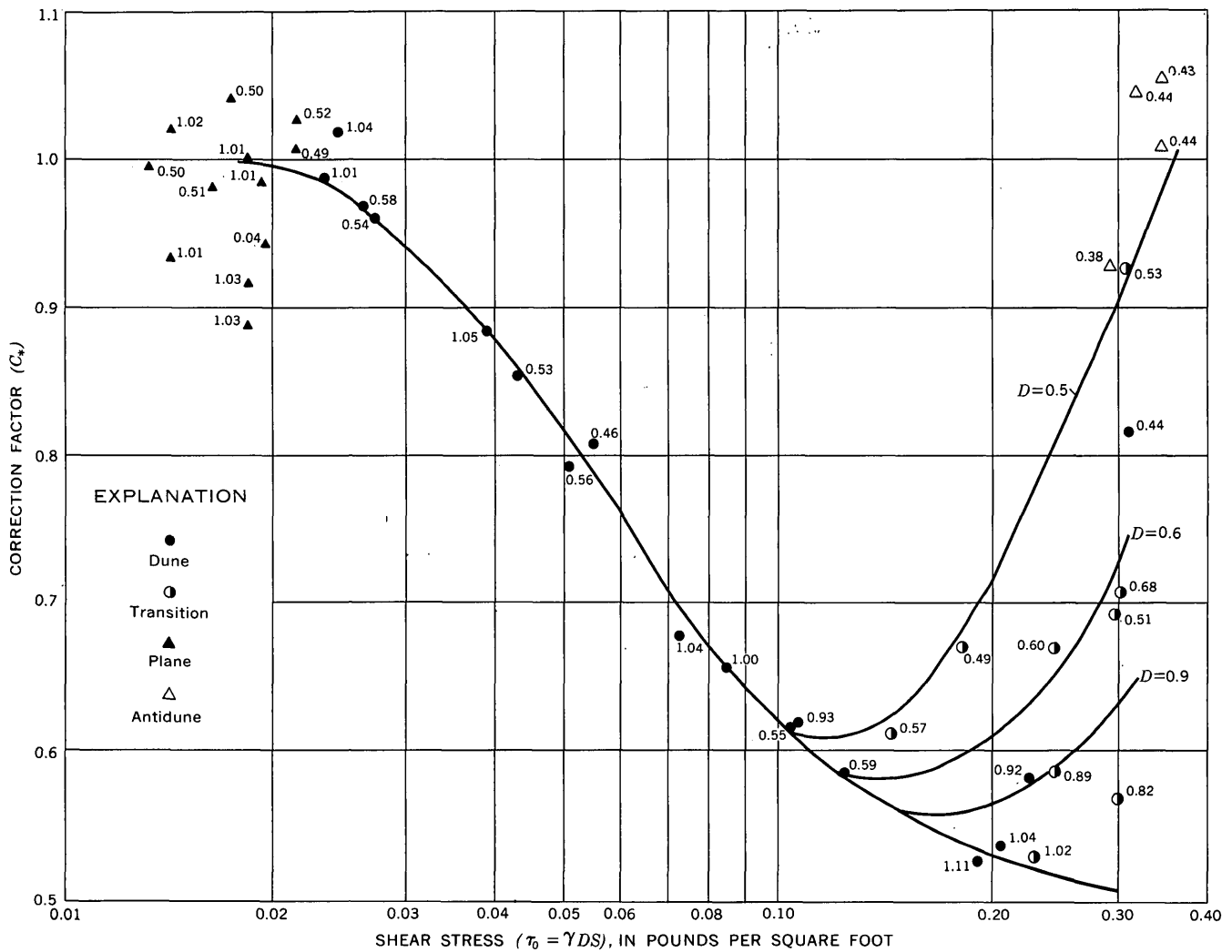


FIGURE 43.—Relation between form roughness correction ( $C_*$ ), shear stress ( $\tau_0$ ), and depth ( $D$ ) for sand IV. Numeral by the point is the depth.

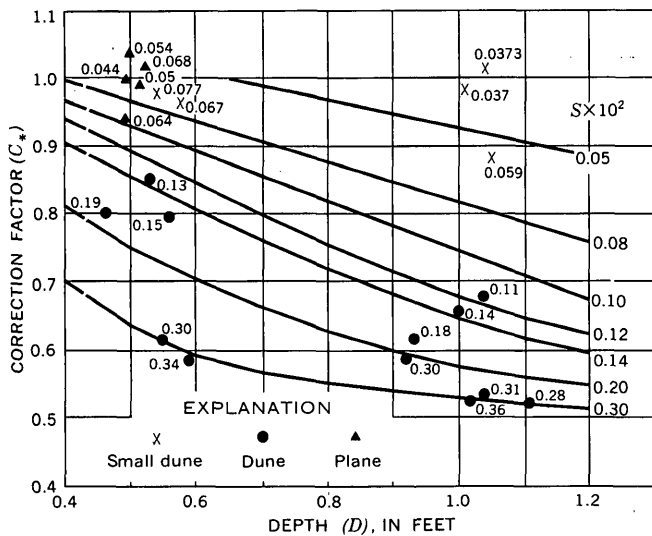


FIGURE 44.—Relation between form roughness correction ( $C_*$ ), depth ( $D$ ), and slope ( $S$ ) for dune-bed configuration in sand IV. Numeral by the point is the slope  $\times 10^2$ .

over the individual roughness elements. For example, downstream from the crest of each ripple and dune is a separation zone in which a part of the fluid rotates about a horizontal axis which passes through the mass of fluid within the zone of separation, as is shown in figure 46.

By careful measurement, it was determined that the length of these separation zones conformed reasonably well with the length of separation zones observed downstream from baffles placed in a wind tunnel (Nagabhushanaiah, 1961). These lengths were approximately 10–12 times the amplitude of the roughness element measured from trough to crest. A study of these separation zones suggested that average velocity based on  $Q/A$  and average depth based on the average distance from the water surface to the bed surface are perhaps misleading. An effective depth ( $D_e$ ) may be defined as the average depth ( $D$ ) reduced to compensate for the zones

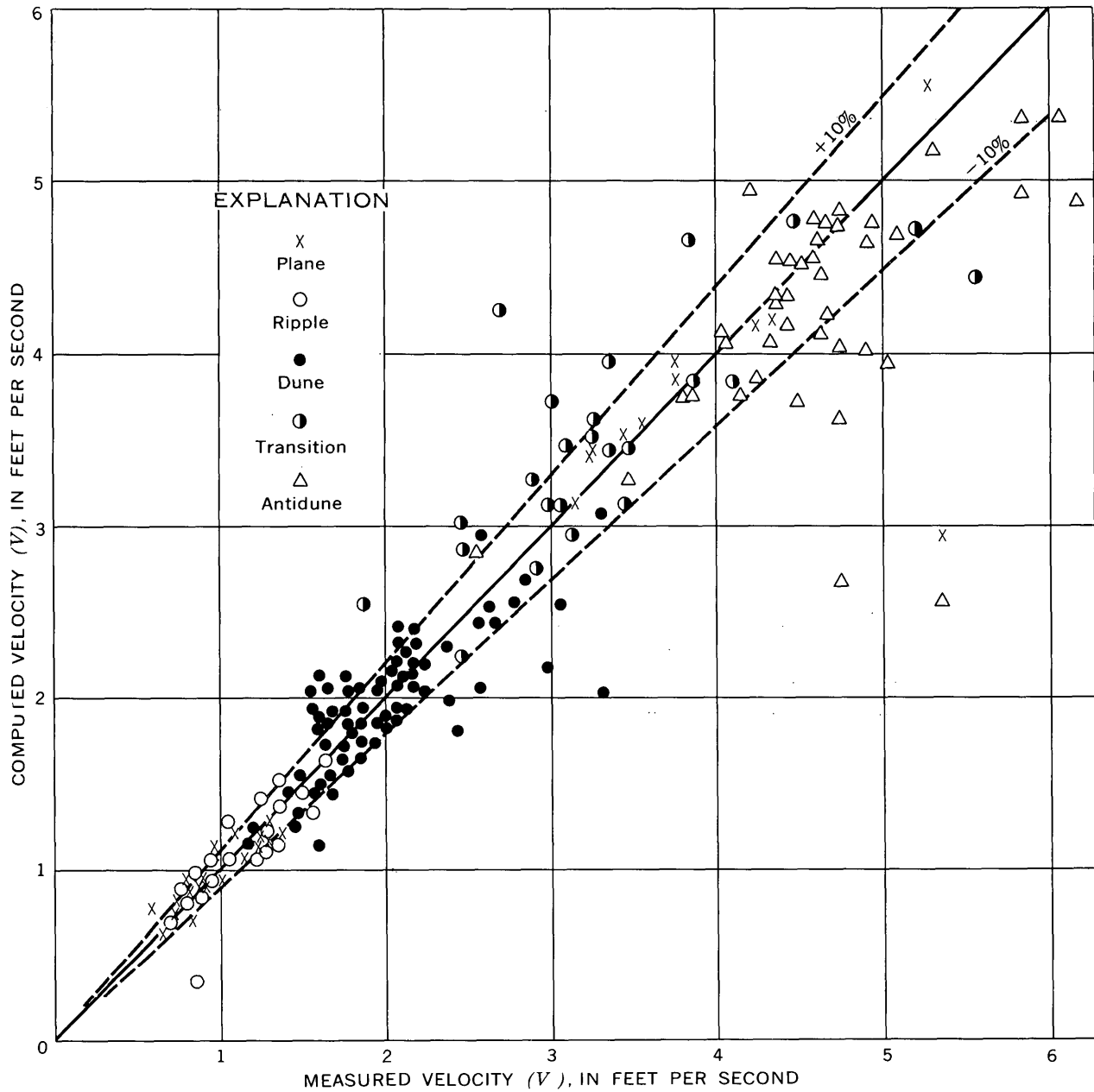


FIGURE 45.—Comparison of the computed velocity and the measured velocity.

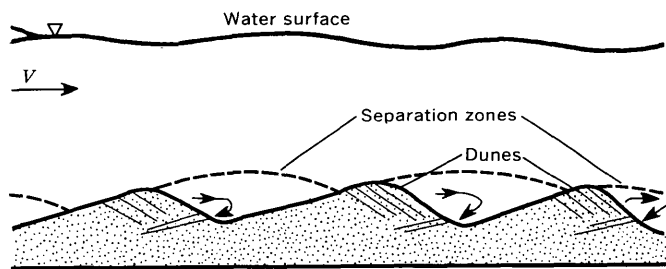


FIGURE 46.—Typical flow pattern over two-dimensional ripple and dune roughness elements.

of separation, and an effective velocity may be defined correspondingly by applying the principle of continuity. The concept of an effective velocity and

depth is further clarified by figure 47, from which it can be seen that the effective depth,

$$D_e = \frac{D_1 + D_2 + D_3 + \dots + D_n}{n} \quad (22)$$

and the effective velocity,  $V_e = q/D_e$ .

The effective depth and velocity given in equation 22 can be approximated in the flumes by mapping the form roughness. This is done using sonic equipment and ejecting dye to define the limits of the separation zone. Knowing effective depth and velocity, the average velocity in the channel can be determined from

$$V = \frac{V_e D_e}{D} \quad (23)$$

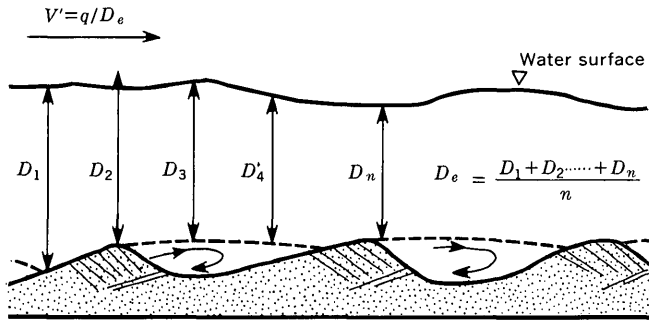


FIGURE 47.—Sketch showing effective depth ( $D_e$ ) and effective velocity ( $V' = q/D_e$ ).

This procedure is extremely difficult and is generally impossible to use. In addition, effective depth and velocity do not consider the increase in energy dissipation resulting from the form roughness. Therefore, in the next sections an adjusted depth ( $D'$ ) and velocity ( $V'$ ) are defined that take into account both correction factors. They are also relatively simple to use to evaluate resistance to flow and velocity.

**ADJUSTING DEPTH TO AVERAGE ALLUVIAL GRAIN ROUGHNESS**

The resistance to flow and the average velocity are evaluated by adjusting the measured depth ( $D$ ) to the depth of flow of an equivalent channel with the same slope, discharge, and average grain roughness. That is,

$$V'D' = VD \tag{24}$$

and

$$D' = D - \Delta D,$$

where

$D'$  = depth of the channel would have for the same slope and discharge if the resistance to flow was the result of an average grain roughness,

$D$  = increase in depth resulting from the form roughness,

$V'$  = mean velocity of the equivalent plane-bed channel,

$$V' = C'/\sqrt{g} \sqrt{gD'S} \tag{25}$$

To obtain  $D'$  it is first necessary to define the average grain roughness. This is done by arbitrarily using the average discharge coefficient (eq 25) obtained for each sand in the plane-bed runs made in the 8-foot-wide flume.

The magnitude of  $C'/\sqrt{g}$  is a function of the median diameter of the bed material:

$C'/\sqrt{g}$	Median diameter of sand (mm)
20.60	0.19
18.28	.28
17.10	.45
16.25	.93

As the tabulation shows,  $C'/\sqrt{g}$  is largest for the finest bed material, because resistance to flow for the plane bed is a function of the magnitude of the grain roughness.

These  $C'/\sqrt{g}$  values ignore the effect of relative roughness (depth range from 0.4 ft to 1.0 ft) and the difference in resistance to flow between static-sand-grain roughness and moving-sand-grain roughness. Average  $C'/\sqrt{g}$  values rather than values obtained from figure 34 are used for the grain roughness because both the relative roughness and the moving-sand-grain effects for the plane-bed condition will be accounted for by the adjustment of the measured depth to the adjusted depth ( $D'$ ).

**ALLUVIAL SAND-BED ROUGHNESS**

**Development of method**

To determine the adjusted depth ( $D'$ ) for an alluvial sand-bed roughness, consider the points plotted in figure 48 for sand I. The points for ripples and dunes fall below and to the right of those for the relation of average grain roughness. Similar figures can be drawn for the other sands. The adjusted depth ( $D'$ ) can be determined by finding the difference necessary to adjust a run with form roughness to the average grain-roughness line. This difference,  $\Delta D$ , between the measured depth ( $D$ ) and the adjusted depth ( $D'$ ) is a measure of the effect of the form roughness on resistance to flow. For the plane bed,  $\Delta D$  is small; for ripples and dunes,  $\Delta D$  is relatively large; for antidunes,  $\Delta D$  is relatively small; and in the transition zone,  $\Delta D$  varies from large to relatively small values. As was indicated previously,  $\Delta D$  should be a function of the depth, slope, size of

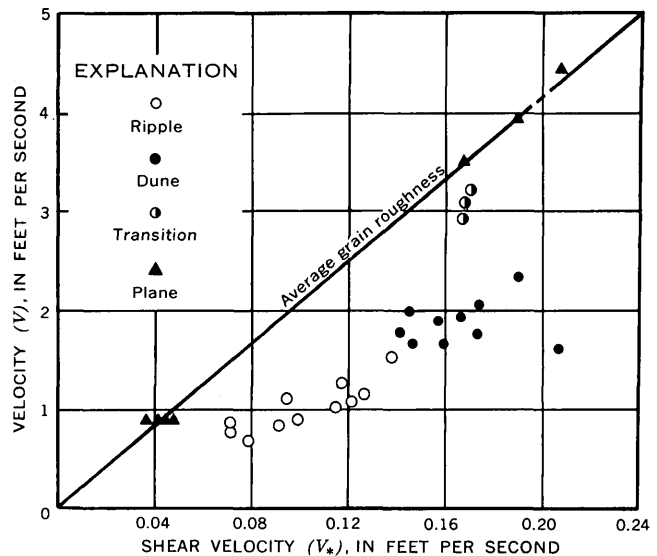


FIGURE 48.—Effect of bed configuration on resistance to flow for sand I.

the bed material, and the bed configuration. If a functional relation can be determined for  $\Delta D$ , then knowing the average depth of flow ( $D$ ), the adjusted depth ( $D'$ ) can be determined. Knowing  $D'$ , the adjusted velocity ( $V'$ ) can be calculated from equation 25 and the mean velocity ( $V$ ) can be determined from the continuity equation, equation 24.

A method of estimating  $\Delta D$  was established by computing it for the ripple and dune runs for each bed material studied in the 8-foot-wide flume. To compute  $\Delta D$ , equation 24 was combined with equation 25 to obtain

$$\Delta D = D - \left[ \frac{q}{(C'/\sqrt{g}) \sqrt{gS}} \right]^{2/3} \quad (26)$$

The computed  $\Delta D$ 's were plotted against depth, with slope as a third variable for each bed material and bed configuration. (See figs. 49-52.) These plots verified that there was a relation between the depth adjustment ( $\Delta D$ ), depth, and bed form for each of the bed materials. The relation between  $\Delta D$  and  $D$  is not a function of the slope for the ripple bed but is a function of slope for the dune bed formed in

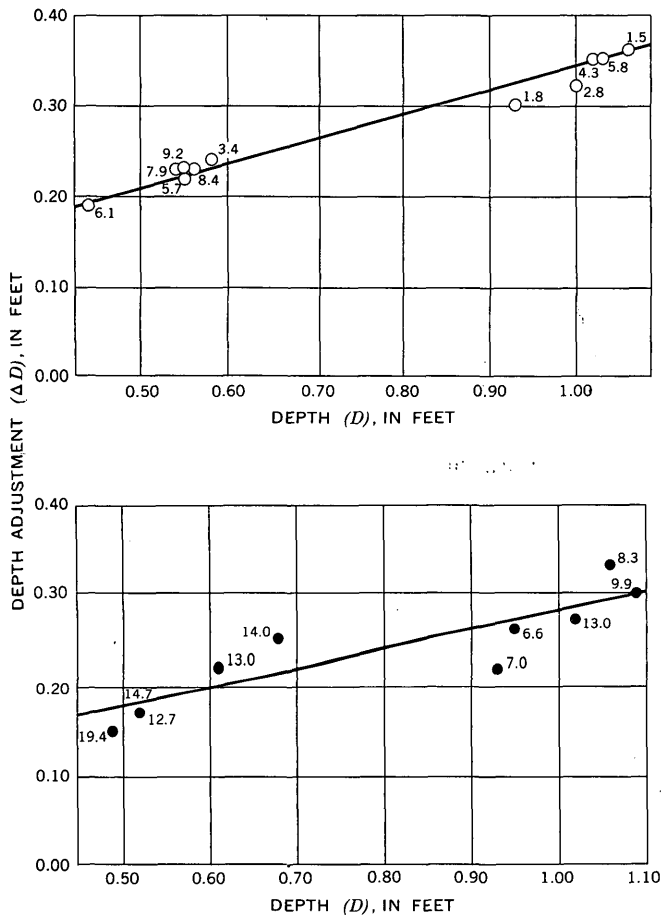


FIGURE 49.—Relation between depth adjustment ( $\Delta D$ ), depth ( $D$ ), and slope ( $S \times 10^4$ ) for ripples (upper part) and dunes (lower part); sand I.

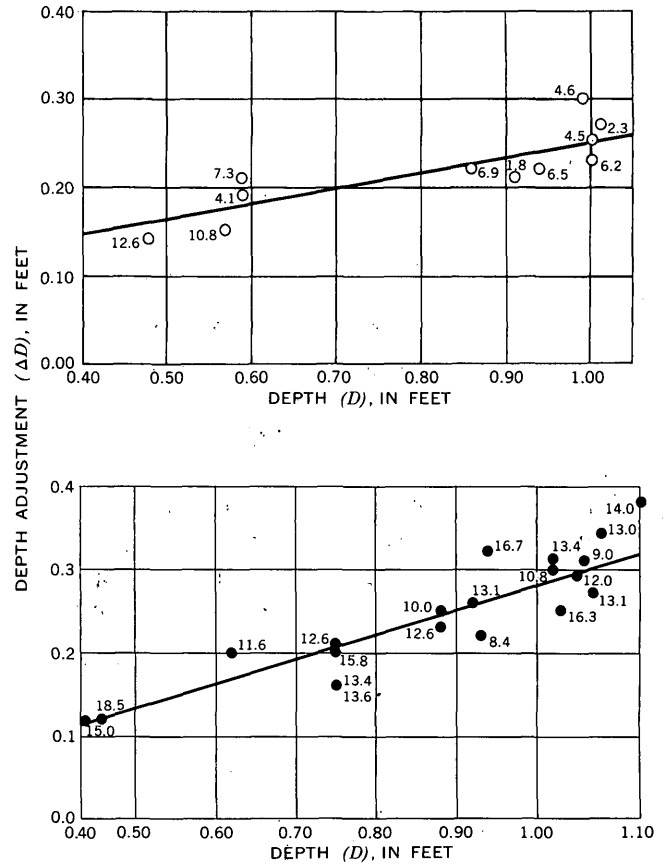


FIGURE 50.—Relation between depth adjustment ( $\Delta D$ ), depth ( $D$ ), and slope ( $S \times 10^4$ ) for ripples (upper part) and dunes (lower part); sand II.

the coarser (sand IV) bed material. The  $\Delta D$  versus  $D$  relation is a function of slope for the dune-bed configuration for all sands if field data are considered. With a significant relation between  $\Delta D$ ,  $D$ , and  $S$  for the different bed forms and bed materials, it is now possible to determine the average velocity by adjusting the depth of flow to an equivalent plane-bed depth.

This method of determining average velocity can be summarized as follows. If the depth, the median fall diameter of the bed material, and the bed configuration are known,  $\Delta D$  can be estimated; then, knowing  $D$ , the term  $D' = D - \Delta D$  can be computed. Next, if the slope of the energy gradient is known, the average plane-bed shear velocity,  $V'_* = \sqrt{gD'S}$ , can be evaluated, and the value of  $V'$  can be computed using equation 25,

$$V' = C'/\sqrt{g} \sqrt{gD'S}. \quad (25)$$

From the continuity relation,

$$V = V'D'/D \quad (24)$$

the average velocity can be computed. The size of bed material and the corresponding text figure to be used in determining  $\Delta D$  for other bed materials with

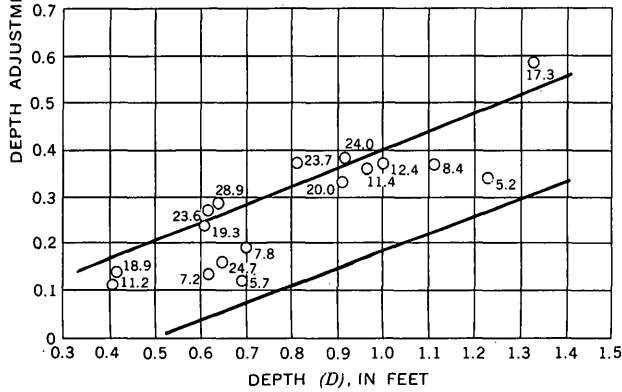
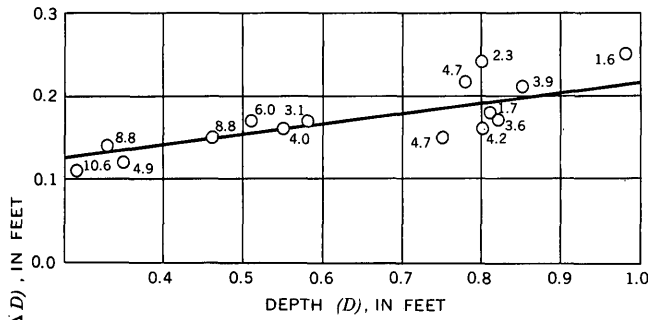


FIGURE 51.—Relation between depth adjustment ( $\Delta D$ ), depth ( $D$ ), and slope ( $S \times 10^4$ ) for ripples (upper part) and dunes (lower part); sand III.

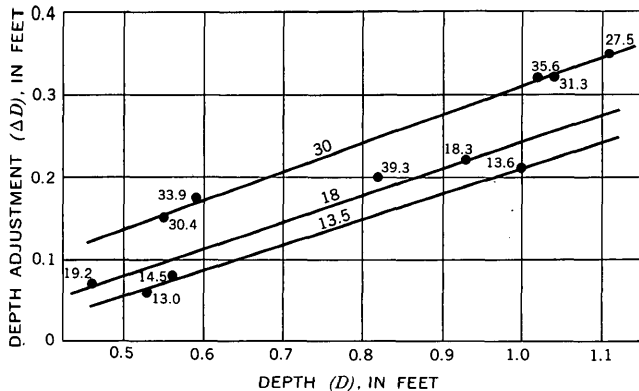


FIGURE 52.—Relation between depth adjustment ( $\Delta D$ ), depth ( $D$ ), and slope ( $S \times 10^4$ ) for dunes; sand IV.

either the ripple- or dune-bed configuration are given in table 6. Similar relations can also be developed for transition or antidune roughness.

Using the data for canals with a dune bed presented by Simons (1957) and by Harza Engineering Co., International (1963) and the average grain-roughness relations developed using data from the 8-foot-wide flume, values of  $\Delta D$ ,  $D$ , and  $S$  for various size ranges of bed material were plotted to give figures 53 and 54. For field conditions, in which

TABLE 6.—Bed configurations and range in size of bed material for which figures 49–52 can be used to determine the  $\Delta D$  adjustment based on an average grain roughness

Figure	Bed configuration	Range of median fall diameters of the bed material for which each figure can be used (mm)
49	Ripples	0.14–0.25
	Dunes	
50	Ripples	0.25–0.35
	Dunes	
51	Ripples	0.35–0.55
	Dunes	
52	Dunes	0.9–1.0

depths are greater, slope is a major variable in the  $\Delta D$ ,  $D$ , and  $S$  relations. For flume conditions, in which depths are shallower, slope is not a major variable. However, the flume data are compatible with the field data. The usefulness of such relations requires further discussion.

**Applications**

Velocity and discharge are determined by using figures 53 and 54 and making an initial estimate of form roughness and then using the other known variables,  $D$ ,  $S$ , and  $d_{50}$ , computing the average velocity ( $V$ ). As a check, it is necessary to enter figure 28 with the stream power, based on computed velocity, and median fall diameter of bed material ( $d_{50}$ ) to see if, in fact, the assumed bed roughness will actually occur. This procedure must be repeated until agreement exists.

In the design of stable channels, the water discharge is known; the form of bed roughness is selected (usually dunes for sand-bed channels); the size of the bed material of the proposed channel is estimated by studying the river characteristics, the diversion conditions, and the natural material in which the channel is to be constructed; and an estimate is made of the bed-material discharge from the river to the canal. A depth of flow is selected from  $D$  versus  $Q$  or  $R$  versus  $Q$  relations based on stable-channel data. These are the regime-type relations described by Simons (1957) and Simons and Albertson (1963). A figure, such as 53 or 54, that is appropriate for the anticipated size of bed material in the canal and form of bed roughness can be entered with the selected depth of flow. A limited choice of slope is available. If the canal must carry a relatively large bed-material discharge, select a steep slope. The depth of flow and the tentative slope fixes the depth adjustment ( $\Delta D$ ). The average velocity is computed using equations 24 and 25. Stream power is then computed. Using the  $d_{50}$  of the bed material, determine if the assumed bed roughness agrees with

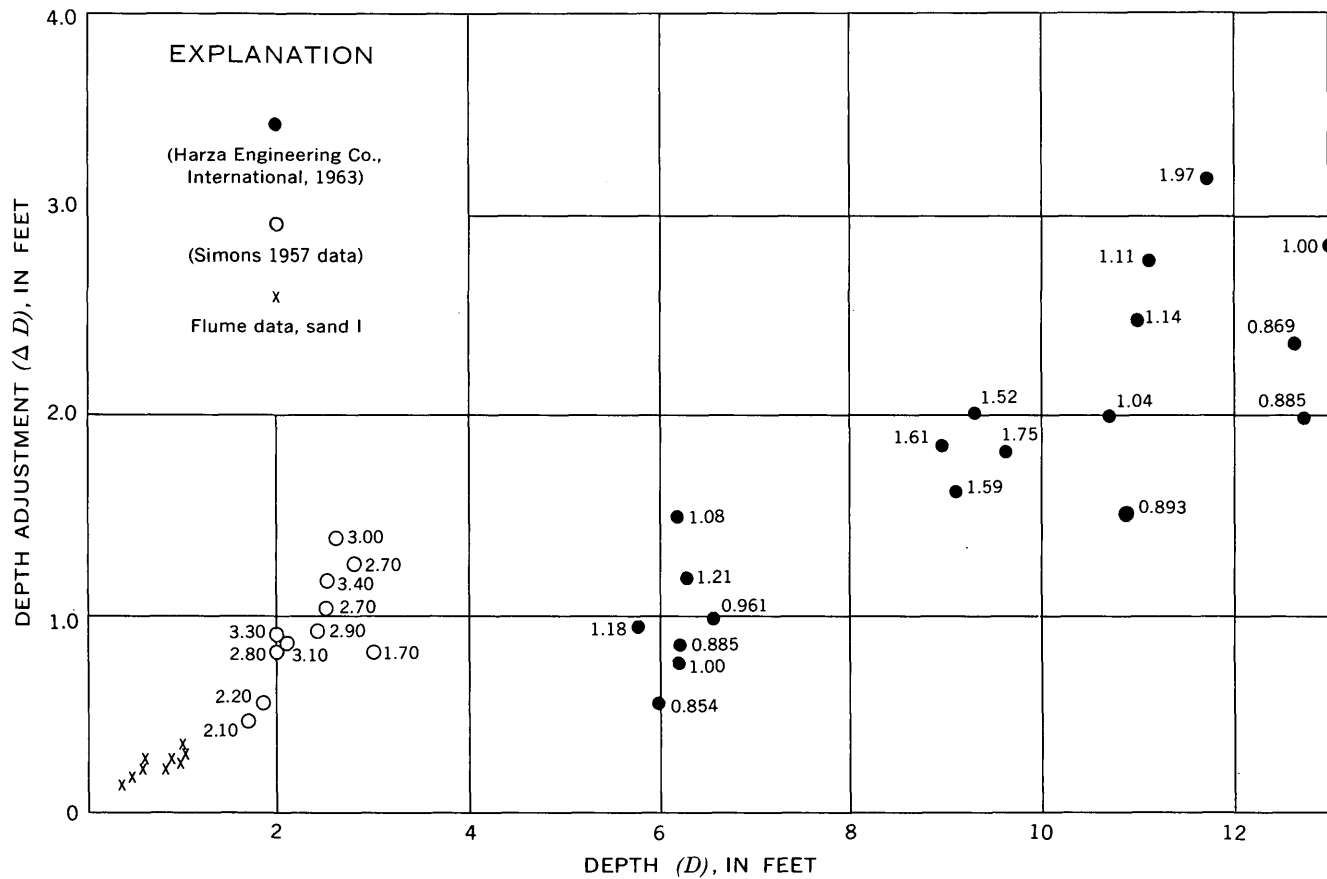


FIGURE 53.—Relation between the depth adjustment ( $\Delta D$ ), depth ( $D$ ), and slope ( $S \times 10^4$ ) for dunes (flume data and field data;  $d_{50}$  ranges from 0.15 to 0.25 mm).

that given in figure 28. If there is disagreement, the geometry of the channel must be modified until there is agreement. When this phase of the design is completed, the bed-material-discharge capacity of the canal is computed using some appropriate procedure, such as that proposed by Colby (1964). If the bed-material discharge differs from the required capacity based on river and canal conditions, another revision is made in the design, such as a change in depth and (or) slope, to increase or decrease the bed-material discharge to as near the required value as possible without changing the bed form. In many channels, conditions for stability can only be achieved by including exclusion and (or) ejection structures to control the quantity of bed material entering the canal from the river. Finally, by dividing the known discharge by the selected depth and computed velocity, the average width of canal is calculated.

If the depth relations and figure 28 are used to design stable channels to convey a given discharge, it will be necessary to avoid designs which have a combination of stream power and median fall diameter that plots close to the dividing line between dunes and upper regime (usually plane bed) flow. In this region a slight error, a change in fall velocity

of bed material, or just the inherent error in figure 28 may be sufficient to give an altogether different form roughness than is desired. This can be a very serious error because the change in resistance to flow between plane bed and dunes is generally on the order of 100 percent. If one designs a channel anticipating dunes as the bed roughness ( $C/\sqrt{g}$  value of about 12) but a plane bed develops ( $C/\sqrt{g}$  value of about 20), the velocity in the channel would be almost double that anticipated. Because the depth would be fairly great, it would be much more difficult to divert flow from the channel, maintain stable banks in the channel, and supply bed material at a rate equal to the channel's new transport capacity.

The accuracy of predicting average velocity by use of the foregoing method for both laboratory and field conditions is indicated in figure 55. The average error is about 5 percent for the laboratory data and about 10 percent for the field data.

To show the usefulness of this approach, resistance diagrams relating  $C/\sqrt{g}$  and  $R$  for different values of  $\Delta D/D$  or  $\Delta R/R$  can be developed. In these diagrams the ratio  $\Delta D/D$  or  $\Delta R/R$  is similar to the measure of relative roughness  $\xi/D$  or  $\xi/R$  in the resistance diagram for pipes. A typical relation

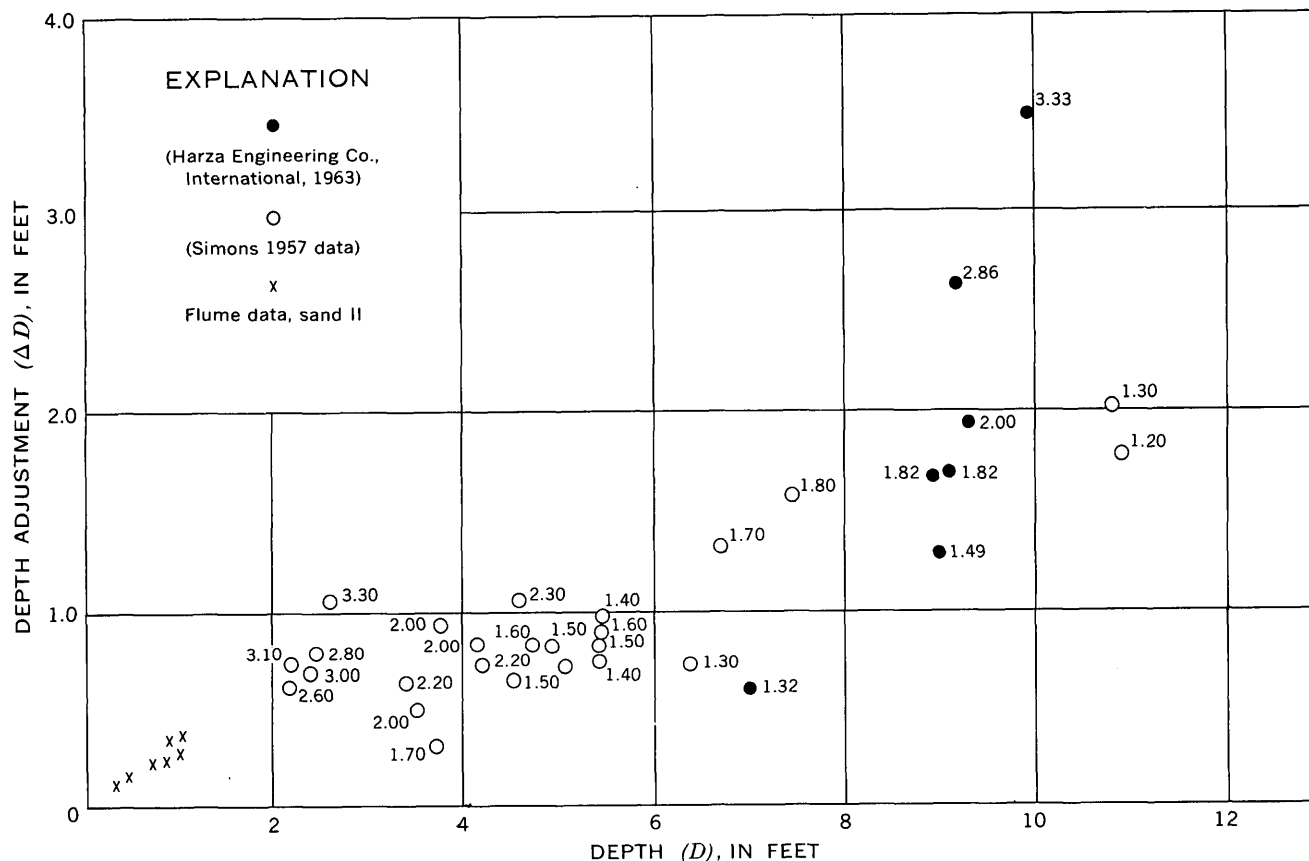


FIGURE 54.—Relation between the depth adjustment ( $\Delta D$ ), depth ( $D$ ), and slope ( $S \times 10^4$ ) for dunes (flume data and field data;  $d_{50}$  ranges from 0.25 to 0.35 mm).

between  $C/\sqrt{g}$ ,  $R$ , and  $\Delta D/D$  for sand II is shown in figure 56. The  $\Delta D/D$  ratio is a function of bed configuration and size of the bed material, so that a general equation cannot be developed as in studies of channels with rigid boundaries. However, this procedure can be applied to rigid-boundary problems.

**BAFFLE AND CUBE ROUGHNESS**

The applicability of the foregoing concept to rigid channels having baffles or cubes as the roughness elements was investigated to test the generality of the method. The baffles and cubes, like dunes, cause zones of separation, turbulence, changes in velocity distribution, and considerable dissipation of energy. A constant resistance coefficient for an average grain roughness can be assumed, and the measured depth in the channel containing baffles and cubes can be adjusted to an equivalent depth in a channel having the same slope and discharge. Then, as in studies of alluvial channels, a relation between the depth adjustment  $\Delta D$  and  $D$  can be determined. With this relation and the assumed resistance coefficient, the velocity can be determined for flow over a boundary having baffle and cube roughness.

If the average grain roughness for a channel containing baffles and cubes is the same as for the 0.19-mm sand, then

$$C'/\sqrt{g} = V/\sqrt{gD'S} = 18.91 \quad (27)$$

or

$$D' = V^2/(18.91^2gS)$$

and

$$\Delta D = D - D' = D - V^2/(18.91^2gS). \quad (28)$$

The depth adjustment ( $\Delta D$ ) is an indirect measure of the total effect of the form roughness in question. If for a given form roughness, values of  $\Delta D$  are plotted against average depth ( $D$ ), a unique relation results for each specific type of roughness. (See fig. 57.) Then, for this type of roughness, if the depth ( $D$ ) and slope ( $S$ ) are known, one can evaluate  $\Delta D$ ,  $D'$ ,  $\sqrt{gD'S}$ ,  $V'$ , and finally, the average velocity,  $V = \frac{V'D'}{D}$ . The whole scheme is shown in figure 57, which is based on data from studies by Sayre and Albertson (1963) and Koloseus and Davidian

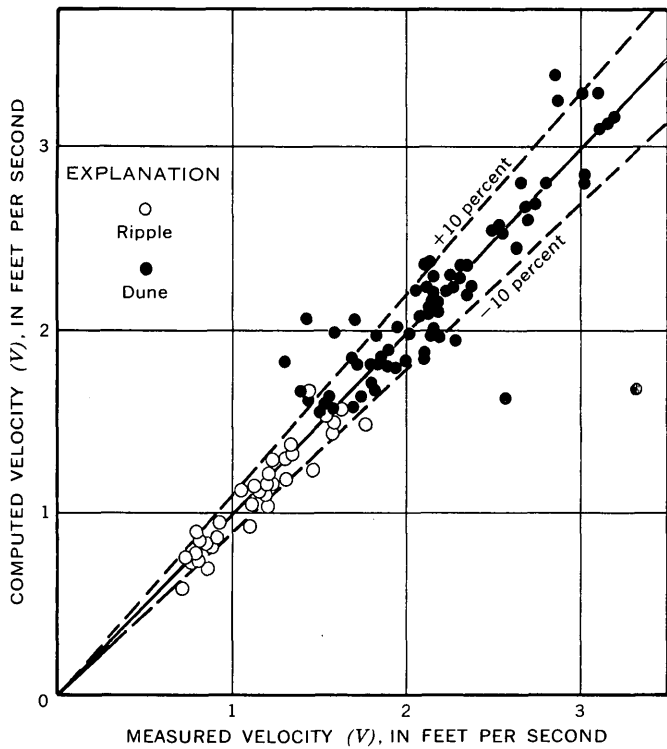


FIGURE 55.—Comparison of the computed velocity with the measured velocity. The velocity was computed by adjusting depth to the equivalent depth for a channel having average grain roughness. Roughness is ripples and dunes, and the data were from the 8-foot-wide flume, Punjab canals (Simons, 1957), and Pakistan canals (Harza Engineering Co., Internat., 1963).

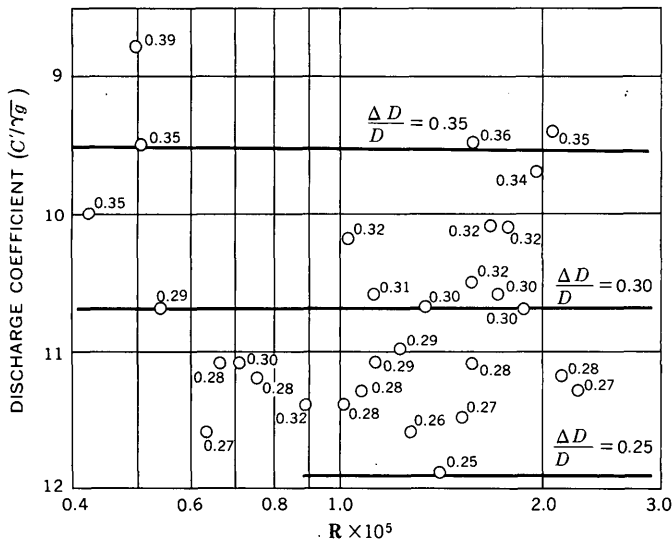


FIGURE 56.—Relation between discharge coefficient ( $C'/\sqrt{g}$ ), and Reynolds number ( $R$ ) for different  $\Delta D/D$  ratios. Bed configuration is ripples and dunes in sand II.

(1961). The upper six lines in the  $\Delta D$  versus  $D$  relation are for Sayre's  $A_1$ ,  $B_1$ ,  $A_2$ ,  $B_2$ ,  $C_1$  and  $C_2$  roughnesses formed by baffles at different spacings. The lower four curves are for Koloseus and Davidian's  $\lambda = 1/8$ ,  $\lambda = 1/32$ ,  $\lambda = 1/128$ , and  $\lambda = 1/512$  cube roughnesses.

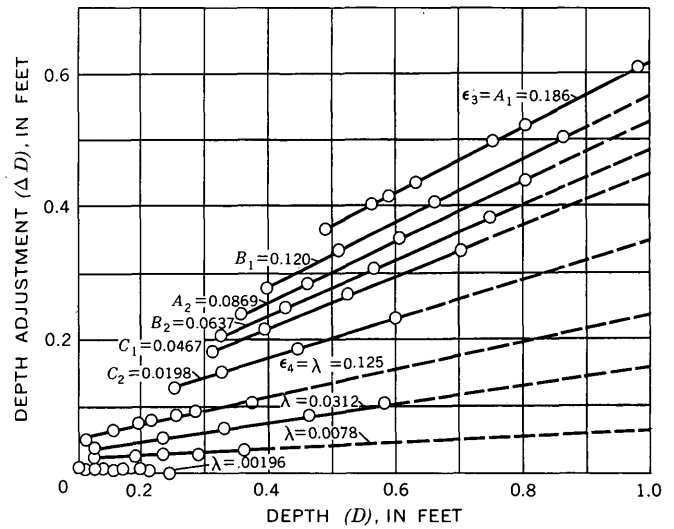


FIGURE 57.—Relation between depth adjustment ( $\Delta D$ ) and depth ( $D$ ) for the type of form roughness in the rigid-boundary flume.  $\xi_3$  refers to Sayre and Albertson's (1963) roughness coefficient, and  $\xi_1$  refers to Koloseus and Davidian's (1961) roughness coefficient.

The general equation for the family of lines in the  $\Delta D$  versus  $D$  relation in figure 57 is

$$\Delta D = MD + b, \tag{29}$$

and the general solution for  $C'/\sqrt{g}$  for these roughness elements is

$$C'/\sqrt{g} = 18.91 \frac{D - (MD + b)^{3/2}}{D}$$

or

$$V = \frac{V'D'}{D} = 18.91 \frac{D - MD - b^{3/2}}{D} \sqrt{gDS}, \tag{30}$$

where

$V$  = the average velocity,

$D$  = the average depth,

$M$  = the slope of the lines in the  $\Delta D$  versus  $D$  relation,

$b$  = a function of the  $Y$ -intercept in the  $\Delta D$  versus  $D$  relation, and

$S$  = the slope of the energy-grade line.

ADJUSTING DEPTH TO SMOOTH BOUNDARY ROUGHNESS

Depth adjustments were determined by adjusting depth and velocity to an equivalent average grain roughness. The same effect is accomplished by correcting data for hydraulically rough channels, both rigid and alluvial, to fit the rigid-channel hydraulically smooth boundary relation presented by Tracy and Lester (1961). That is,

$$C'/\sqrt{g} = 5.75 \log \frac{R}{C'/\sqrt{g}} + 2.38, \tag{31}$$

where

$C'/\sqrt{g}$  = Chezy discharge coefficient for hydraulically smooth rigid open channels, and

$R$  = Reynolds number,  $VR/\nu$ , which becomes  $VD/\nu$  for channels where sidewall effect can be neglected.

Equation 31 indicates that the discharge coefficient is a function of depth, slope, and temperature.

$$C'/\sqrt{g} = \phi(D'_s, S, T) \quad (32)$$

where

$D'_s$  = equivalent smooth-channel depth for the same slope ( $S$ ) and discharge, and

$T$  = temperature of the flow.

If both discharge and temperature are constant, a relation between  $C'/\sqrt{g}$ ,  $D'_s$ , and  $S$  can be developed. (See fig. 58.) A quantitative relation can be written which expresses  $C'/\sqrt{g}$  versus  $D'_s$  and, holding the slope ( $S$ ) and the unit discharge ( $q$ ) constant, figure 59 is obtained. Using the results shown in figures 58 and 59, the smooth-boundary resistance ( $C'/\sqrt{g}$ ) given by equation 31 can be expressed as

$$C'/\sqrt{g} = \phi(D'_s, S, T) = 8.4 \left[ \log \frac{D'_s S^{1/3}}{3.52 - 1.415 \log T} + 4.132 \right] \quad (33)$$

To develop a general method of adjusting the hydraulic radius of a particular run to the smooth-boundary relation, first assume that the change in the wetted perimeter ( $P$ ) is incorporated into the

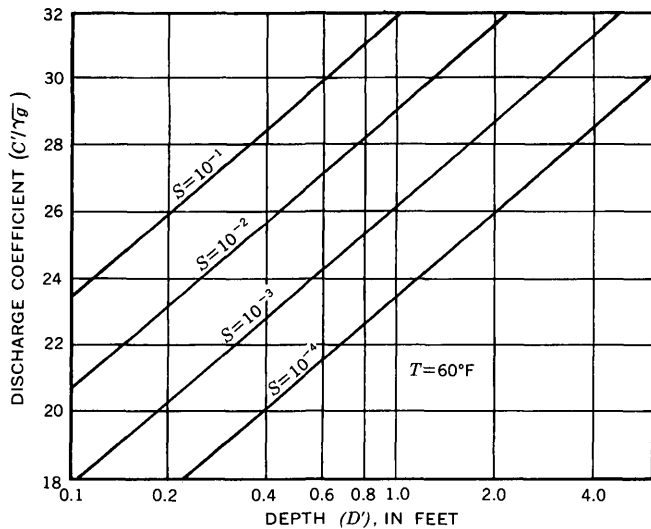


FIGURE 58.—Relation between discharge coefficient ( $C'/\sqrt{g}$ ), depth ( $D'$ ), and slope ( $S$ ). Unit discharge ( $q$ ) and temperature ( $T$ ) are constant.

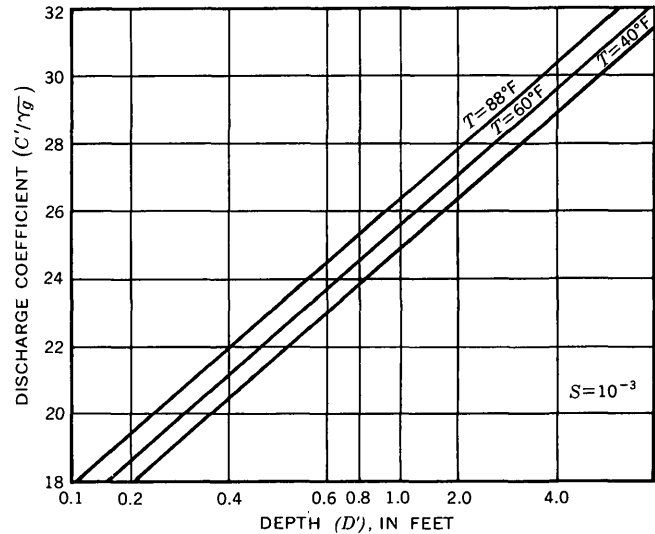


FIGURE 59.—Relation between discharge coefficient ( $C'/\sqrt{g}$ ), depth ( $D'$ ), and temperature ( $T$ ). Unit discharge ( $q$ ) and slope ( $S$ ) are constant.

adjusted hydraulic radius. Then, from the continuity equation,

$$Q = AV = A'V', \quad RPV = R'P'V', \quad RV = R' \frac{P'}{P} V' = R'_s V', \quad (34)$$

and for constant temperature,  $\frac{V'R'_s}{\nu} = \frac{V'R}{\nu}$ .

The Chezy relation for smooth or equivalent boundary flow is

$$V' = C'/\sqrt{g} \sqrt{gR'_s S}. \quad (35)$$

Solving equations 34 and 35 simultaneously for  $R'_s$ ,

$$R'_s = \left[ \frac{VR}{C'/\sqrt{g} \sqrt{gS}} \right]^{2/3}. \quad (36)$$

The correction to the hydraulic radius ( $\Delta R$ ) required to plot a particular run on the smooth boundary relation is

$$\Delta R = R - R'_s = R - \left[ \frac{VR}{C'/\sqrt{g} \sqrt{gS}} \right]^{2/3}, \quad (37)$$

or for channel conditions such that  $R \approx D$ ,

$$\Delta D = D - \left[ \frac{VD}{C'/\sqrt{g} \sqrt{gS}} \right]^{2/3} = D - \left[ \frac{q}{C'/\sqrt{g} \sqrt{gS}} \right]^{2/3}. \quad (38)$$

Values of  $\Delta R$  or  $\Delta D$  can be computed using either equation 37 or 38, and from these values  $\Delta R$  versus  $R$  or  $\Delta D$  versus  $D$  relations can be developed.

For a particular roughness it appears that using  $\Delta R$  versus  $R$  or  $\Delta D$  versus  $D$  relations to adjust  $R$

or  $D$  to  $R'_s$  or  $D'_s$ , and using equations 33, 34, and 35, the average velocity can be estimated. This procedure will be discussed in detail after the required relations are developed.

An alternative for determining the average velocity is suggested by referring to the resistance diagram in figure 56, which relates  $C/\sqrt{g}$ ,  $R$ , and  $\Delta D/D$ . If in such a resistance diagram a new parameter,

$$R \left[ \frac{C}{\sqrt{g}} \right]^{-1} = R_* = \frac{V_* D}{\nu} \text{ or } \frac{V_* R}{\nu}, \quad (39)$$

is adopted, a new resistance diagram relating  $C/\sqrt{g}$ ,  $V_* D/\nu$ , and  $\Delta D/D$  can be developed. It is then possible to use the  $\Delta D$  versus  $D$  relation and the new resistance diagram to establish average velocity for a given boundary roughness. This concept will also be tested and discussed in more detail.

**BAFFLE AND CUBE ROUGHNESS**

Using the data of Sayre and Albertson (1961) and Koloseus and Davidian (1961), in which the

bed roughness and the width of channel are large so that  $R \approx D$ , the value of  $\Delta D$  for each run for each roughness was computed using equation 38.

The relations between  $\Delta D$  and  $D$  for each of the families of roughness patterns studied are shown in figure 60. Resistance diagrams relating  $C/\sqrt{g}$ ,  $R_* = V_* D/\nu$ , and  $\Delta D/D$  were prepared as outlined in the preceding section for both Sayre and Albertson's (1961) and Koloseus and Davidian's (1961) data. These diagrams are presented in figures 61 and 62, respectively.

As with the  $\Delta D$  versus  $D$  relations, where  $\Delta D$  was based on plane-bed roughness, the results based on the smooth bed are excellent.

**GRAVEL AND COBBLE ROUGHNESS**

The flume data of Kharrufa (1962) and equation 38 were used to compute  $\Delta D$ . The relations between  $\Delta D$  and  $D$  for Kharrufa's type  $B$  and  $H$  rock roughnesses, which have diameters of 4 and 2 inches, respectively, are given in figure 63. Also, a resistance diagram was developed using the flume rock

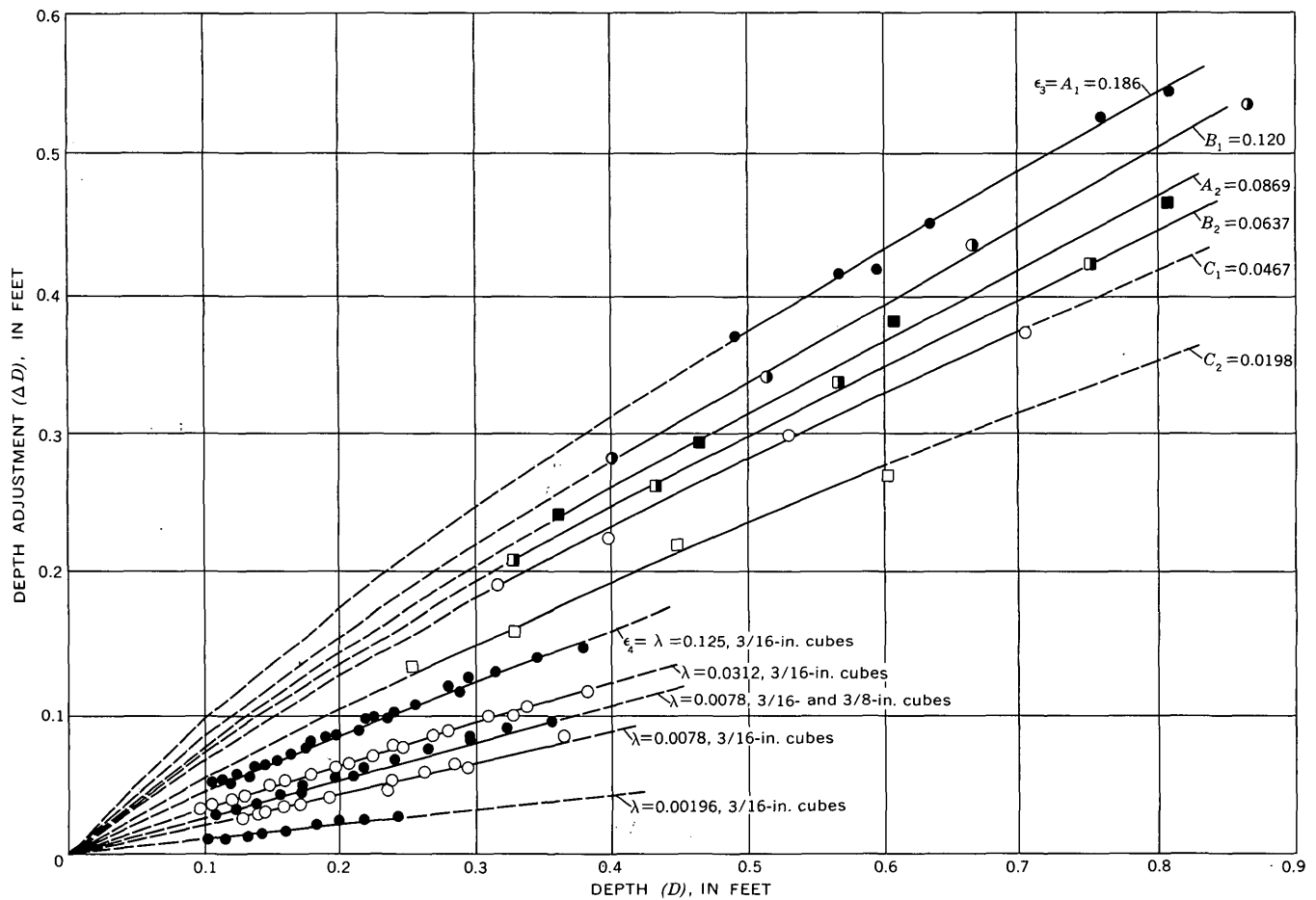


FIGURE 60.—Relation between the depth adjustment ( $\Delta D$ ) and depth ( $D$ ) for baffle and cube roughness elements.  $\xi_3$  refers to Sayre and Albertson's roughness coefficient, and  $\xi_4$  refers to Koloseus and Davidian's (1961) roughness coefficient.

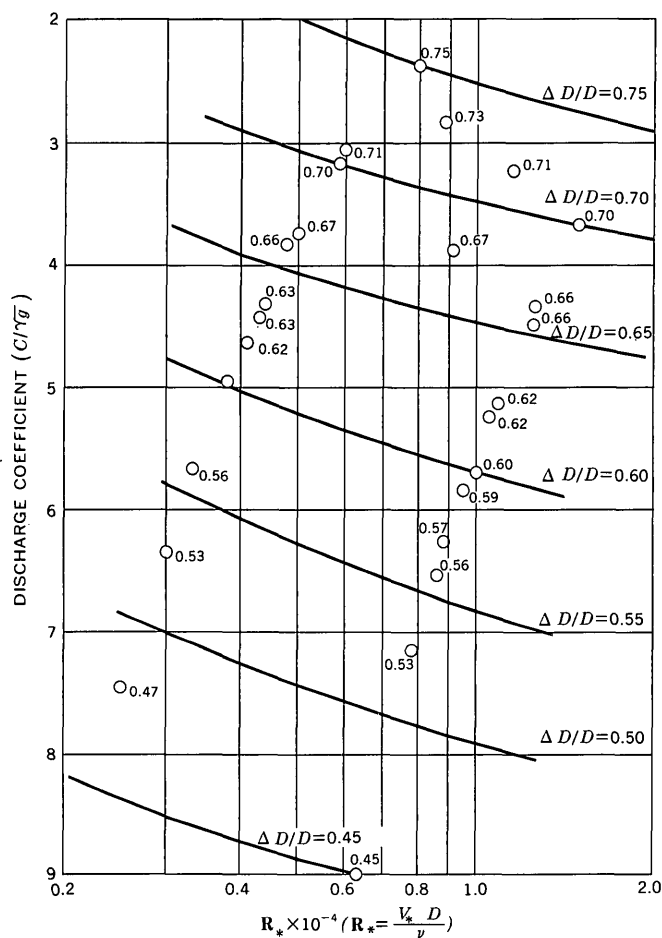


FIGURE 61.—Resistance diagram relating  $C/\sqrt{g}$ ,  $R_*$ , and  $\Delta D/D$  for the baffle roughness (Sayre and Albertson, 1963).

roughness for a limited number of these runs. (See fig. 64.)

Study of natural cobble roughness was possible using data from Lane and Carlson's (1953) examination of irrigation canals in the San Luis Valley, Colo. (fig. 65). The resultant roughness, a paved cobble bed, resulted from the interaction of the bed material and the flow. Values of  $\Delta D$  for these canals were determined using equation 38. The canals were divided into three groups on the basis of the median size of the bed material at the streambed-water interface. The bed material in one group had a median diameter of about 3 inches, that in another group, about 2 inches, and that in the last group, about 1½ inches. The  $\Delta D$  versus  $D$  relations for each of these groups of canals are given in figure 66. The corresponding resistance diagram is given in figure 67. As with the rigid-boundary roughnesses previously considered,  $\Delta D$  is independent of slope; but in canals it can remain independent of slope only as long as the bed material is stable. If a large dis-

charge was turned into any of these canals, a boundary shear could develop that would cause movement of bed material. The bed material would ultimately become a little coarser through transportation of some of the smaller particles and movement of larger roughness elements into new positions. The previous  $\Delta D$  versus  $D$  relation may no longer hold after such a flow condition, because a new boundary condition is developed by the flow. Also, a dune-bed configuration may develop that would be residual at lower discharge.

#### ALLUVIAL SAND-BED ROUGHNESS

Sand-bed roughness is much more complex than the baffle, cube, and rock roughnesses. Form roughness is a function of flow. A small change in any variable affecting the form of bed roughness will cause a change in the bed roughness and the resistance to flow. However,  $\Delta R$  versus  $R$  or  $\Delta D$  versus  $D$  relations can be developed for the bed form shown in figure 3.

For the flume data,  $D \approx R$ , and the relations are in terms of  $\Delta D$  and  $D$ .

As can be seen in equation 32,  $C'/\sqrt{g}$  and, hence,  $\Delta D$ , for a constant ( $q$ ) are a function of the slope and depth of the channel. Also,  $\Delta D$  is more strongly dependent on slope when the bed form is dunes in the coarser sands. (See figs. 68 and 69.)

In contrast to the previous study for sand bed roughness where  $\Delta D$  was determined by correcting to an average sand-grain roughness, in this section  $\Delta D$  is determined by correcting to the hydraulically smooth, rigid-boundary conditions, and it will not be zero for the plane bed. The  $\Delta D$  versus  $D$  relation for plane-bed runs using sand I is given in figure 70. A similar relation using slope as the abscissa for plotting antidune flow is given in figure 71. Similar relations for the other forms of bed roughness and other bed materials can be developed.

Although the resistance diagram for the flume data could be more precise if separate diagrams were made for each form roughness and size of bed material, only one diagram has been prepared. (See fig. 72.) This diagram relates  $C/\sqrt{g}$ ,  $R$ , and  $\Delta D/D$  for all the ripple and dune flume data. To show the possibilities of using this procedure to estimate the average velocity in alluvial channels, the foregoing analysis was applied to the Punjab canal data reported by Simons (1957) and the more recently collected Pakistan canal data reported by Harza Engineering Co., International (1963). Relations based on these data were prepared in terms of the hydraulic

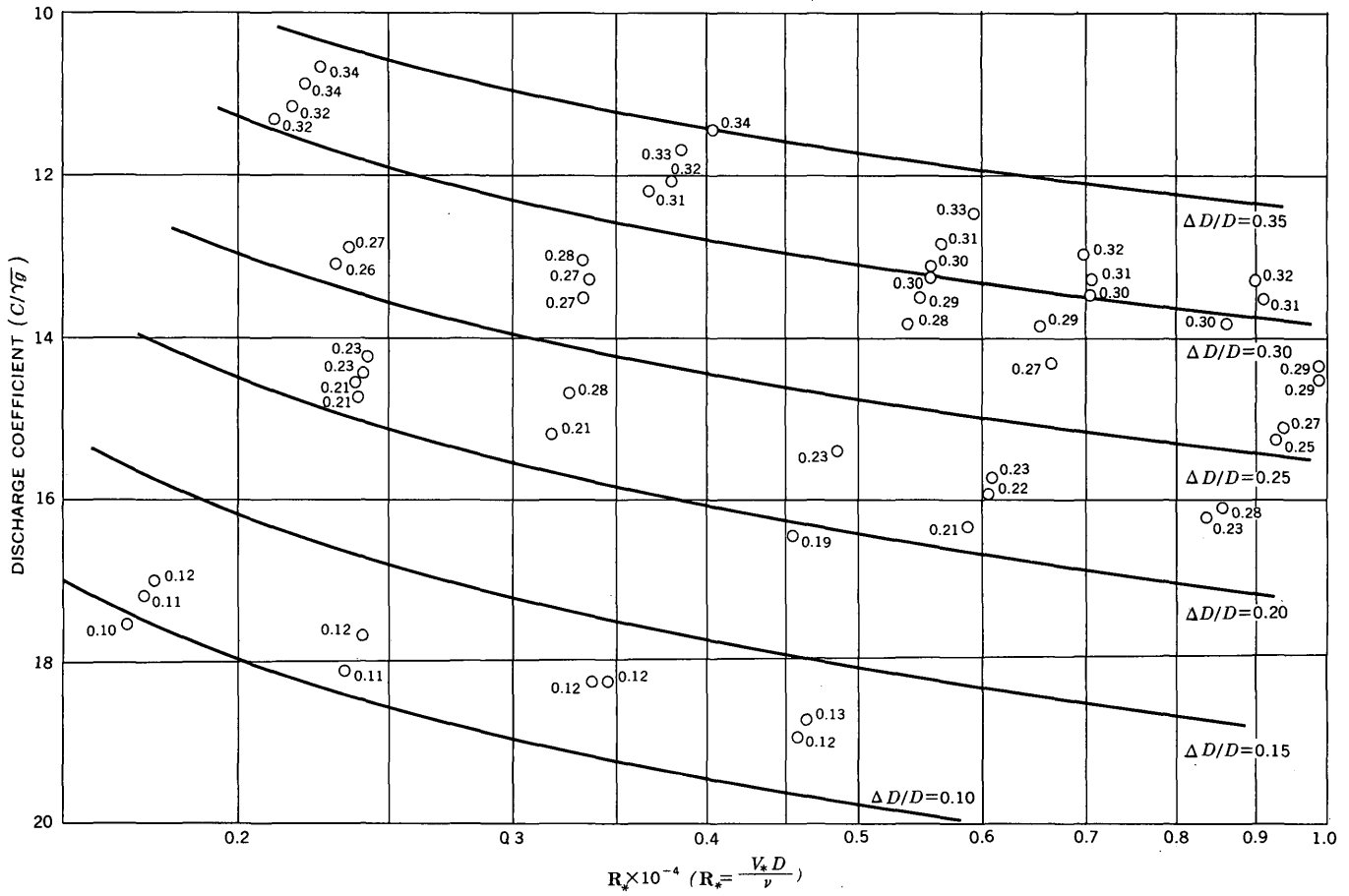


FIGURE 62.—Resistance diagram relating  $C/\sqrt{g}$ ,  $R_*$ , and  $\Delta D/D$  for cube roughness (Koloseus and Davidian, 1961).

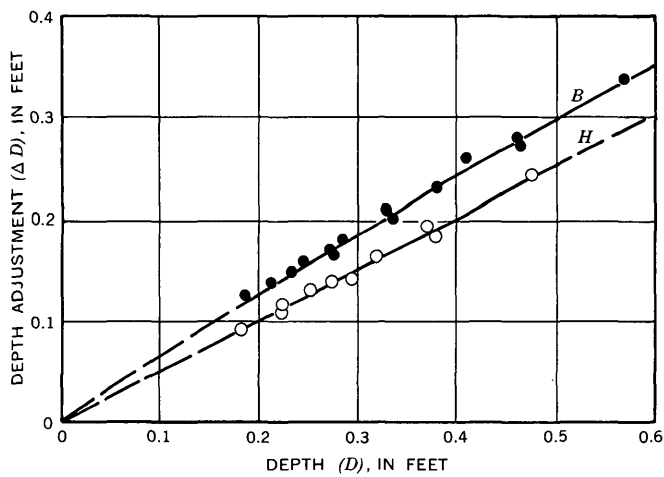


FIGURE 63.—Relation between depth adjustment ( $\Delta D$ ) and  $D$  for rock roughness in a flume.  $B$  and  $H$  rock roughness of Kharrufa (1962). Slope ranged from 0.001 to 0.09 foot per foot.

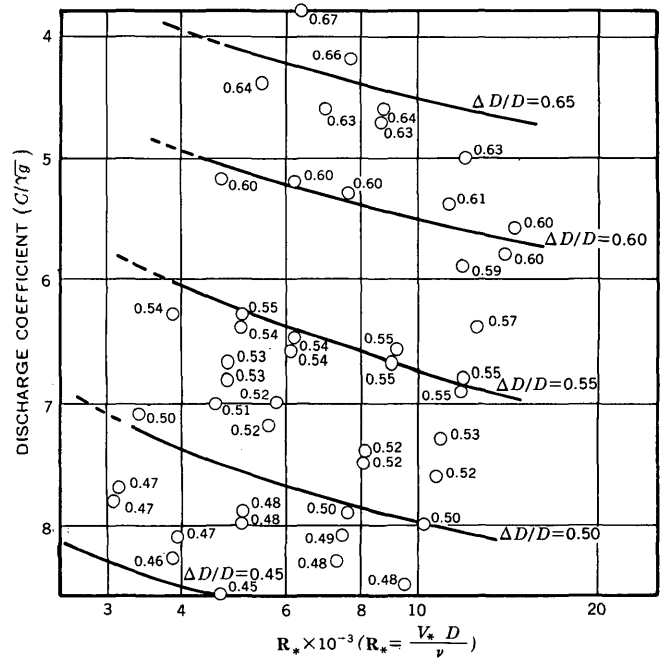


FIGURE 64.—Resistance diagram relating  $C/\sqrt{g}$ ,  $R_*$ , and  $\Delta D/D$  for rock roughness in a flume.  $B$  and  $H$  rock roughness of Kharrufa (1962).



FIGURE 65.—Typical San Luis Valley, Colo., canal with cobble roughness.

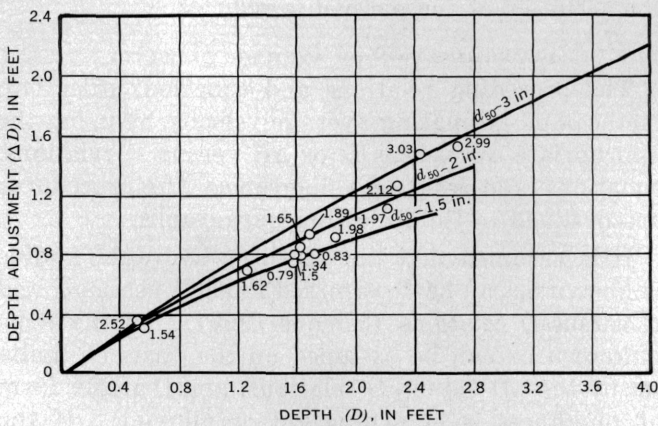


FIGURE 66.—Relation between depth adjustment ( $\Delta D$ ) and depth ( $D$ ) for the San Luis Valley, Colo., canals with cobble roughness (Lane and Carlson, 1953). The third variable is median diameter of the bed material, in inches.

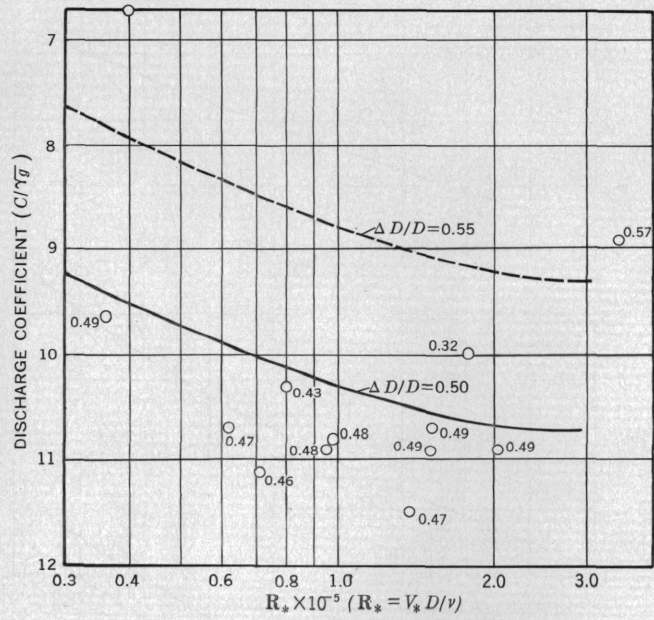


FIGURE 67.—Resistance diagram relating  $C/\sqrt{g}$ ,  $R_*$ , and  $\Delta D/D$  for the San Luis Valley, Colo., canals with cobble roughness.

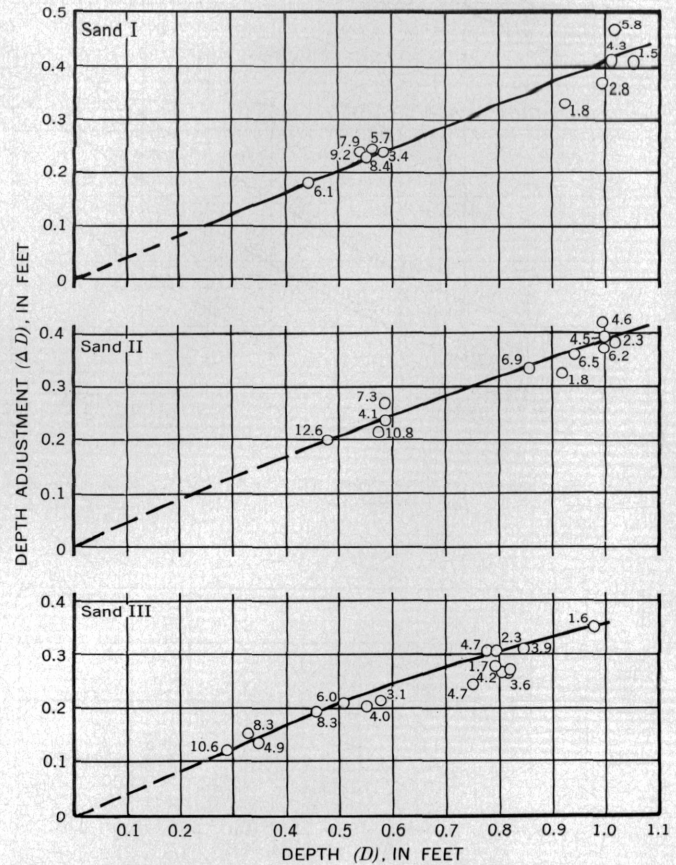


FIGURE 68.—Relation between depth adjustment ( $\Delta D$ ), depth ( $D$ ), and slope ( $S \times 10^4$ ) for the ripple-bed configuration in sands I, II, and III.

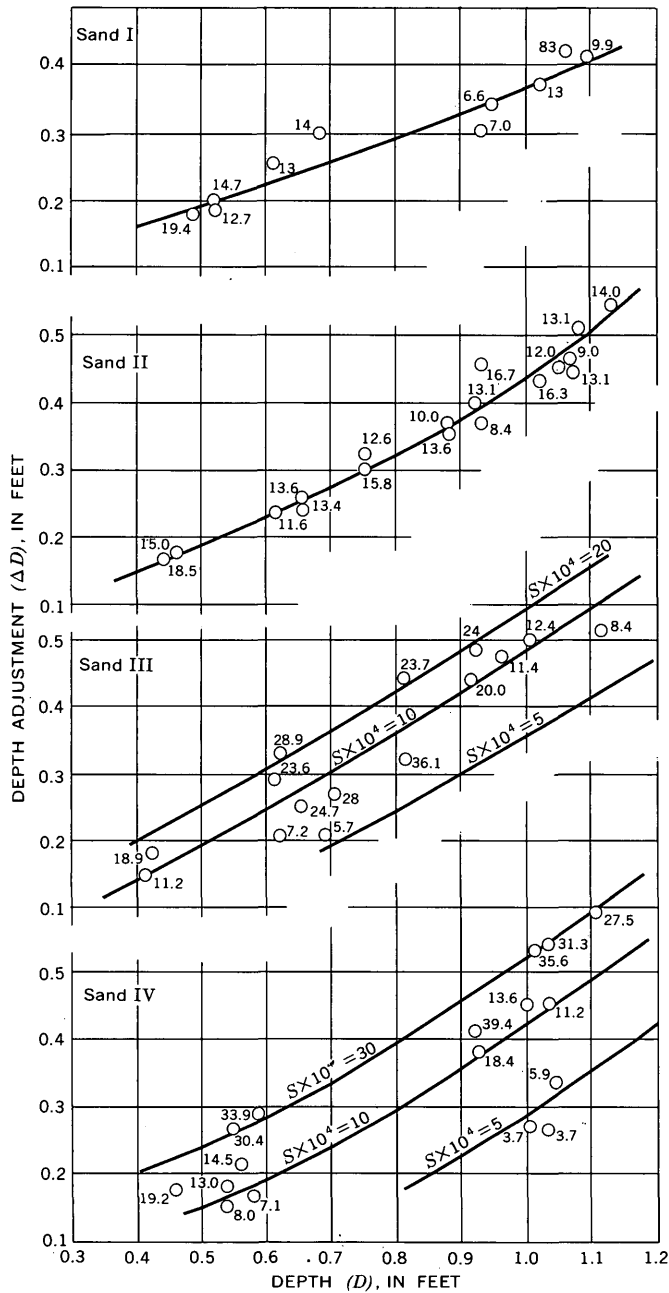


FIGURE 69.—Relation between depth adjustment ( $\Delta D$ ), depth ( $D$ ), and slope ( $S \times 10^4$ ) for the dune-bed configuration in sands I, II, III, and IV.

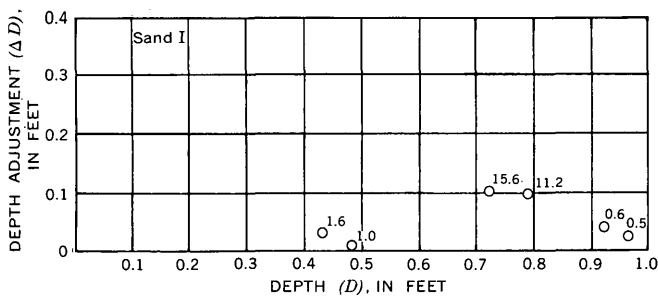


FIGURE 70.—Relation between depth adjustment ( $\Delta D$ ), depth ( $D$ ), and slope ( $S \times 10^4$ ) for a plane bed in sand I.

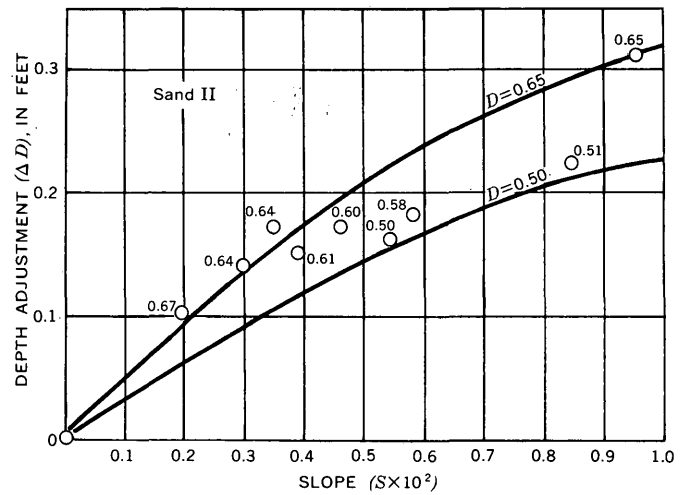


FIGURE 71.—Relation between depth adjustment ( $\Delta D$ ), depth ( $D$ ), and slope ( $S \times 10^2$ ) for antidune flow in sand II.

radius, although the relations would be equally valid if expressed in terms of depth and a depth correction.

Figure 73 presents the  $\Delta R$  versus  $R$  relation for the Punjab canals, which, according to the relationship given in figure 28, have a dune-bed roughness. The slope in the canals is a very significant third variable. The accompanying resistance relation for the Punjab canals is presented in figure 74.

Following an identical procedure, the  $\Delta R$  versus  $R$  relation for the Pakistan canals is presented in figure 75, and the resistance diagram is given in figure 76.

Similar relations were tested for field conditions using river-channel data. Very good results were obtained for channels having the same pattern throughout—that is, dunes, plane bed, or antidunes. However, if multiple roughness patterns and other complicating factors occur, such as a braided stream, the accuracy of the method is reduced.

DETERMINATION OF AVERAGE VELOCITY

The preceding relations and equations offer two methods of estimating average velocity by using the appropriate  $\Delta D$  versus  $D$  or  $\Delta R$  versus  $R$  relations, equations, and resistance diagrams. The procedures are outlined in the following paragraphs.

It is assumed that the depth or hydraulic radius is known or can be determined from  $D$  versus  $Q$  and  $R$  versus  $Q$  relations (Simons 1957), that the slope is known or can be assumed on the basis of limits set by the  $\Delta D$  versus  $D$  relations, and that the form of roughness is known (rigid or alluvial). If the boundary is alluvial, the median fall diameter of the bed material  $d_{50}$  must also be known. For many channels only an estimate of  $d_{50}$  is possible.

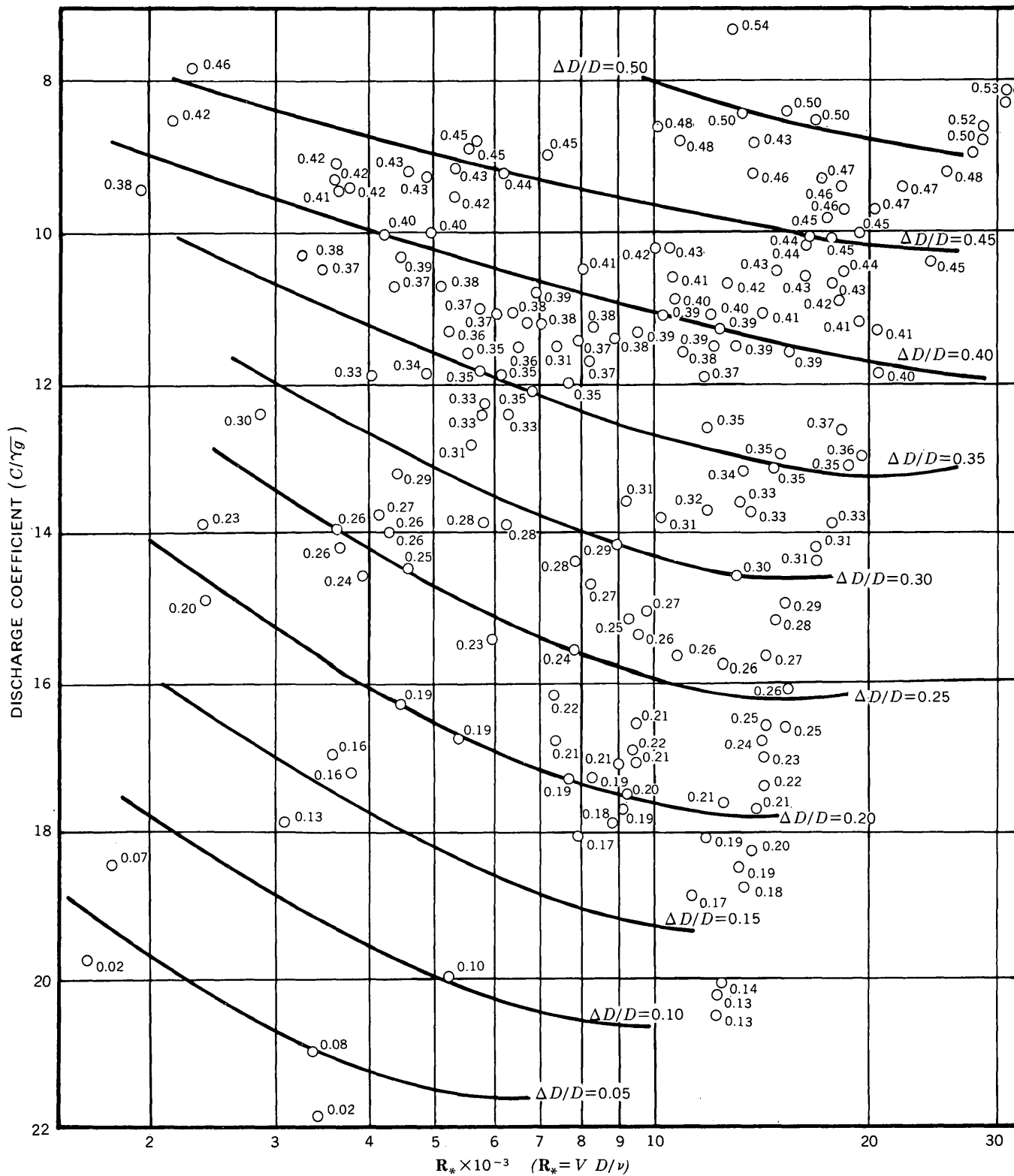


FIGURE 72.—Resistance diagram relating  $C/\sqrt{g}$ ,  $R_*$ , and  $\Delta D/D$  for ripples and dunes. Data for sands I, II, III, and IV in the 8-foot-wide flume.

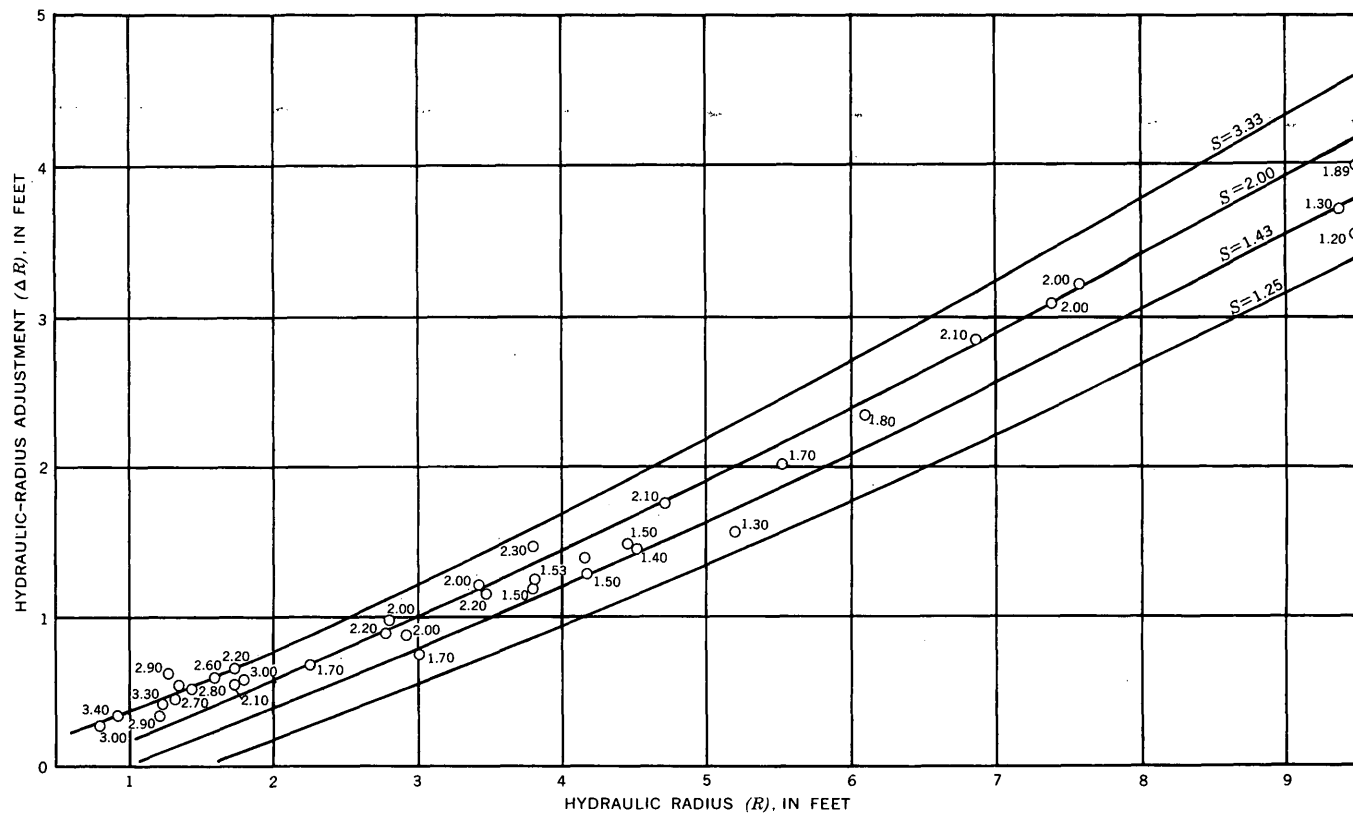


FIGURE 73.—Relation between the hydraulic-radius adjustment ( $\Delta R$ ), hydraulic radius ( $R$ ), and slope ( $S \times 10^4$ ) for Punjab canals (Simons, 1957).

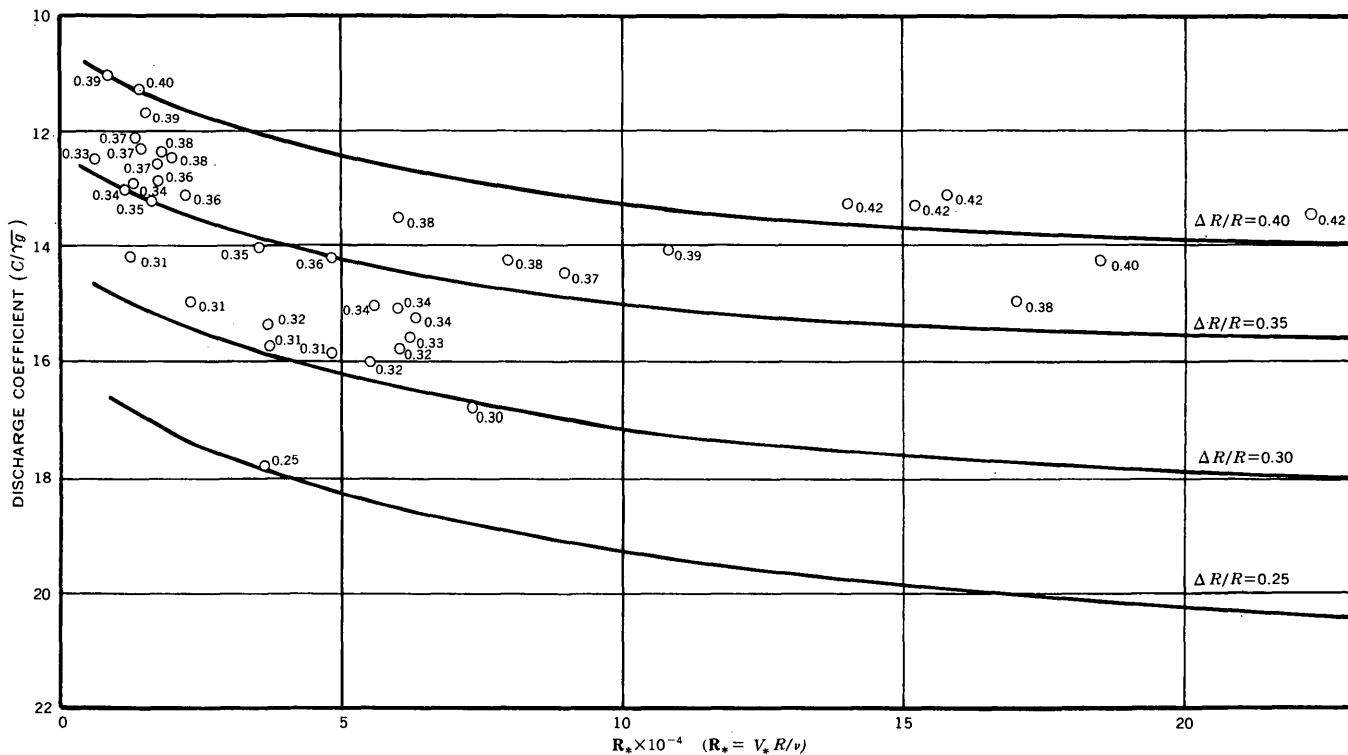


FIGURE 74.—Resistance diagram relating  $C/\sqrt{g}$ ,  $R_*$ , and  $\Delta R/R$  for Punjab canals (Simons, 1957).

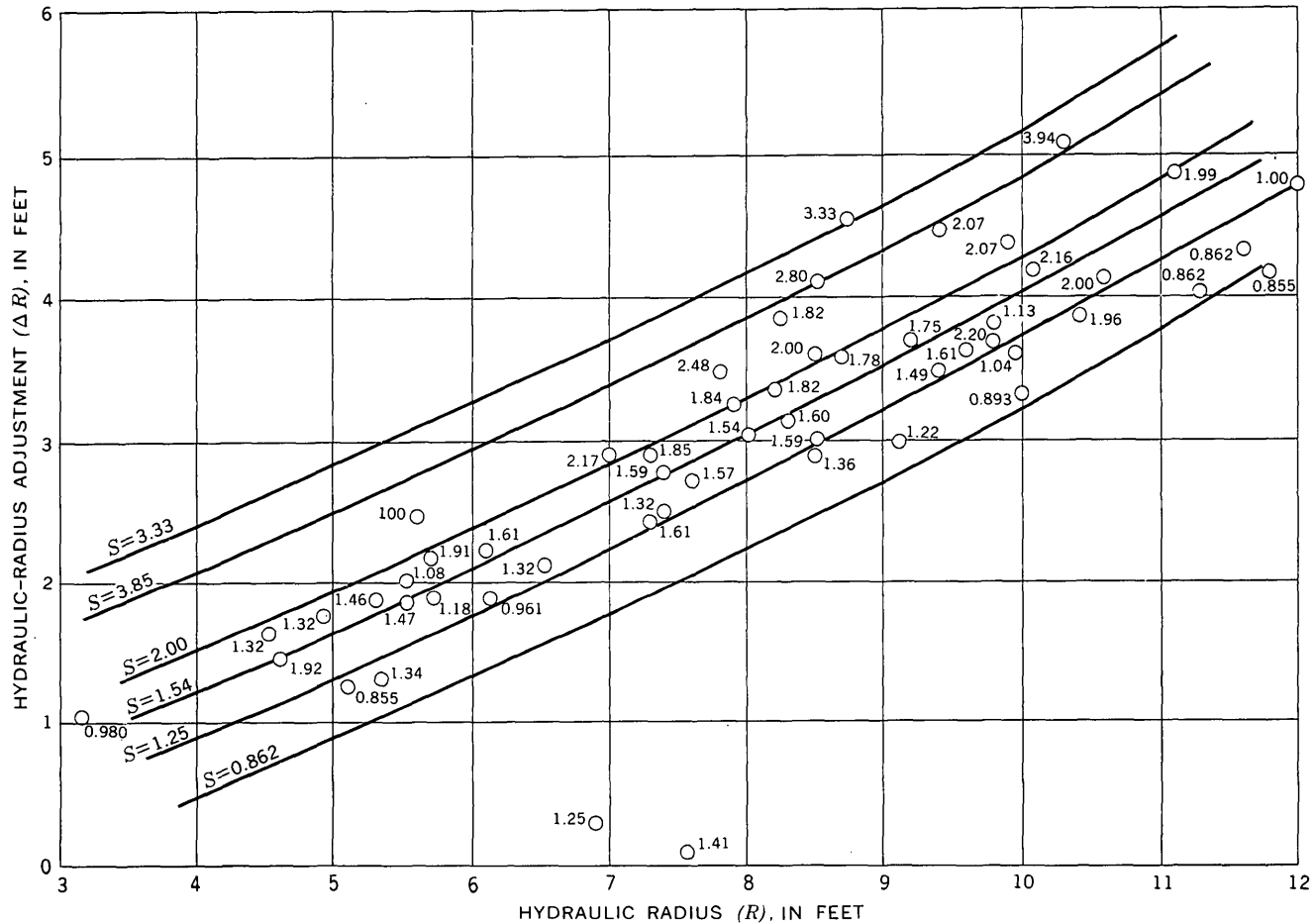


FIGURE 75.—Relation between the hydraulic-radius adjustment ( $\Delta R$ ), hydraulic radius ( $R$ ), and slope ( $S \times 10^4$ ) for Pakistan canals (Harza Engineering Co., Internat., 1963).

In the first method, if the depth ( $D$ ) or hydraulic radius ( $R$ ), the slope ( $S$ ), and the temperature ( $T$ ) are known or assumed,  $\Delta R$  or  $\Delta D$  can be determined from the appropriate relation. Then  $C'/\sqrt{g}$  can be computed using equation 31 or 33. Knowing  $C'/\sqrt{g}$ , equation 35 can be used to compute  $V'$ , and  $V$  determined from equation 34.

The second method of determining  $V$ , in which knowledge of  $D$  or  $R$  and of  $S$  is assumed, is as follows:

1. Read  $\Delta D$  or  $\Delta R$  directly from the appropriate  $\Delta D$  versus  $D$  or  $\Delta R$  versus  $R$  relation, in which slope may be a significant third variable.
2. Having determined a depth adjustment and knowing the corresponding values of  $S$ ,  $D$  or  $R$ , form roughness, and size of bed material when dealing with alluvial channels:
  - A. Compute  $\Delta D/D$  or  $\Delta R/R$ ;

B. Compute  $R_* = V_* D/\nu$ ;

C. Enter the appropriate  $C/\sqrt{g}$ ,  $R_*$  relation in which  $\Delta D/D$  or  $\Delta R/R$  is the third variable, and read the value of  $C/\sqrt{g}$  corresponding to the values of  $R_*$  and of  $\Delta R/R$  or  $\Delta D/D$ .

3. Compute the average velocity from the relation  $V = C/\sqrt{g} \sqrt{gRS}$ , using  $D = R$  when appropriate.

If determining the average velocity in a sand-bed channel, for which it has been necessary to assume a form of bed roughness prior to the determination of  $\Delta D$  or  $\Delta R$ , it is also necessary to compute the stream power,  $\tau_0 V$ . Then, with  $d_{50}$ , enter figure 28 to determine whether the preselected roughness will occur. To conform with the selected bed roughness, it may be necessary to make another trial computation using a different slope and (or) depth. For the design of a stable sand-bed canal, the bed-material

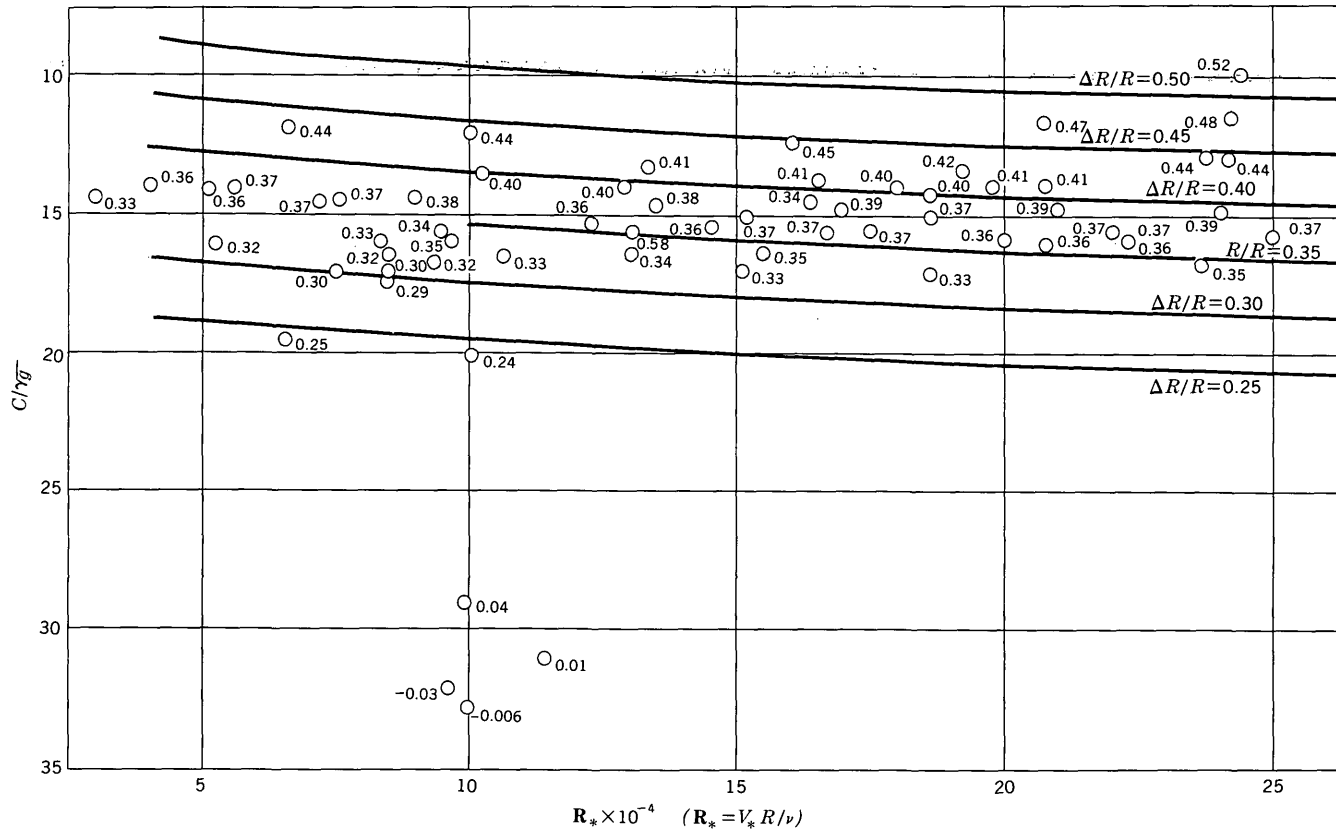


FIGURE 76.—Resistance diagram relating  $C/\sqrt{g}$ ,  $R_*$ , and  $\Delta R/R$  for Pakistan canals (Harza Engineering Co., Internat., 1963).

discharge is computed and compared with the desired bed-material discharge. If they are not approximately equal, the design should be modified by changing slope and (or) depth without changing the form of bed roughness.

**SUMMARY AND CONCLUSIONS**

The forms of bed roughness and resistance to flow in alluvial channels are functions of many inter-related variables, which are sensitive to changes in each other. In flume experiments and in natural rivers, the bed forms that occur (depending on the flow, fluid, geometry, and sediment characteristics) are ripples, ripples on dunes, dunes, plane bed, antidunes, and chutes and pools. These bed forms are classified into a lower or an upper flow regime or into an intermediate transition zone. Classification is based on similarity of bed form, mode of sediment transport, and magnitude of resistance to flow. This classification and the range in resistance to flow, as measured by  $f$  or  $C/\sqrt{g}$ , associated with each bed roughness are:

*Lower flow regime*

1. Ripples ( $0.052 \leq f \leq 0.13$ , or  $7.8 \leq C/\sqrt{g} \leq 12.4$ )
2. Dunes ( $0.042 \leq f \leq 0.16$ , or  $7.0 \leq C/\sqrt{g} \leq 13.2$ )

*Upper flow regime*

1. Plane bed ( $0.02 \leq f \leq 0.03$ , or  $16.3 \leq C/\sqrt{g} \leq 20$ )
2. Antidunes  
 Standing waves ( $0.02 \leq f \leq 0.035$ , or  $15.1 \leq C/\sqrt{g} \leq 20$ )  
 Breaking waves ( $0.03 \leq f \leq 0.07$ , or  $10.8 \leq C/\sqrt{g} \leq 16.3$ )
3. Chutes and pools ( $0.07 \leq f \leq 0.09$ , or  $9.4 \leq C/\sqrt{g} \leq 10.7$ )

The bed roughness and flow regime are not mutually exclusive occurrences in time and space. They may occur side by side in a cross section (multiple roughness) or one after another in time (variable roughness).

Resistance to flow in the lower flow regime is relatively large and results mainly from form roughness but also from grain roughness. Resistance to flow in the upper flow regime is relatively small except in chute-and-pool flow and is caused by the grain roughness, wave formation and subsidence, and the breaking of waves. Resistance to flow for a plane

bed is less when the bed material is moving than when the bed material is not moving.

The bed form and resistance to flow are extremely variable in the transition between the two flow regimes, ranging from those typical of the lower flow regime to those typical of the upper flow regime. The bed form in the transition (in addition to being dependent on flow, fluid, geometry, and bed-material characteristics) depends on the antecedent form of the bed. That is, if the bed configuration is dunes, depth and (or) slope can be increased, without changing the bed form, to values more consistent for the upper flow regime; or, if the bed is plane, depth and (or) slope can be decreased, without a change in bed form, to values more consistent with the lower flow regime. At certain depths and slopes, other variables being constant, the bed form in a flume or in a reach of a river will oscillate between dunes and either plane bed or antidunes. This oscillation to and from dunes is caused by the change in resistance to flow and, consequently, the change in depth and slope with a change in bed form. On a plane bed, resistance to flow is small, so that the shear stress on the bed decreases to a value that is incompatible for a plane bed, and a dune bed forms. The increases in resistance to flow and shear stress resulting from the dune bed cause the dunes to be replaced by a plane bed, and the oscillations continue.

Ripples are not small-scale dunes; although the two are similar in shape, they differ in size. Ripples range from 0.4 foot to 2.0 feet in length and from 0.02 foot to 0.2 foot in amplitude; dunes range from 2.0 feet to more than 100 feet in length and from 0.2 foot to more than 10 feet in amplitude. Resistance to flow for flow over ripples is independent of grain size and decreases with an increase in depth. Resistance to flow for flow over dunes is dependent on grain size and may either increase or decrease with an increase in depth. Ripples will not form in bed material having a median fall diameter coarser than 0.6 mm, but dunes may form in any size non-cohesive bed material. Ripples appear to move mostly in one horizontal plane because of their small amplitude, but they actually move in many horizontal planes because they have many amplitudes. Knowing these fundamental differences between ripples and dunes is extremely important, because it explains the difficulty of extrapolating the results of small-scale laboratory studies to natural streams. Ripples are the dominant bed form in the lower flow regime in small flumes, whereas dunes are the dominant bed form in the lower flow regime in the field.

The variables that govern the form of bed roughness and, thus, resistance to flow under the restraint of equilibrium flow,

$$\left[ \frac{\partial \bar{C}_r}{\partial t} = \frac{\partial \bar{C}_r}{\partial x} = \frac{\partial \bar{V}}{\partial t} = \frac{\partial \bar{V}}{\partial x} = 0 \right],$$

are slope of the energy grade line; depth of flow; fall velocity, physical size, and gradation of the bed material; concentration of fine sediment; seepage force; and shape and sinuosity of the channel. Concentration of the bed-material discharge is not included as a variable because the definition of equilibrium flow eliminates it as an independent variable. However, bed-material discharge can be substituted for resistance to flow or bed form if the purpose of the investigation is to evaluate sediment transport.

The independent variables in alluvial channels are often interdependent in their effect on bed form, resistance to flow, and each other. That is, a change in one of the variables not only affects resistance to flow but may interact and affect one or more of the other independent variables. Owing to this interaction it is impossible to completely isolate the effect of an independent variable. The following conclusions resulted from the flume experiments and field studies.

1. With only slope and discharge varying, and with the original slope being the slope at which motion begins, an increase in slope will produce, in order, the bed forms listed on page J11. Even if bed form does not change, resistance to flow will still vary with slope. The magnitude and direction of the change in resistance to flow with a change in slope will depend on the bed form and the other independent variables.

2. With only depth and discharge varying, a change in depth can cause a change in bed form. The change occurring with an increase in depth may be from ripples to dunes, dunes to plane bed, or plane bed to antidunes. With a large increase in depth, the bed form can change from dunes to plane bed or even to antidunes. The order will be reversed by decreasing depth. If the bed configuration does not change with a change in depth, resistance to flow will change. With either ripples or a plane bed as the bed form, an increase in depth will cause a decrease in resistance to flow as a result of changing relative roughness. With dunes as the bed form, an increase in depth will cause an increase in resistance to flow if the median diameter of the bed material is larger than 0.3 mm, because the increase in the length and amplitude of dunes caused by the

increase in depth is more rapid than the decrease in relative roughness. With dunes as the bed form in bed material having a median diameter of less than 0.3 mm, an increase in depth either will not change or will cause a decrease in the resistance to flow. This is because the length of the dunes increases more than the amplitude, and because the angularity of the dunes decreases with increasing depth. If the bed form is antidunes, an increase in depth will cause the antidunes to increase in length, amplitude, and activity until a maximum is reached, and then further increases in depth will cause the antidune characteristics to decrease. These changes in the antidunes with an increase in depth results in resistance to flow increasing to some maximum value and then decreasing.

3. Fall velocity of the sediment is the primary variable that determines the interaction between the bed material and the fluid. The experiments proved that for a given depth and slope, fall velocity is more important than physical size in determining the bed forms that will occur, the dimensions of the bed form, and the intensity of any flow phenomenon associated with the bed form. If both depth and slope are constant, an increase in fall velocity will cause a decrease in the length and an increase in the angularity of the dunes; thus, resistance to flow will be increased. If the bed form is antidunes, a decrease in fall velocity will cause the antidunes to increase in occurrence and activity, thereby increasing resistance to flow. A decrease in fall velocity can cause a plane bed to change to antidunes, whereas an increase in fall velocity can cause a plane bed to change to dunes. For either change (plane bed to antidunes or plane bed to dunes), resistance to flow will increase, although the increase is much larger when a change from plane bed to dunes occurs.

Fall velocity, in addition to depending on the physical size of bed material, depends on the viscosity of the fluid and the density and shape of the particle. The effect of the fluid viscosity on fall velocity, and thus on resistance to flow, is very important because within the range of changes in temperature or fine-sediment concentration that occur naturally in streams, the bed form may range from dunes to antidunes. With an increase in viscosity the fall velocity decreases and a dune bed may become plane, decreasing resistance to flow. This same change in viscosity and fall velocity may cause a plane bed to change to antidunes or, if antidunes are already present, may increase the antidune activity, thus causing a corresponding increase in resistance to flow. Although density and shape of the particles

are factors in determining fall velocity, their effect on resistance to flow in natural streams is small because their variation in nature is small. However, varying density and shape of the bed material is a common technique employed when attempting to model natural river behavior.

4. The physical size of the bed material is a fundamental variable in determining fall velocity and the bed configuration that will form for a given shear stress or stream power. Physical size is also important because grain roughness occurs to a certain degree with all bed forms. Whether resistance to flow will increase or decrease with an increase or decrease in physical size of the bed material depends on the bed form that will occur with the associated fall velocity of the sand grains and the relative importance of the dissipation of energy by grain roughness and form roughness.

5. Fine sediment dispersed in water affects the specific weight and apparent viscosity of the mixture. The apparent viscosity of a fine-sediment dispersion in water depends on the concentration of the fine sediment; the chemical and physical properties of the fine sediment; the amount and type of any base added as a dispersing agent; and, with some fine sediments at certain concentrations, the temperature of the fluid. The ratio of the apparent viscosity of an aqueous dispersion of bentonite, as measured with a Stormer viscometer, to the viscosity of water is independent of the temperature at concentrations of less than about 5 percent by weight but is dependent on the temperature at concentrations greater than about 5 percent. At 40°C the apparent viscosity of an aqueous dispersion of 10 percent (by weight) bentonite is 11 times the viscosity of water.

The specific weight of the aqueous dispersions of fine sediment increases in accordance with the amount and density of the fine material into the flow.

The change in fluid properties that results from the presence of fine sediment has a definite effect upon the fall velocity of the bed material and, thus, on resistance to flow. For example, at 24°C the fall velocity of a 0.47-mm median fall diameter sand in an aqueous dispersion of bentonite is decreased by 65 percent. This decrease of fall velocity is equivalent to the difference between the fall velocities of a 0.47-mm and a 0.24-mm sand particle in water at 24°C. With fine sediment in the flow, the bed configuration, resistance to flow, and transport of bed material for the 0.47-mm sand have the attributes

of a 0.24-mm sand at the same slope, depth, and discharge.

6. Gradation of the bed material has a major effect on the resistance to flow. Resistance to flow is larger for the bed configuration formed in a uniform sand than in a graded sand.

7. Seepage force resulting from the flow of water into or out of the bed of a stream can increase or decrease the effective weight and, thus, the mobility of the bed material. The change in mobility can cause a change in the bed form and resistance to flow.

8. The shape of the cross section and the sinuosity of the flow affect the distribution of the shear stress or stream power on the bed and thus affect the bed configuration and resistance to flow. These changes in bed configuration and resistance to flow were observed even in laboratory flumes which had only slightly different widths. In natural rivers the shape of the cross section and the sinuosity of the flow may cause antidunes to form in one part of the channel and dunes or other features to form adjacent to the antidunes. The dunes formed in deeper parts of the cross section of a natural stream may be much larger than those formed in the shallow parts. These variations in bed form across a stream (called multiple roughness) considerably affect resistance to flow.

The velocity distribution in an alluvial channel is as complex as the bed forms that occur there. Except over a plane bed, the velocity distribution is variable, and many measurements are needed to determine its average form. Over a plane bed, however, the velocity distribution in the vertical can be described by  $v_v/V_* = 3.2 [\ln(D/\xi) + 1]$ , and the mean velocity by  $V/V_* = 3.2 \ln(D/\xi)$ . For flume data, the roughness coefficient ( $\xi$ ) is the  $d_{85}$  size of bed material. The value of von Karman's kappa in the equations for plane-bed velocity distribution is 0.31; it does not vary systematically with concentration, size of bed material, or any other variable when computed using flume data.

Knowledge of the bed configuration that will form for a given slope, depth, viscosity, bed-material size distribution, and shape of channel would greatly simplify the determination of resistance to flow and sediment transport. A satisfactory method or relation between the independent variables and the bed configuration has not been developed. However, a relation between stream power (involving the velocity of flow) and the median fall diameter of the bed material separates the different bed configurations for both the laboratory and field data.

Because of the large range of bed forms that may occur in an alluvial channel, the large variation of resistance to flow among the different bed forms, and the large number of interrelated independent variables affecting bed form, it has been impossible to write a generalized function to predict resistance to flow or the velocity of flow. However, if the bed configuration is known or can be determined by trial-and-error computation, there are methods for determining resistance to flow and average velocity. The methods are based on adjustment of measured slope to compensate for the increase in energy loss caused by the form roughness or on adjustment of depth or hydraulic radius to compensate for the energy loss and increase in cross-sectional area caused by the form roughness. The magnitude of depth or slope adjustment varies with the bed configuration. Therefore, the methods for determining resistance to flow and average velocity depend on knowledge of the bed configuration.

In the slope adjustment method, the plane-bed equation (eq 13) developed from the study of the velocity profile is multiplied by a parameter  $C_*$  to obtain the discharge coefficient  $C/\sqrt{g}$  for the flow. The parameter  $C_*$  depends on bed configuration, sand size, slope, and depth. Equations and graphs were developed for determining  $C_*$  when these variables are known.

In the depth adjustment method, two methods were used to determine the depth adjustment ( $\Delta D$ ) required to compensate for energy losses and cross-sectional area losses. In one method the depth of flow is adjusted to the depth of an equivalent plane bed having the same average grain roughness as defined by the plane-bed conditions studied in the 8-foot-wide flume. In the other method the depth or hydraulic radius of flow is corrected to the depth or hydraulic radius of an equivalent channel with a hydraulically smooth boundary as defined by the equation of Tracy and Lester (1961). The increase in depth resulting from the form roughness systematically varies with depth, slope, and bed form for the different sand sizes; so it is possible to develop relations for predicting  $\Delta D$ . If  $\Delta D$  is known, the resistance to flow and average velocity can be determined. The depth correction ( $\Delta D$ ) or the hydraulic radius correction ( $\Delta R$ ) is analogous to the protuberance height ( $\xi$ ) referred to in resistance diagrams for pipes, and the ratio of  $\Delta D/D$  or  $\Delta R/R$  is a measure of the relative roughness. Resistance diagrams relating the discharge coefficient ( $C/\sqrt{g}$ ), the Reynolds number, and the measure of relative roughness ( $\Delta D/D$ ) are developed for both methods

of depth correction and for both rigid and alluvial channels. Also, a very useful relation is obtained by using the ratio of the Reynolds number to the discharge coefficient instead of the Reynolds number as a parameter in the resistance diagrams. (See figs. 75, 77, 79.) This procedure eliminates a trial-and-error solution for the velocity.

By correcting the plane-bed equation with the correction factor ( $C_*$ ) or by computing the depth correction ( $\Delta D$ ) and working it into a resistance relation, a more meaningful method of estimating average velocity for alluvial channels is developed. This method can be extended to all types of roughness in all types of channels, both for analysis and design. The methods are verified using laboratory and field data for both rigid and alluvial channels.

#### LITERATURE CITED

- Albertson, M. L., Simons, D. B., and Richardson, E. V., 1958, Discussion of mechanics of sediment-ripple formation: *Am. Soc. Civil Engineers Jour.*, v. 84, no. HY-1, 9 p.
- Bagnold, R. A., 1954, Experiments on a gravity-free dispersion of large solid spheres in a Newtonian fluid under shear: *Royal Soc. [London] Philos. Trans.*, ser. A, v. 225, p. 49-63.
- Beckman, E. W., and Furness, L. W., 1962, Flow characteristics of Elkhorn River near Waterloo, Nebraska: U.S. Geol. Survey Water-Supply Paper 1498-B, 34 p.
- Bingham, E. C., 1922, Fluidity and plasticity. New York, McGraw Hill Book Co., 440 p.
- Blench, T., 1952, Normal size distribution found in samples of river bed sand: *Am. Soc. Civil Engineers Mag.*, v. 22, no. 2, 2 p.
- Brooks, N. H., 1958, Mechanics of streams with movable beds of fine sand: *Am. Soc. Civil Engineers Trans.*, v. 123, p. 526-594.
- Carey, W. C., and Keller, M. D., 1957, Systematic changes in the beds of alluvial rivers: *Am. Soc. Civil Engineers Jour.*, v. 83, no. HY-4, 24 p.
- Colby, B. C., and Christensen, R. P., 1956, Visual accumulation tube for size analysis of sand: *Am. Soc. Civil Engineers Jour.*, v. 82, no. HY-3, 17 p.
- Colby, B. R., 1960, Discontinuous rating curves for Pigeon Roost and Cuffawa Creeks in Northern Mississippi: U.S. Dept. Agriculture, Agr. Research Service Rept. 41-36, 31 p.
- 1964, Discharge of sands and mean-velocity relationships in sand-bed streams: U.S. Geol. Survey Prof. Paper 462-A, 47 p.
- Culbertson, J. K., and Dawdy, D. R., 1964, A study of fluvial characteristics and hydraulic variables, Middle Rio Grande, New Mexico: U.S. Geol. Survey Water-Supply Paper 1498-F, 74 p.
- Daranandana, Niwate, 1962, A preliminary study of the effect of gradation of bed material on flow phenomena in alluvial channels: Fort Collins, Colo., Colorado State Univ., Dept. Civil Eng., Ph. D. dissertation.
- Dawdy, D. R., 1961, Depth-discharge relations of alluvial streams—discontinuous rating curves: U.S. Geol. Survey Water-Supply Paper 1498-C, 16 p.
- Einstein, A., 1906, Eine Neue Bestimmung der Molekular dimensionen: *Ann. Physik.*, Leipsig., v. 19, p. 289.
- Einstein, H. A., 1950, The bed load function for sediment transportation in open channel flows: U.S. Dept. Agriculture Tech. Bull. 1026, 70 p.
- Einstein, H. A., and Barbarossa, N. L., 1952, River channel roughness: *Am. Soc. Civil Engineers Trans.*, v. 117, p. 1121-1146.
- Einstein, H. A., and Kalkanis, G., 1959, Project report on sand deposit in canals: Berkeley, Calif., Univ. California Inst. Engineering Research, Ser. 93, Issue 6, 62 p.
- Elata, C., and Ippen, A. T., 1961, The dynamics of open-channel flow with suspensions of neutrally buoyant particles: Cambridge, Mass., Massachusetts Inst. Technology, Dept. Civil and Sanitary Eng. Tech. Rept. 45.
- Garde, R. J., 1959, Total sediment transport in alluvial channels: Fort Collins, Colo., Colorado State Univ., Dept. Civil Eng., Ph. D. dissertation.
- Gilbert, G. K., 1914, The transport of debris by running water: U.S. Geol. Survey Prof. Paper 86, 263 p.
- Guy, H. P., Simons, D. B., and Richardson, E. V., 1966, Summary of alluvial channel data from flume experiments, 1956-1961. U.S. Geol. Survey Prof. Paper 462-I, 96 p.
- Harza Engineering Co., International, 1963, West Pakistan Water and Power Development Authority canal and head works observation program, 1962, data tabulation: Chicago, Ill., 322 p.
- Harms, J. C., and Fahnestock, R. K., 1965, Stratification, bed forms and flow phenomena: *Soc. Econ. Paleontologists and Minerologists Special Pub.* 12, p. 84-115.
- Hubbell, D. W., and Al-Shaikh Ali, K. S., 1961, Qualitative effects of temperature on flow phenomena in alluvial channels: U.S. Geol. Survey Prof. Paper 424-D, p. D-21.
- Hubbell, D. W., and Matekja, D. Q., 1959, Investigations of sediment transportation, Middle Loup River at Dunning, Nebraska: U.S. Geol. Survey Water-Supply Paper 1476, 123 p.
- Hubbell, D. W., and others, 1956, Progress report No. 1, Investigations of some sedimentation characteristics of a sand bed stream: U.S. Geol. Survey open-file report, 78 p.
- Inglis, Sir Claude, 1948, Historical note on empirical equations developed by engineers in India for flow of water and sand in alluvial channels: *Internat. Assoc. Hydraulic Research*, 2d mtg., Stockholm, 7-9, VI, app. 5, p. 1-14.
- Ippen, A. T., and Drinker, A. M., 1962, Boundary shear stresses in curved trapezoidal channels: *Am. Soc. Civil Engineers Jour.*, v. 88, no. HY-5, p. 143-179.
- Ismail, H. M., 1952, Turbulent transfer mechanism and suspended sediment in closed canals: *Am. Soc. Civil Engineers Trans.*, v. 117, p. 409-434.
- Kennedy, J. F., 1961, Stationary waves and antidunes in alluvial channels: Pasadena, Calif., California Inst. Technology Rept. KH-R-2, 146 p.
- 1963, The mechanics of dunes and antidunes in erodible-bed channels: *Fluid Mechanics Jour.*, v. 16, pt. 4, p. 521-544.
- Kharrufa, Najib S., 1962, Flume studies of steep flow with large graded natural roughness elements: Logan, Utah, Utah State Univ., Dept. Civil Eng., Ph. D. dissertation.
- Knoroz, V. S., 1959, The effect of the channel macro-roughness on its hydraulics resistance: *Inst. Gidrotekaniki*, v. 62, p. 75-96 (in Russian). Translated by Ivan Mittin, U.S. Geol. Survey, Denver, Colo.

- Koloseus, H. J., and Davidian, J., 1961, Flow in an artificially roughened channel: U.S. Geol. Survey Paper 424-B, 25 p.
- Kramer, H., 1935, Sand mixtures and sand movement in fluvial models: Am. Soc. Civil Engineers Trans., v. 100, p. 798-838.
- Lane, E. W., 1955, The importance of fluvial morphology in hydraulic engineering: Am. Soc. Civil Engineers Proc., v. 81, no. 745, p. 1-17.
- Lane, E. W., and Carlson, E. J., 1953, Some factors affecting the stability of canals constructed in coarse granular materials: Internat. Assoc. Hydraulic Research, 5th Gen. Mtg., Minneapolis, group 18-31-58, p. 37-38.
- Laursen, E. M., and Lin, Pin-Nam, 1952, Discussion of turbulent transfer mechanism and suspended sediment in closed channels: Am. Soc. Civil Engineers Trans., v. 117, p. 435.
- Leopold, L. B., and Langbein, W. B., 1962, The concept of entropy in landscape evolution: U.S. Geol. Survey Prof. Paper 500-A, 20 p.
- Leopold, L. B., and Maddock, T., 1953, The hydraulic geometry of stream channels and some physiographic implications: U.S. Geol. Survey Prof. Paper 252, 57 p.
- Liu, H. K., 1957, Mechanics of sediment ripple formation: Am. Soc. Civil Engineers Jour., v. 83, no. HY-2, 23 p.
- Nagabhushanaiah, H. S., 1961, Separation flow downstream of a plate set normal to a plane boundary: Fort Collins, Colo., Colorado State Univ., Dept. Civil Eng., Ph.D. dissertation.
- Richardson, E. V., Simons, D. B., and Haushild, W. L., 1962, Boundary form and resistance to flow in alluvial channels: Internat. Assoc. Sci. Hydrology Bull. 1, v. 7, 5 p.
- Richardson, E. V., Simons, D. B., and Posakony, G. J., 1961, Sonic depth sounder for laboratory and field use: U.S. Geol. Survey Cir. 450, 7 p.
- Rouse, H., 1959, Advanced mechanics of fluids: New York, John Wiley & Sons, 444 p.
- Sayre, W. W., and Albertson, M. L., 1963, Roughness spacing in rigid open channels: Am. Soc. Civil Engineers Trans., v. 128, p. 343-372.
- Shields, I. A., 1936, Application of similarity principles and turbulence research to bed-load movement: A translation from the German by W. P. Ott and J. C. van Vchelin, U.S. Soil Conserv. Service Coop. Lab., California Inst. Technology, Pasadena, 21 p.
- Simons, D. B., 1957, Theory and design of stable channels in alluvial material: Fort Collins, Colo., Colorado State Univ., Dept. Civil Eng., Ph. D. dissertation.
- Simons, D. B., and Albertson, M. L., 1963, Uniform water convergence channels in alluvial material: Am. Soc. Civil Engineers Trans., v. 128, p. 65-167.
- Simons, D. B., and Richardson, E. V., 1962a, Resistance to flow in alluvial channels: Am. Soc. Civil Engineers Trans., v. 127, p. 927-1006.
- 1962b, The effect of bed roughness on depth-discharge relations in alluvial channels: U.S. Geol. Survey Water-Supply Paper 1498-E, 26 p.
- 1963, Form of bed roughness in alluvial channels: Am. Soc. Civil Engineers Trans., v. 128, p. 284-323.
- 1965, A study of variables affecting flow characteristics and sediment transport in alluvial channels: Federal Inter-Agency Sed. Conf. 1963 Proc., Agr. Research Service Misc. Pub. 970, p. 193-207.
- Simons, D. B., Richardson, E. W., and Albertson, M. L., 1961, Flume studies using medium sand (0.45 mm): U.S. Geol. Survey Water-Supply Paper 1498-A, 76 p.
- Simons, D. B., Richardson, E. V., and Haushild, W. H., 1963, Some effects of fine sediment on flow phenomena: U.S. Geol. Survey Water-Supply Paper 1498-G, 46 p.
- Straub, L. G., 1954, Transportation characteristics of Missouri River sediment: Minneapolis, Minn., U.S. Army Corps Engineers M.R.D. Sediment Ser. 4, 33 p.
- Taylor, R. H., and Brooks, N. H., 1962, Discussion of resistance to flow in alluvial channels: Am. Soc. Civil Engineers Trans., v. 127, p. 246-256, 927-1006.
- Tracy, H. J., and Lester, C. M., 1961, Resistance coefficients and velocity distribution in a smooth rectangular channel: U.S. Geol. Survey Water-Supply Paper 1592-A, 18 p.
- Vanoni, V. A., 1946, Transport of suspended sediment by water: Am. Soc. Civil Engineers Trans., v. 111, p. 67-102.
- Vanoni, V. A., and Brooks, N. H., 1957, Laboratory studies of the roughness and suspended load of alluvial streams: Pasadena, Calif., California Inst. Technology Rept. E-68, 121 p.
- Vanoni, V. A., Brooks, N. H., and Kennedy, J. F., 1961, Lecture notes on sediment transportation and channel stability: Pasadena, Calif., California Inst. Technology Rept. KH-R-1, 129 p.
- Vanoni, V. A., and Nomicos, G. N., 1960, Resistance properties of sediment-laden streams: Am. Soc. Civil Engineers Trans., v. 125, p. 1140-1175.
- White, C. M., 1940, Equilibrium of grains on bed of streams: Royal Soc. [London] Philos. Trans., Ser. A, Mathematical and Physical Sciences, v. 174, p. 322-334.